Dynamic refractive tensor field tomography as an inverse problem for a transport equation

Dissertation

zur Erlangung des Grades des Doktors der Naturwissenschaften der Fakultät für Mathematik und Informatik der Universität des Saarlandes

von
Lukas Vierus

Saarbrücken, 2024

UNIVERSITÄT
DES
SAARLANDES

Tag des Kolloquiums:	14.11.2024
Dekan:	Prof. Dr. Roland Speicher
Vorsitzender:	Prof. Dr. Michael Bildhauer
Berichterstatter:	Prof. Dr. Thomas Schuster
	Prof. Dr. Sergej Rjasanow
	Prof. Dr. E. Todd Quinto
Protokollführer:	Dr. Dimitri Rothermel

Acknowledgements

First and foremost, I would like to acknowledge my supervisor, Professor Thomas Schuster. I am grateful to him for arousing my interest in inverse problems during my Bachelor's thesis. I would also like to thank him for the trust he placed in me and the offer to continue the exciting research question from my Master's thesis over the past few years.

I am grateful to the late Professor Alfred K. Louis for his collaboration in our joint DFG project and for initially agreeing to serve as a co-referee for this thesis. His passing is a profound loss to the academic community, and I am honored to have had the privilege of working with him. I also sincerely thank Professor Sergej Rjasanow, who kindly stepped in for Professor Louis, and Professor E. Todd Quinto for serving as co-referees for this thesis.

Furthermore, I would like to thank my maths teacher Katharina Backes, who got me interested in mathematics when I was a junior at grammar school and made me want to study mathematics very early on.

I would like to thank Clemens Meiser, Dr. Dimitri Rothermel and Alice Oberacker for the many mathematical and friendly discussions that greatly helped me in completing this thesis. I would also like to thank Dr. Rebecca Rothermel, Dean Zenner, Petra Schuster-Gentes, Claudia Stoffer and Cindy Ernst for the pleasant working atmosphere.

I am very grateful to Clemens Meiser and Alice Oberacker for proofreading this thesis.

Finally, I would like to thank my family for their unwavering support. Special thanks go to my parents Stefanie and Markus, my sibling Leno and my partner Michelle.

Abstract

The model of the X-ray transform from computed tomography can be transferred to numerous applications, for example by increasing the dimension of the problem. There are already many publications in which generalizations of this transformation are investigated. For example, instead of scalar functions, vector or tensor fields are reconstructed. In addition, there are also treatments of time-varying quantities, intensity losses due to absorption, or deviations of ray trajectories from exact straight lines. However, these phenomena have so far been discussed only individually or in pairs, not all simultaneously.

In the first part of this work, a holistic model of tensor tomographic applications of any rank and dimension is developed. For this purpose, a generalized beam transformation is derived that considers absorption and refraction effects as well as temporal variability. By reformulating the integral equation into a transport equation, the adjoint problem can be derived. Through the approximation of this parabolic equation by elliptic equations, its unambiguous solvability is shown. This makes it possible to develop an efficient algorithm for the reconstruction of tensor fields, which is then applied to synthetic data generated using the model from the first part. It turns out that the modified model leads to a significant improvement in the reconstructions.

Zusammenfassung

Das Modell der Röntgen-Transformation aus der Computertomographie kann auf zahlreiche Anwendungen übertragen werden, indem beispielsweise die Dimension des Problems erhöht wird. Es gibt bereits viele Veröffentlichungen, bei denen Verallgemeinerungen dieser Transformation untersucht werden. Dabei werden zum Beispiel statt skalaren Funktionen Vektor- oder Tensorfelder rekonstruiert. Hinzu kommen auch die Behandlungen von zeitlich variierenden Größen, Intensitätsverlusten durch Absorption, beziehungsweise Abweichungen der Strahlverläufe von exakten Geraden. Allerdings wurden diese Phänomene bisher nur einzeln oder paarweise diskutiert, nicht aber alle zur selben Zeit.

In dieser Arbeit wird im ersten Teil ein ganzheitliches Modell tensortomographischer Anwendungen beliebigen Ranges und Dimension ausgearbeitet. Dazu wird eine verallgemeinerte Strahltransformation hergeleitet, die sowohl Absorptions- und Brechungseffekte als auch zeitliche Veränderlichkeit berücksichtigt. Durch Umformulierung der Integralgleichung zu einer Transportgleichung kann das adjungierte Problem hergeleitet werden. Für die Approximation dieser parabolischen Gleichung durch elliptische Gleichungen wird dessen eindeutige Lösbarkeit gezeigt. Dadurch ist es möglich einen effizienten Algorithmus zur Rekonstruktion von Tensorfeldern zu entwickeln. Dieser wird auf synthetische Daten angewendet, die mithilfe des Modells aus dem ersten Teil generiert werden. Es stellt sich heraus, dass das modifizierte Modell zu einer deutlichen Verbesserung der Rekonstruktionen führt.

Contents

List of Symbols

Designations

α	attenuation coefficient
$a(u, v)$	bilinear form with test functions u and v
$b(v)$	linear form with test function v
δ	noise level or symbol for variation
Δ	Laplace-Beltrami operator
d	superscript indicating time-dependence
$D_\xi Y$	directional derivative of Y in direction ξ
ε	viscosity parameter
$\mathrm{err}(A^*)$	relative error in dual condition generated by A^*
$\mathcal{F}_\alpha^{\varepsilon(,d)}$	parameter-to-solution mappings regarding the perturbed equation
$f_{i_1,\ldots,i_m}(x)$	static tensor field of rank m at x, $f(x)$ for short
$f_{i_1,\ldots,i_m}(t, x)$	dynamic tensor field of rank m at x and time t, $f(t, x)$ for short
$\gamma_{x,\xi}$	geodesic curve starting at x in direction ξ
γ_+	trace operator restricting to $\partial_+ \Omega M$
Γ_{ij}^k	Christoffel symbols
$g_{ij}(x)$	entries of metric tensor at x
$\mathcal{H}$	geodesic vector field
h	boundary values of forward problem
$\mathcal{I}_\alpha^{(d)}$	static/dynamic attenuated ray transform
$\mathcal{J}_\beta$	Tikhonov functional with parameter β
m	rank of the tensor field
ν	outward normal vector
∇_{euclid}	Euclidean gradient
$\nabla_\xi Y$	covariant derivative of Y in direction ξ
n	refractive index
N	dimension of manifold M
$\mathfrak{p}$	operator for inner differentiation of tensor fields
P	number of angles in the polar grid
Q	number of directions
R	number of radii in the polar grid
$\mathfrak{s}$	divergence operator for tensor fields
$\mathcal{S}_\alpha^{\varepsilon(,d)}$	forward operator using the perturbed transport equation
$\tau_\pm(x, \xi)$	exit and entry time of geodesic starting in x into direction ξ
u	solution of the PDE of the forward problem
w	solution of the PDE of the adjoint problem
Ξ_n	damping function appearing in adjoint operator

Spaces and manifolds

M	manifold representing the body
(M, g)	Riemannian manifold with manifold M and Riemannian metric g
$S^m\tau'_M$	space of symmetric tensor fields of rank m on τ'_M
τ_M	tangent bundle
τ'_M	cotangent bundle
T_pM	tangent space at p
T'_pM	cotangent space at p
TM	union of all T_pM
$T'M$	union of all T'_pM
ΩM	submanifold of TM with unit tangent vectors
$\partial_\pm \Omega M$	outflow and inflow boundary of ΩM
$\Omega_x M$	sphere of possible directions given a fixed vector x

Surface and volume forms

$\mathrm{d}\omega_x^N(\xi)$	angular measure on $\Omega_x M$ for dimension N
$\mathrm{d}\sigma_+^N$	surface element on $\partial_+\Omega M$ for dimension N
$\mathrm{d}\Sigma^N$	volume element on ΩM for dimension N
$\mathrm{d}V_x^N(\xi)$	volume form on T_xM for dimension N

List of Figures

List of Tables

Introduction

Inverse problems are a very large part of numerical mathematics. The aim is to deduce the underlying cause of a system from an observed effect. The direct problem is often easier to solve because a physical model is known. In the case of inverse problems, this model has to be inverted to determine the cause of the effect, as in the case described below. This is not possible without further effort, as the following two examples show.

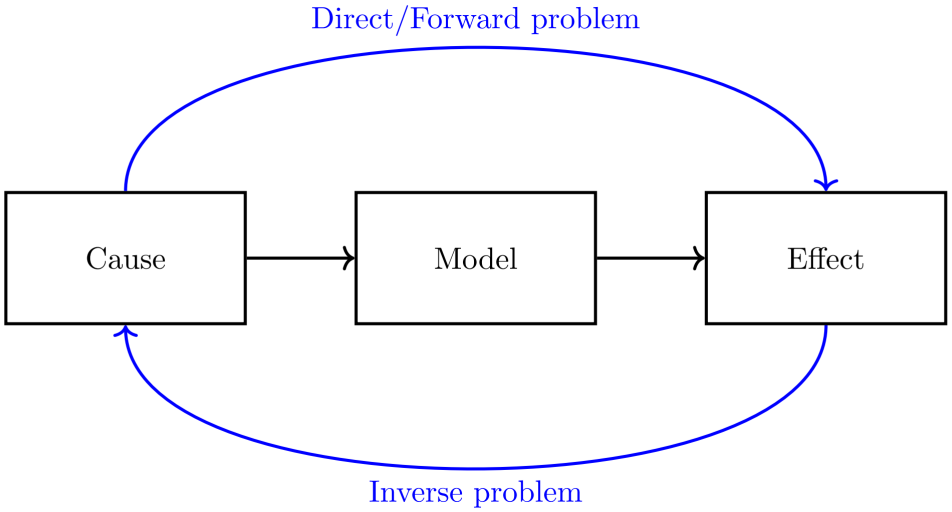

Figure 0.1: Sketch of direct/forward and inverse problem

A good example of an inverse problem is the reconstruction of an accident. In this context, one typically observes the consequences of an accident, such as marks on the road, damage to vehicles, or injuries to people. The aim could be to retrospectively determine the exact circumstances and parameters of the accident from these visible indications of how it happened. This inverse problem often requires complex analysis, as several factors can influence the accident. These include the speeds of the vehicles, their positions before and after the collision, the frictional properties of the road and many other parameters. The physical representation of the course of the accident therefore corresponds to the model. The cause would be the actual course of the accident, including the specific actions of the drivers involved, road conditions and other relevant factors. We take the observable results of the accident, such as marks on the road, damage to vehicles, and injuries to people, as the effect. The following problems arise: It could be, for example, that two different accident sequences lead to identical lanes on the road or the same damage to the vehicles. If no further information is available, there would be no clear explanation for the accident. Another

aspect could be that the tracks were falsified due to other external circumstances, so without this knowledge, there is no logical hypothesis. It could also happen that tracks that cannot be measured exactly lead to a completely different conclusion. Let us assume, for example, that the exact position of the tire tracks on the road cannot be precisely determined due to measurement inaccuracies or other uncertainties. A minimal deviation in the interpretation of the tracks could lead investigators to conclude that the vehicle involved was braking when it was accelerating, or that it was swerving to the left when it was instead swerving to the right.
In mathematical applications, too, it quickly becomes clear that the inverse problem is often much more difficult to solve. Let us take the simplified approach that the population of some bacteria behaves according to the following function: At time t the function

$$f(t) = 10^8 t e^{-t}, \quad t \in [0, \infty)$$

gives the number of bacteria present in an observed area.

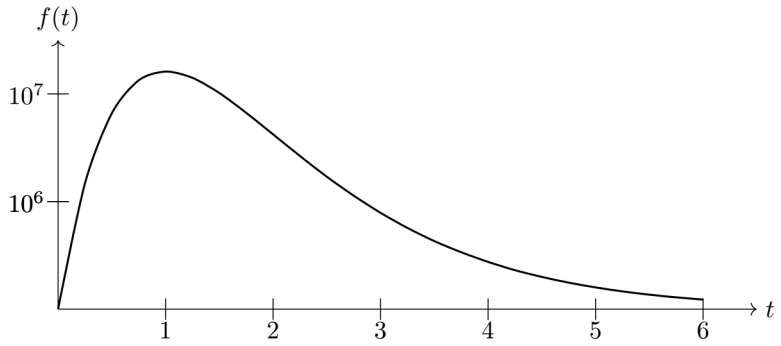

Figure 0.2: Plot of bacteria population

The function f therefore corresponds to the model with which the number of bacteria can easily be determined for a specific point in time by simply inserting the respective value into the function and evaluating everything. Conversely, if you want to determine the possible point in time for a given number, another problem arises: No explicit inverse function can be written for this function. If you have enough data points, the function f can be plotted and you can find an approximation for the value you are looking for by reading it off. However, the exact time cannot usually be determined in this way. To obtain the best possible approximation in this case, you can use the Newton method, for example. This is an iterative procedure which, under certain conditions, converges at least locally to the required solution. As a result, a decision must be made at a certain point as to which sequence element you are satisfied with. For example, as a rule, this happens when the distance between successive iterations falls below a predetermined value. In the case of a non-injective function such as f, where there is no unique preimage for certain function values. In such cases, a selection for the physically most sensible solution must be made based on a priori information.
These two examples show that even for supposedly simple forward problems, the corresponding inverse problems can present some difficulties. As mentioned above,

one of the biggest challenges is dealing with inverse mappings which, if they exist, are not bijective and continuous. Things become much more complicated when considering mappings between higher or even infinite-dimensional spaces. Especially in the latter case, exact inversion formulas can rarely be given. However, if this is the case, they are usually not continuous. This means that even small measurement inaccuracies of the effect lead to large differences in the possible cause. In addition, there may also be several causes that lead to the same result. In the previous example, this would correspond to the case where the number of bacteria is the same at several points in time. For complex inverse problems, it, therefore, takes a large number of theoretical considerations to develop a method that decides in favor of the physically most sensible solution when several solutions exist and does not react too sensitively to possible inaccuracies.
In this thesis, we only refer to linear inverse problems, i.e., the effect depends linearly on the cause. Tomographic problems are a large area of such problems. This involves sending signals of an acoustic, mechanical, or electromagnetic nature through an object that cannot be seen from the outside to obtain and visualize information about its interior. In this work, we deal with the tomography of tensors. In general, tensors are multi-linear mappings. Tensor tomography refers to the reconstruction of matrices as representatives of bilinear mappings, i.e., second-rank tensors. However, vector-valued functions can also be understood as tensors, more precisely as 1st-rank tensors. This is because vectors v can be interpreted as a linear mapping by $\langle v, \cdot \rangle$. Analogously, scalar functions describe a 0th-rank tensor. It therefore makes sense to investigate the theory for tensors with maximum degree that appear in applications and then to obtain information about the treatment of lower rank tensors as simplified special cases.

Computerized Tomography (CT), often regarded as one of the most classical applications of the 2D X-ray transform, revolutionized medical diagnostics by enabling non-invasive visualization of internal anatomical structures. By collecting X-ray data from various angles and employing mathematical algorithms, CT scanners reconstruct detailed cross-sectional images, offering clinicians unprecedented insights into tissues, organs and abnormalities. The inverse problem mathematically involves determining the absorption coefficient f based on integral data If, given by

$$If(x, \xi) = \int_{\mathbb{R}} f(x + \tau\xi) \mathrm{d}\tau, \tag{1}$$

providing information about the intensity of an outcoming ray at x in direction ξ, cf. [64].
There are plenty of inverse problems that exhibit a similar integral model to (1). For example, in Single Photon Emission Computed Tomography (SPECT), the same formula but with an additional damping term is used but f describes a radioactive source that is to be determined, c.f. [18] and [37]. But also reconstructions of higher-dimensional quantities are encountered in certain applications. The field of vector tomography has evolved from various sources and applications that cover a wide range of topics and challenges. A pioneering work in this field was done by Norton in 1988, which stands as a precursor to two-dimensional vector tomography and is documented in [66]. The image of the vectorial beam transformation is a scalar

function. This is because instead of the vector field, only projections on the ray's direction vector of the propagation are considered. Consequently, all parts of a vector field that are orthogonal to this direction are ignored. Therefore, this transformation is only injective for divergence-free vector fields. More detailed information can be found in [28], [70], [95] and [99]. This theory can be used to visualize blood flows in human bodies, see [48]. Another major application is the detection of velocity anomalies of seismic wave propagation in the Earth's interior, which can be used to predict earthquakes, see [5], [7] and [17]. In some cases, the consideration of absorption effects is also important. These then appear as an additional weighting factor in the integral transformation. This problem, among others, was dealt with in [15], [44], [63] and [82].[24] and [30] show that this concept can also be applied to tensor fields. Here, too, analytical results such as injectivity or results regarding the stability or range of the transformation can be proven, see [3], [8], [21], [72], [73], [90], [96], [97] and [98]. It is noteworthy that this problem can be reformulated as a boundary value problem, see [27]. In [25], the unambiguous solvability of the partial differential equation under certain conditions on the absorption coefficient is shown. The applications of tensor fields are far-reaching. They can be found, for example, in the calculation of internal stresses in optic fibers, c.f. [76] and [77], strain tensors in polycrystalline materials [56], diffusion tensors [71] and in the field of photoelasticity, see [1],[2],[49] and [55].

In all the sources mentioned so far, it is assumed that the signals move in a straight line through the object under investigation. In practice, however, there are always deviations from these lines, although to a small extent in certain cases. This is particularly the case if the object is inhomogeneous, i.e., consists of several materials. To take these deviations into account, Riemannian manifolds must be considered. Their comprehensive theory is for example dealt with in sources [6], [47] and [88]. In [86] it is explained how time-of-flight measurements can be used to approximately determine the refractive index inside an object. This also leads to a better approximation of the signal propagation although there are no more inversion formulas as in the Euclidean case, see [52]. Here, too, it can be seen that only the divergence-free components of a field can be reconstructed without taking absorption into account. There is a large number of numerical results that include refraction effects, limited to the vector undamped case, c.f. [61], [75], or the scalar damped case, c.f. [26], [29]. Another aspect that is dealt with in the context of beam transformations is the time dependence of a field. Sources like [50] and [51] on theory and [83] and [84] on numerical analysis provide theory on general dynamic inverse problems. Specifically, e.g. [32], [39], [40], [41] deal with dynamic computed tomography. The aim is to deal with possible artifacts caused by any movement of the patient during the scan.

In summary, the above sources have generalized the model of the original X-ray transformation from (1) by extending the dimension from static scalar to dynamic tensor fields to be reconstructed and by including both absorption and refraction effects. This work aims to develop a holistic approach that unifies all these aspects.

In the first chapter, all mathematical theories are introduced, which are necessary for the modeling of the problem and the numerical implementation. This includes the theory of inverse problems as operator equations. In particular, it describes how, at least in theory, reasonable solutions can be computed by iterative methods, even if the available measured data are subject to errors. After that, some important

definitions and properties of tensors are given, to be able to describe tensor tomography mathematically precisely. The third aspect is an introduction to Riemannian geometry. This is needed to be able to describe the exact course of the rays in a medium. In the second chapter, some examples of physical problems in different dimensions are investigated, which can be modeled with a ray transformation. It is shown that the transformations can all be brought to a similar form. However, it also becomes clear that some things such as absorption, time dependence and refraction effects are not taken into account. All these phenomena are embedded in the model one after the other. Finally, a closed integral transformation is obtained again. Although continuity can be proved for this one, unfortunately, the formula is too complex to give direct inversion formulas. Instead, one derives an equivalent formulation via a transport equation with appropriate initial and boundary conditions. For this problem, with the help of a perturbation term, we show the existence of a unique weak solution and thus the well-definiteness of the problem. For the numerical implementation, using the transport equation, we compute the adjoint operator, which again consists of the solution of a differential equation. From the derivation, we also see what the adjoint integral operator looks like. In the last chapter, we then perform some numerical experiments with both forward and adjoint operators. For simplicity, we restrict ourselves to the time-independent setting and concentrate on the reconstruction of vector fields because of better visualization. For reasons of symmetry, it makes sense to choose a polar grid for the reconstruction of the fields on an area M. For this purpose, we test which combination of radii and angles leads to the best results. For certain simple vector fields and an Euclidean metric (propagation of the waves along straight lines), the forward operator can also be determined analytically. We use these examples to test the quality of the forward integral operator. As it turns out, it can be approximated very efficiently with appropriate quadrature formulas. Then we test the quality of the adjoint operator by determining the absolute error for different numbers of propagation directions. After careful analysis, we have identified the most effective grid dimensions. We generate synthetic data with refraction effects calculated into varying degrees and then apply noise of varying magnitudes to these data. With these data, we check the above-mentioned constraint from the derivation of the problem, which only allows certain relations from refraction and absorption.
Finally, there is given a brief outlook on future research.

1 Mathematical preliminaries

In the first chapter we provide the basics for our work. Here we first deal with linear inverse problems. In the second part, definitions and notations from tensor analysis and Riemannian geometry are given.

1.1 Inverse Problems

In this subsection, we deal with some useful tools from the theory of inverse problems. These include regularization methods in the form of iterative procedures as well as the possible acceleration of these calculations. This section is mainly based on the monographs from [54], [58] and [79]. All other sources are listed as usual.
Inverse problems usually consist of reconstructing causes from observed effects. The connection between cause and effect can be expressed by the following equation

$$Af = g. \tag{1.1}$$

The mathematical model, expressed by a mapping $A\colon X \to Y$, maps the set of causes X to the set of effects Y. Almost all inverse problems that are of practical relevance are ill-posed in the sense of Hadamard [38]. This is the case if at least one of the following conditions does not apply.

Definition 1.1. *Let X and Y be Hilbert spaces, $A\colon X \to Y$ a linear mapping. The equation $Af = g$ is called properly-posed or well-posed if the following holds:*

a) Existence: For every $g \in Y$ there is (at least one) $f \in X$ such that $Af = g$.

b) Uniqueness: For every $g \in Y$ there is at most one $f \in X$ with $Af = g$.

c) Stability: The inverse mapping $A^{-1}\colon Y \to X$ is continuous, i.e., the solution f depends continuously on the data g.

Equations for which (at least) one of these properties does not hold are called ill-posed.

We first need some notations. In the following, we focus on continuous linear mappings between Hilbert spaces X and Y and define

$$\mathcal{L}(X,Y) \coloneqq \{B\colon X \to Y | B \text{ is linear and } ||B|| \coloneqq \sup_{||x||_X=1} ||Bx||_Y < \infty\}.$$

Further, we set

$$\mathcal{N}(A) = \{f \in X | Af = 0\} \qquad \text{and} \qquad \mathcal{R}(A) = \{Af | f \in X\}$$

as the *null space* and *range* of A. For a closed subspace $U \subset X$ we denote by $\mathcal{P}_U \colon X \to X$ the orthogonal projection from X on U. For $A \in \mathcal{L}(X, Y)$ there exists a unique operator $A^* \in \mathcal{L}(Y, X)$ which is called *the adjoint operator of* A satisfying

$$\langle Ax, y\rangle_Y = \langle x, A^* y\rangle_X \qquad \text{for all } x \in X,\ y \in Y. \tag{1.2}$$

where $\langle \cdot, \cdot \rangle_Y$ and $\langle \cdot, \cdot \rangle_X$ denote the scalar product in Y, respectively in X.
We will now extend the solution concept for non-bijective operators A. Therefore, we consider elements $f \in X$ that are characterized in the following way:

Theorem 1.2. *Let $g \in Y$ and $A \in \mathcal{L}(X, Y)$. Then the following are equivalent.*

a) $f \in X$ satisfies $Af = \mathcal{P}_{\overline{\mathcal{R}(A)}} g$.

b) $f \in X$ minimizes the functional

$$\mathcal{J}_0 = \frac{1}{2}\|Af - g\|_Y^2. \tag{1.3}$$

c) $f \in X$ satiesfies the normal equation

$$A^* Af = A^* g. \tag{1.4}$$

Proof. See [79]. □

This theorem provides a way to cope with operators that are not surjective: If there is no solution of the operator equation $Af = g$ we seek for one that at least minimizes the residual $\|Af - g\|_Y$. For non-injective operators, we make use of the following statement:

Lemma 1.3. *Let $g \in Y$. Then:*

a) The set of solutions of the normal equation $\mathbb{L}(g) = \{\varphi \in X | A^* A\varphi = A^* g\}$ is non-empty if and only if $g \in \mathcal{R}(A) \oplus \mathcal{R}(A)^\perp$.

b) For $g \in \mathcal{R}(A) \oplus \mathcal{R}(A)^\perp$ there is exactly one element $f^\dagger$ on $\mathbb{L}(g)$ with a minimal norm, i.e., $\|f^\dagger\|_X < \|\varphi\|_X$ for all $\varphi \in \mathbb{L}(g) \backslash \{f^\dagger\}$.

Proof. See [79]. □

Definition 1.4. *The operator* $A^\dagger\colon \mathcal{D}(A^\dagger) = \mathcal{R}(A) \oplus \mathcal{R}(A)^\perp \subset Y \to X$ *that maps any* $g \in \mathcal{D}(A^\dagger)$ *to the uniquely determined element* $f^\dagger \in \mathbb{L}(g)$ *with minimal norm, is called generalized inverse of* $A \in \mathcal{L}(X, Y)$*. We call* $f^\dagger = A^\dagger g$ *the minimum-norm solution of* $Af = g$*.*

It can easily be verified that $f^\dagger \in \mathcal{N}(A)^\perp$. We arbitrarily selected the element with the smallest norm from the set $\mathbb{L}(g)$. It would also be conceivable to minimize the distance to a certain element $f_0 \in X$. In that case, it is possible to insert some prior information about the solution as we will see later. The corresponding solution is also clearly determined. We call it the f_0-minimum norm solution and also denote it by $f^\dagger$. For the f_0-minimum norm solution, it holds that

$$f^\dagger = A^\dagger g + \mathcal{P}_{\mathcal{N}(A)} f_0. \tag{1.5}$$

Compact operators are a class of operators that typically lead to ill-posed problems. If their range is not finite-dimensional their generalized inverse cannot be continuous.

Definition 1.5. *Let* X *and* Y *be normed spaces. The linear operator* $A\colon X \to Y$ *is called compact if one of the following equivalent properties applies:*

a) Each bounded set $U \subset X$ *has a relatively compact image, i.e.,* $\overline{A(U)}$ *is compact in* Y*.*

b) Is $\{\varphi_n\}_{n\in\mathbb{N}} \subset X$ *a bounded sequence then the sequence of images* $\{A\varphi_n\}_{n\in\mathbb{N}} \subset Y$ *has a convergent subsequence.*

We set

$$\mathcal{K}(X, Y) \coloneqq \{A\colon X \to Y | A \text{ is linear and compact}\}.$$

Theorem 1.6. *Let* X, Y *be Hilbert spaces and* $A \in \mathcal{K}(X, Y)$*. There are a monotonic decreasing sequence* $\{\sigma_j\}_{j\in\mathbb{N}} \subset \mathbb{R}^+$ *that is finite or converges to* 0*, and complete orthonormal bases* $\{u_j\}_{j\in\mathbb{N}} \subset Y$ *of* $\overline{\mathcal{R}(A)}$ *and* $\{v_j\}_{j\in\mathbb{N}} \subset X$ *of* $\mathcal{N}(A)^\perp$ *such that*

$$Av_j = \sigma_j u_j, \qquad A^* u_j = \sigma_j v_j \qquad \text{for all } j \in \mathbb{N}. \tag{1.6}$$

Given $x \in X$*,* Ax *can be written as a series expansion as*

$$Ax = \sum_{j=1}^{\infty} \sigma_j \langle x, v_j \rangle_X u_j. \tag{1.7}$$

Consequently, compact operators can be seen as a generalization of finite dimensional linear operators (matrices) to infinite dimensional spaces.

Note that $A^\dagger$ is not continuous if $\dim(\mathcal{R}(A)) = \infty$ because the $(\sigma_j)_{j\in\mathbb{N}}$ in (1.7) must have an accumulation point in 0. This brings us to the discussion of the third bullet of Definition 1.1:
So far, we know how to treat the first two points of Theorem 1.2. If the operator A is not surjective, we are satisfied with an appropriate projection, which hopefully is close enough to a physically meaningful solution. If the operator is not injective, i.e., there are several solutions to the inverse problem, we consider the one with the minimum norm or the one that has the smallest distance to another element $f_0 \in X$. What remains is the problem of the discontinuity of the inverse A^{-1}. In reality, we want to solve a linear operator equation

$$Af = g, \qquad g \in \mathcal{R}(A),$$

where we are only given some noisy data g^δ with

$$\|g - g^\delta\|_Y \leq \delta.$$

We call $\delta > 0$ the *noise level*. With the definition of a generalized inverse, it was possible to manage the operator not being bijective. The problem of inverting the operator continuously remains. In fact, if $\mathcal{R}(A) \neq \overline{\mathcal{R}(A)}$ then the generalized inverse $A^\dagger$ is discontinuous (c.f. [79]). As a remedy, one has to regularize and stabilize the inverse problem. This can be done by approximating $A^\dagger$ by a family of continuous operators $\{R_t\}_{t>0}$ that is defined on Y. From that we need to choose a proper element from the family $\{R_t g^\delta\}_{t>0} \subset X$ which approximates $A^\dagger g$ the best. One may think of the element $R_{t_{\text{opt}}} g^\delta$ that minimizes the error $\|A^\dagger g - R_t g^\delta\|_X$ but this fails with the missing knowledge of $A^\dagger g$. All this can be summarized in the following definition.

Definition 1.7. *Let $A \in \mathcal{L}(X, Y)$ and $\{R_t\}_{t>0}$ be a family of continuous operators from Y to X with $R_t 0 = 0$. If there is a mapping $\gamma\colon (0,\infty) \times Y \to (0,\infty)$ such that for each $g \in \mathcal{R}(A)$*

$$\sup\{\|A^\dagger g - R_{\gamma(\delta,g^\delta)} g^\delta\|_X \mid g^\delta \in Y,\ \|g - g^\delta\|_Y \leq \delta\} \to 0 \quad \text{for } \delta \to 0, \tag{1.8}$$

then $(\{R_t\}_{t>0}, \gamma)$ is called a regularization for $A^\dagger$. The mapping γ is called parameter choice and satisfies

$$\lim_{\delta\to 0} \sup\{\gamma(\delta, g^\delta) | g^\delta \in Y,\ \|g - g^\delta\|_Y \leq \delta\} = 0. \tag{1.9}$$

There is

a) *a priori* choices only depending on δ,

b) *a posteriori* choices depending on δ and g^δ.

Equation (1.8) yields

$$\lim_{\delta \to 0} \|R_{\gamma(\delta, g^\delta)} g - A^\dagger g\|_X = 0 \qquad \text{for all } g \in \mathcal{R}(A).$$

From (1.9) it is clear that $\Gamma := \{\gamma(\delta, g) | \delta > 0,\ g \in \mathcal{R}(A)\}$ has an accumulation point at 0 and hence,

$$\lim_{\Gamma \ni \lambda \to 0} \|R_\lambda g - A^\dagger g\|_X = 0 \qquad \text{for all } g \in \mathcal{R}(A). \tag{1.10}$$

We obtain the following lemma.

Lemma 1.8. *Let $A \in \mathcal{L}(X, Y)$ and $(\{R_t\}_{t>0}, \gamma)$ be a regularization for $A^\dagger$. Then, $\{R_\lambda\}_{\lambda \in \Gamma}$ converges pointwise to $A^\dagger$ on $\mathcal{R}(A)$ as $\lambda \to 0$.*

The reconstruction error $\|A^\dagger g - R_t g^\delta\|_X$ of regularization can be divided into an approximation error and a data error:

$$\|A^\dagger - R_t g^\delta\|_X \leq \underbrace{\|A^\dagger g - R_t g\|_X}_{\text{approximation error}} + \underbrace{\|R_t (g - g^\delta)\|_X}_{\text{data error}}.$$

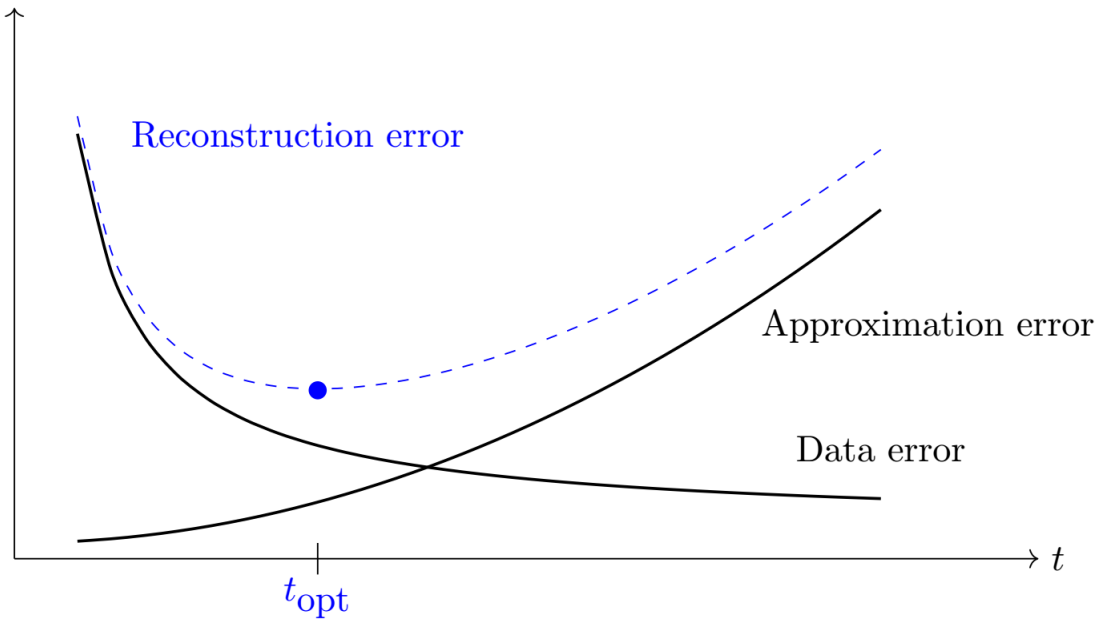

Figure 1.1: Behavior of approximation and data error

Figure 1.1 is a sketch of the typical behavior of the reconstruction error and its components. For $t \to 0$, the approximation error tends to 0 while the data error diverges. For $t \to \infty$ it is the opposite way. Therefore, the reconstruction error tends

to infinity as $t \to 0$ and $t \to \infty$. The important question is how to choose an optimal regularization parameter t_{opt} that minimizes that error.
Some regularization procedures are now presented: The first method is the so-called Landweber Method. It is based on transforming the normal equation from (1.4) into a fixed point equation and then solving it iteratively. The regularized solution is then obtained as the m^*-th iterated of

$$f_{m+1} = f_m - \omega A^*(Af_m - g^\delta), \qquad f_0 = 0,$$

where m^* is the stopping index of the iteration. The relaxation parameter $\omega > 0$ must be chosen to be smaller than $\frac{2}{\|A\|^2}$ so that the iteration converges according to Banach's theorem. Thus $\gamma = \frac{1}{m^*}$ is the regularization parameter. It works similarly to the iterative Tikhonov regularization, see [11], [42] or [62]. Here, however, instead of (1.3), the modified functional

$$\mathcal{J}_\beta(f) = \frac{1}{2}\|Af - g^\delta\|_Y^2 + \frac{\beta}{2}\|f\|_X^2$$

is considered. The difference is that not only the defect $\|Af - g^\delta\|_Y$ is minimized but also the norm of f. Depending on how large β is, the first or the second summand is weighted more. The larger β is chosen, the smoother the solution becomes. However, for $\beta \to \infty$ we naturally move further and further away from the actual physical solution. It holds for any $f \neq 0$ that $\langle \mathcal{J}_\beta''(f), f\rangle_X > 0$. Hence, $\mathcal{J}_\beta$ is positive definite for any $\beta > 0$ and the minimum is guaranteed and unique. The minimizer f^β of $\mathcal{J}_\beta$ can be characterized as the solution of the shifted normal equation

$$(A^*A + \beta \mathbb{1})f^\beta = A^*g^\delta. \tag{1.11}$$

It can also be given explicitly for this equation, namely

$$f^\beta = \sum_{j=1}^{\infty} \frac{\sigma_j}{\sigma_j^2 + \beta}\langle g^\delta, u_j\rangle_Y v_j.$$

This can be verified easily by using (1.6) and (1.7) and plugging f^β into (1.11). Here, one can see how small singular values are shifted away from 0 which means that the solution gets smoother for increasing β. In case the singular values are not easy to compute, one can solve (1.11) iteratively as in Landweber's method. We obtain the iteration rule

$$f_{m+1} = f_m - \omega\left(A^*(Af_m - g^\delta) + \beta f_m\right), \qquad f_0 = 0.$$

Let us now return to the question of regularization: How long do we have to iterate until we have found an optimal solution? In Figure 1.1 we have seen that it makes

no sense to calculate infinitely many sequence elements. There is a point from which the defect function increases again. Therefore, we follow the discrepancy principle of Morozov, which says that we choose the regularization parameters $\gamma = \gamma(\delta) = \frac{1}{m^*}$ for some stopping index m^* such that

$$\|Af_{m^*}^\delta - g^\delta\|_Y \approx \delta.$$

Definition 1.9. *(Morozov's discrepancy principle) Let $\tau > 1$ be fixed. Choose $m^* = m^*(\delta, g^\delta)$ as the well-defined number such that for all $m = 1, \dots, m^* - 1$,*

$$\frac{1}{2}\|Af_{m^*}^\delta - g^\delta\|_Y^2 \leq \tau\delta < \frac{1}{2}\|Af_m^\delta - g^\delta\|_Y^2.$$

In [33] and [34] it is proven that for both methods the stopping index $m^*(\delta, g^\delta) \in \mathcal{O}(\delta^{-2})$. For better results, one has to require some smoothness condition on $A^\dagger g$. We define

$$X_\nu = \mathcal{R}(A^*A)^{\frac{\nu}{2}} = \{(A^*A)^{\frac{\nu}{2}} z \mid z \in \mathcal{N}(A)^\perp\},\ \nu \geq 0.$$

Therefore, $X_\nu \subset X_\mu$ for $\nu > \mu$. If $g \in \mathcal{R}(A)$ and $A^\dagger g \in X_\nu$ with $\nu > 0$ then the stopping index $m^*(\delta, g^\delta)$ obtained by Morozov's discrepancy principle satisfies

$$m^*(\delta, g^\delta) = \mathcal{O}(\delta^{-\frac{2}{2\nu+1}}).$$

But still, especially for small $\delta > 0$ the two methods may converge very slowly.
A faster way to achieve convergence of Landweber's or Tikhonov's iteration is the Nesterov acceleration that was first introduced by Y. Nesterov in his seminal paper [65]. The basic idea is to add a correction term to the iterative sequence generated by the iterative algorithm. This correction term is designed to compensate for the error in the previous iteration and is computed using a linear combination of the previous two iterations.
Specifically, let f_k be the iterative sequence generated by the iterative algorithm, and let z_k be the accelerated sequence generated by a linear combination of the last two iterates. Then the Nesterov acceleration can be defined by the following update rule:

$$\begin{aligned} z_{m+1} &= f_m + \lambda_m^k (f_m - f_{m-1}) \\ f_{m+1} &= z_{m+1} - \omega A^*(Az_{m+1} - g^\delta) \end{aligned}$$

where

$$\lambda_m^k = \frac{m-1}{m+k-1}$$

is a weight parameter that depends on the iteration number m. The value of k is chosen in such a way that the accelerated sequence converges faster than the original one. For example, [9] and [45] suggest that $k = 3$ is an appropriate choice.

1.2 Riemannian geometry

This section is about the comprehension of curves and tensors on Riemannian manifolds. Riemannian manifolds are manifolds with a corresponding metric. Their benefit becomes illustrative when we look at distances on Earth, for example. For two points on the surface, we can define a distance that is different from the Euclidean distance. Instead of determining the length of the Euclidean direct line running through the Earth's interior, in practice, we measure the length of the shortest curve on the Earth's surface that connects the two points. We proceed similarly with diffractive media: We want to define distances between two points by the course of the rays in a medium that passes through both points.
We therefore need an alternative concept of distance. This works with Riemannian manifolds. After we have defined these and understood operators and mappings on such objects, we will explain how the course of the rays can be calculated given a metric.
For this chapter, we mainly refer to [36], [74], [87], [94] and [103].

1.2.1 Tensor analysis and Riemannian manifolds

A N-dimensional differentiable manifold or N-manifold is a set M equipped with a family $(M_i)_{i\in I}$ of subsets such that the following conditions are satisfied:

- $M = \bigcup_{i\in I} M_i$,
- for each $i \in I$ there is an injective mapping (a so-called *chart*) $\varphi_i \colon M_i \to \mathbb{R}^N$ such that $\varphi_i(M_i) \subset \mathbb{R}^N$ is open,
- for $M_i \cap M_j \neq \emptyset$ is $\varphi_i(M_i \cap M_j) \subset \mathbb{R}^N$ open, and the composition

$$\varphi_j \circ \varphi_i^{-1} \colon \varphi_i(M_i \cap M_j) \to \varphi_j(M_i \cap M_j)$$

  is differentiable for all $i, j = 1, \ldots, N$.

We call the mappings φ_i^{-1} parameterizations. The definition of a N-dimensional differentiable manifold is illustrated in Figure 1.2.
Next, we want to consider vector fields on such a manifold. In the N-dimensional real space, one can define them easily by mapping each point p to a N-dimensional vector $v(p)$. Such a vector points in a direction and has a specific length. In that way, we can describe, for example, velocity fields of fluids. The reason for generalizing this definition is that we want to describe refractional media.
For a better understanding, we first assume that the manifold M is a two-dimensional spherical surface embedded in three-dimensional space. At every point p on this spherical surface, we can imagine a flat two-dimensional plane that touches the sphere at p. We call this plane tangent space. It contains all the velocity vectors that can be used to walk through p on the surface. Let $\gamma \colon \mathbb{R} \to \mathbb{R}^3$ be a differentiable curve on the attached surface with $\gamma(0) = p$. Then,

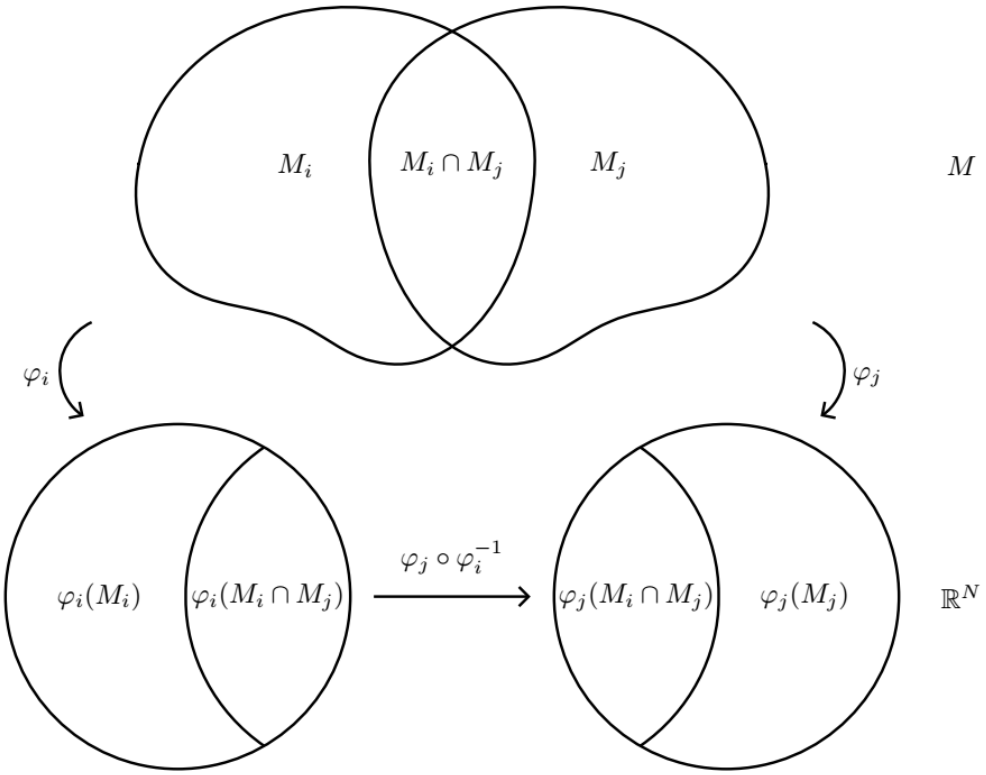

Figure 1.2: Illustration of a manifold

$$\frac{\mathrm{d}}{\mathrm{d}\tau}\gamma(\tau)\Big|_{\tau=0} = \lim_{\tau\to 0}\frac{\gamma(\tau)-\gamma(0)}{\tau}$$

is a tangent vector in p. But on a manifold, the difference $\gamma(\tau)-\gamma(0)$ is not defined at all. We can only define the tangent space here by embedding the vectors $\gamma(\tau)$ and $\gamma(0)$ into $\mathbb{R}^3$ and also obtain the difference as a 3-dimensional vector. We now want to understand how the tangent space can also be defined without a surrounding space. For this, we need the notion of a directional derivative. Let $\phi\colon M \to \mathbb{R}$ be a scalar function. The directional derivative is used to indicate with which rate ϕ in $p \in M$ changes in direction ξ. To do this, we choose a curve $\gamma\colon \mathbb{R} \to M$ on the surface such that $\gamma(0) = p$ and $\dot{\gamma}(0) = \xi$. Then, the directional derivative is given by

$$\frac{\mathrm{d}}{\mathrm{d}\tau}\phi(\gamma(\tau))\Big|_{\tau=0}.$$

Thus, we have a one-to-one mapping of the directional derivative to the tangential vector ξ. Since $\xi = \frac{\mathrm{d}}{\mathrm{d}\tau}\gamma(\tau)\Big|_{\tau=0}$ can not be defined without the embedding, we define for arbitrary N-manifolds M the tangential vector $\xi(p)$ as an operator as follows

$$\xi(p)\phi = \frac{\mathrm{d}}{\mathrm{d}\tau}\phi(\gamma(\tau))\Big|_{\tau=0}, \tag{1.12}$$

which thus assigns a real number to a scalar function in p. Next, assuming that one chart φ covers M completely, we use (1.12) to compute

$$\begin{aligned}\xi(p)\phi &= \frac{\mathrm{d}}{\mathrm{d}\tau}(\phi \circ \varphi^{-1} \circ \varphi \circ \gamma)(\tau)\Big|_{\tau=0} \\ &= \sum_{i=1}^{N} \frac{\partial(\phi \circ \varphi^{-1})}{\partial x_i}\Big|_{\varphi(p)} \cdot \frac{\mathrm{d}}{\mathrm{d}\tau}(\varphi \circ \gamma)_i(\tau)\Big|_{\tau=0}. \end{aligned} \tag{1.13}$$

Setting

$$\xi^i(p) \coloneqq \frac{\mathrm{d}}{\mathrm{d}\tau}(\varphi \circ \gamma)_i(\tau)\Big|_{\tau=0}$$

and defining

$$\frac{\partial}{\partial x_i}\Big|_p \phi \coloneqq \frac{\partial(\phi \circ \varphi^{-1})}{\partial x_i}\Big|_{\varphi}(\varphi(p))$$

we obtain a shorter representation for $\xi(p)$:

$$\xi(p) = \sum_{i=1}^{N} \xi^i \frac{\partial}{\partial x_i}\Big|_p.$$

The operators

$$\frac{\partial}{\partial x_1}\Big|_p, \ldots, \frac{\partial}{\partial x_N}\Big|_p$$

form a basis of the tangent space T_pM, each of them pointing in the direction of one changing coordinate while all others are constant. Consequently, vector fields ξ on M can be expressed by

$$\xi = \sum_{i=1}^{N} \xi^i \frac{\partial}{\partial x_i}. \tag{1.14}$$

Note that we used subindices for the basis vectors and superindices for the components to avoid future confusion. While the definition of the tangent vectors is independent of φ, the representation in the basis, however, obviously depends on the respective coordinate system. Let us now look at how the representation behaves after a change of coordinates. Let ψ be another chart with coordinates $\hat{x}_i(p)$. Then the components $\xi^i(p)$ can be written as

$$\begin{aligned}
\xi^i(p) &= \frac{\mathrm{d}}{\mathrm{d}\tau}(\varphi \circ \gamma)_i(\tau)\Big|_{\tau=0} \\
&= \frac{\mathrm{d}}{\mathrm{d}\tau}(\varphi \circ \psi^{-1} \circ \psi \circ \gamma)_i(\tau)\Big|_{\tau=0} \\
&= \sum_{i=1}^{N} \frac{(\varphi \circ \psi^{-1})_i}{\partial \hat{x}_j}\Big|_{\psi(p)} \frac{\mathrm{d}}{\mathrm{d}\tau}(\psi \circ \gamma)_j(\tau)\Big|_{\tau=0} \\
&= \sum_{j=1}^{N} \frac{\partial x_i}{\partial \hat{x}_j}\Big|_{\psi(p)} \hat{\xi}^j(p) \qquad (1.15)
\end{aligned}$$

where $\hat{\xi}^j(p)$ are the components in the new coordinates. Hence, we also have

$$\hat{\xi}^j(p) = \sum_{i=1}^{N} \frac{\partial \hat{x}_j}{\partial x_i} \xi^i(p). \qquad (1.16)$$

We call such a transformation behavior like that of the components of the tangential vectors in (1.16) *contravariant* and in the following, we continue to characterize it with the superindex. The reason for this notation is that there are also quantities which are opposite. We now want to define the cotangent space $T_p'M$, i.e., the dual space to the tangent space T_pM. This space contains all linear mappings from T_pM into the real numbers. To do this, let ϕ again be a scalar function on M defined in a neighborhood of p, and let $\xi(p)$ be a tangent vector in p. Then the cotangent vector $\mathrm{d}\phi(p)$ is given by

$$\mathrm{d}\phi(p)\xi(p) \coloneqq \xi(p)\phi.$$

In the definition of the tangent vector, the function ϕ is arbitrary and the uniqueness of the directional derivative depends on the curve γ. Here, γ and, therefore, $\xi(p)$ are arbitrary and the function ϕ defines the cotangent vector. In order to find a representation of $\mathrm{d}\phi(p)$ in a proper basis, we compute

$$\mathrm{d}\phi(p)\xi(p) = \xi(p)\phi = \left(\sum_{i=1}^{N} \xi^i(p) \frac{\partial}{\partial x_i}\Big|_p\right)\phi.$$

Defining the basis $\mathrm{d}x^1, \ldots, \mathrm{d}x^N$ of the cotangent space by

$$\mathrm{d}x^i|_p \xi(p) \coloneqq \xi^i(p),$$

we conclude that

$$\mathrm{d}x^j|_p \left(\frac{\partial}{\partial x_i}\Big|_p\right) = \delta_i^j. \qquad (1.17)$$

Using (1.13), we can write

$$\mathrm{d}\phi(p) = \sum_{i=1}^{N} \frac{\partial(\phi \circ \varphi^{-1})}{\partial x_i}\Big|_{\varphi(p)} \mathrm{d}x^i|_p.$$

Note that for any cotangential vector

$$\omega(p) = \sum_{i=1}^{N} \omega_i \mathrm{d}x^i|_p \tag{1.18}$$

and fixed p we find a scalar function ϕ such that

$$\omega(p) = \mathrm{d}\phi(p)$$

by demanding that

$$\omega_i(p) = \frac{\partial(\phi \circ \varphi^{-1})}{\partial x_i}\Big|_{\psi(p)}.$$

In contrast to (1.14), we use superindices for the cotangent basis vectors and subindices for the components. Since the right-hand side of (1.17) is constant and does not depend on the choice of variables, the components $\omega_i(p)$ must transform in the opposite direction, i.e., using the same chart and local variables as in (1.15), we get the new components

$$\hat{\omega}_i(p) = \sum_{j=1}^{N} \frac{\partial x_i}{\partial \hat{x}_j} \omega_j(p). \tag{1.19}$$

We call such behavior of transforming components as in (1.19) *covariant*.
Let us introduce Einstein's convention which means that any unrepeated suffix in a term is understood to take all the values $1, 2, \ldots, N$ whereas in the repeated case the suffix leads to a summation over $1, 2, \ldots, N$. Hence, (1.19) can be expressed by

$$\hat{\omega}_i(p) = \frac{\partial x_i}{\partial \hat{x}_j} \omega_j(p).$$

The understanding of how tangent and cotangent vectors behave, leads to the definition of tensors, i.e., multilinear mappings, acting on tangent and cotangent spaces. A *s-fold covariant and r-fold contravariant tensor* or *(r, s)-tensor* for short, defined at point p of a differentiable manifold M is a multilinear mapping

$$\mathcal{T}_p\colon \underbrace{(T_p'M)\times\cdots\times(T_p'M)}_{r\text{ times}}\times\underbrace{(T_pM)\times\cdots\times(T_pM)}_{s\text{ times}}\to\mathbb{R}.$$

The space of all these (r,s)-tensors has the canonical basis

$$\left(\frac{\partial}{\partial x_{i_1}}\Big|_p\otimes\cdots\otimes\frac{\partial}{\partial x_{i_r}}\Big|_p\otimes\mathrm{d}x^{j_1}|_p\otimes\cdots\otimes\mathrm{d}x^{j_s}|_p\right)_{i_1,\ldots,i_r,j_1,\ldots,j_s=1,\ldots,N}$$

such that

$$\left(\frac{\partial}{\partial x_{i_1}}\Big|_p\otimes\cdots\otimes\mathrm{d}x^{j_s}\right)\left(\mathrm{d}x^{k_1},\ldots,\mathrm{d}x^{k_r},\frac{\partial}{\partial x_{l_1}},\ldots,\frac{\partial}{\partial x_{l_s}}\right)\coloneqq\delta_{i_1}^{k_1}\cdot\ldots\cdot\delta_{i_r}^{k_r}\cdot\delta_{l_1}^{j_1}\cdot\ldots\cdot\delta_{l_s}^{j_s}.$$

This means that

$$\mathcal{T}_p=\mathcal{T}_{j_1,\ldots,j_s}^{i_1,\ldots,i_r}\cdot\left(\frac{\partial}{\partial x_{i_1}}\otimes\cdots\otimes\frac{\partial}{\partial x_{i_r}}\otimes\mathrm{d}x^{j_1}\otimes\cdots\otimes\mathrm{d}x^{j_s}\right)$$

has the coefficients

$$\mathcal{T}_{j_1,\ldots,j_s}^{i_1,\ldots,i_r}=\mathcal{T}_p\left(\mathrm{d}x^{i_1},\ldots,\mathrm{d}x^{i_r},\frac{\partial}{\partial x_{j_1}},\ldots,\frac{\partial}{\partial x_{j_s}}\right).$$

Due to (1.16) and (1.19), these coefficients transform as follows after changing variables:

$$\hat{\mathcal{T}}_{j_1,\ldots,j_s}^{i_1,\ldots,i_r}=\frac{\partial x_{k_1}}{\partial\hat{x}_{i_1}}\cdots\frac{\partial x_{k_r}}{\partial\hat{x}_{i_r}}\frac{\partial\hat{x}_{j_1}}{\partial x_{l_1}}\cdots\frac{\partial\hat{x}_{j_s}}{\partial x_{l_s}}\mathcal{T}_{l_1,\ldots,l_s}^{k_1,\ldots,k_r}.$$

This transformation leads to the fact that for a $(0,m)$-tensor $\mathcal{A}$ and a $(m,0)$-tensor $\mathcal{B}$ the expression $\mathcal{A}_{i_1,\ldots,i_m}\mathcal{B}^{i_1,\ldots,i_m}$ is invariant, i.e., it does not depend on the choice of variables. We verify that by the following computation

$$\begin{aligned}\hat{\mathcal{A}}_{i_1,\ldots,i_m}\hat{\mathcal{B}}^{i_1,\ldots,i_m}&=\left(\mathcal{A}_{p_1,\ldots,p_m}\frac{\partial x_{p_1}}{\partial\hat{x}_{i_1}}\cdots\frac{\partial x_{p_m}}{\partial\hat{x}_{i_m}}\right)\left(\mathcal{B}^{q_1,\ldots,q_m}\frac{\partial\hat{x}_{i_1}}{\partial x_{q_1}}\cdots\frac{\partial\hat{x}_{i_m}}{\partial x_{q_m}}\right)\\&=\mathcal{A}_{p_1,\ldots,i_m}\mathcal{B}^{q_1,\ldots,q_m}\delta_{q_1}^{p_1}\cdots\delta_{q_m}^{p_m}\\&=\mathcal{A}_{p_1,\ldots,i_m}\mathcal{B}^{p_1,\ldots,p_m}.\end{aligned}$$

To shorten longer expressions somewhat, we also sometimes use the notation of the inner product, i.e.,

$$\langle \mathcal{A}, \mathcal{B} \rangle \coloneqq \mathcal{A}_{i_1,\dots,i_m} \mathcal{B}^{i_1,\dots,i_m}.$$

It will always be clear from the context whether the pairing meant by $\langle \cdot, \cdot \rangle$ is this pairing or a scalar product.

Next, we summarize the tangent and cotangent spaces for all $p \in M$ in the following way:

$$\begin{aligned} TM &= \{(p, \xi) | p \in M,\ \xi \in T_p M\}, \\ T'M &= \{(p, \xi) | p \in M,\ \xi \in T'_p M\}. \end{aligned}$$

Based on this one can define $\tau_M = (TM, \pi, M)$ as the tangent bundle and $\tau'_M = (T'M, \pi', M)$ as the cotangent bundle on M, where

$$\begin{aligned} \pi &\colon TM \to M, \\ \pi' &\colon T'M \to M \end{aligned}$$

are corresponding projections to M. For integers $r, s \geq 0$ we set $\tau^r_s M$ as the product

$$\tau^r_s M = \tau'_M \otimes \cdots \otimes \tau'_M \otimes \tau_M \otimes \cdots \otimes \tau_M,$$

where the factor τ_M is repeated r times and τ'_M is repeated s times. On this occasion, we set the space of all symmetric covariant tensors of rank m as $S^m \tau'_M$. The symmetry here means that the tensor is invariant under the interchange of two indices and thus invariant under all arbitrary permutations. We will use this set in the next chapter.

In the following, we will give an example of a $(0, 2)$-tensor, the so-called *metric tensor*, which will give us a tool for computing distances on the manifold. Let $\{x_1, \dots, x_N\}$ be Cartesian coordinate system and $\{\hat{x}_1, \dots, \hat{x}_N\}$ some local coordinate system at a point p on a manifold M. Writing $(e_1, \dots, e_N)$ for the canonical orthonormal basis of $T_p M$ embedded into $\mathbb{R}^N$, we get the tangent vectors $\partial_1, \dots, \partial_N$ by

$$\partial_i = \frac{\partial x_k}{\partial \hat{x}_i} e_k.$$

The Euclidean product

$$\langle \partial_i, \partial_j \rangle = \left\langle \frac{\partial x_k}{\partial \hat{x}_i} e_k, \frac{\partial x_l}{\partial \hat{x}_j} e_l \right\rangle = \frac{\partial x_k}{\partial \hat{x}_i} \frac{\partial x_k}{\partial \hat{x}_j} = g_{ij} \tag{1.20}$$

yields the components of the metric $(0,2)$-tensor

$$g_p = \sum_{i,j=1}^{N} g_{ij}(p)\mathrm{d}x^i \otimes \mathrm{d}x^j, \tag{1.21}$$

where g_{ij} has the matrix representation

$$(g_{ij}(p)) = \begin{pmatrix} \left\langle \frac{\partial x}{\partial \hat{x}_1}, \frac{\partial x}{\partial \hat{x}_1} \right\rangle & \cdots & \left\langle \frac{\partial x}{\partial \hat{x}_1}, \frac{\partial x}{\partial \hat{x}_N} \right\rangle \\ \vdots & \ddots & \vdots \\ \left\langle \frac{\partial x}{\partial \hat{x}_N}, \frac{\partial x}{\partial \hat{x}_1} \right\rangle & \cdots & \left\langle \frac{\partial x}{\partial \hat{x}_N}, \frac{\partial x}{\partial \hat{x}_N} \right\rangle \end{pmatrix}.$$

Analogously, for the contravariant basis $\{\partial^k\}$, we compute for each of the $\hat{x}_i(x_1, \ldots, x_N)$ the gradient

$$\hat{x}_i(x_1, \ldots, x_N) = \frac{\partial \hat{x}_i}{\partial x_k} e_k = \partial^i.$$

Hence,

$$\partial^i = \frac{\partial \hat{x}_i}{\partial x_k} e_k = \frac{\partial \hat{x}_i}{\partial x_k} e^k.$$

Thus, we obtain the components g^{ij} of the contravariant metric tensor by

$$\langle \partial^i, \partial^j \rangle = \frac{\partial \hat{x}_i}{\partial x_k} \frac{\partial \hat{x}_j}{\partial x_k} = g^{ij}. \tag{1.22}$$

Using (1.20) and (1.22), we observe that

$$g_{ij} g^{jk} = \frac{\partial x_m}{\partial \hat{x}_i} \frac{\partial x_m}{\partial \hat{x}_j} \frac{\partial \hat{x}_j}{\partial x_l} \frac{\partial \hat{x}_k}{\partial x_l} = \delta_i^k. \tag{1.23}$$

This equation will be a useful tool for later calculations.

Finally, it is possible to define a Riemannian manifold:

Let M be a N-dimensional differentiable manifold. A *Riemannian metric* g on M is a mapping $p \mapsto g_p$ where each g_p is an element of $C_0^\infty(S^2\tau'_M)$, i.e., each

$$g_p \colon T_pM \times T_pM \to \mathbb{R}$$

fulfills the following three conditions:

- $g_p(X,Y) = g_p(Y,X)$ for all $X, Y \in T_pM$
- $g_p(X,X) > 0$ for all $X \neq 0$
- the coefficients g_{ij} are differentiable functions for any local representation (i.e., in every chart)

$$g_p = \sum_{i,j=1}^{N} g_{ij}(p) \cdot \mathrm{d}x^i|_p \otimes \mathrm{d}x^j|_p. \tag{1.24}$$

Note that the metric tensor defined in (1.21) satisfies all the conditions of a Riemannian metric since the matrix $(g_{ij}) = \partial_i \otimes \partial_j$ is positive definite. The pair (M, g) is called *Riemannian manifold*.

On a Riemannian manifold, the metric tensor defines for any $p \in M$ a scalar product on T_pM. Therefore, it is possible to calculate the length of a tangent vector and the angle between two elements of (T_pM).

1.2.2 Differential operators on Riemannian manifolds

This subsection is about computing differential operators of a Riemannian manifold (M, g). We refer to [46] and [59]. Let $V = v^i\partial_i$ be a vector field on M. We write the gradient of a scalar function u on M at p as $\nabla u(p) = a^i\partial_i$ for some coefficients a^i. For a given curve $\gamma \colon (-\varepsilon, \varepsilon) \to M$ with $\gamma(0) = p$ and $\dot\gamma(0) = \xi$ we write

$$\mathrm{d}u_p(\xi) = \frac{\mathrm{d}}{\mathrm{d}\tau} u(\gamma(\tau))\Big|_{\tau=0}$$

for the directional derivative of u in direction ξ. Choosing any local chart φ going through p we can define $\tilde u \coloneqq u \circ \varphi^{-1}$ and, by the chain rule, it holds

$$\frac{\partial \tilde u}{\partial x_i} = \frac{\partial(u \circ \varphi^{-1})}{\partial x_i} = \mathrm{d}u\left(\frac{\partial \varphi^{-1}}{\partial x_i}\right) = \mathrm{d}u(\partial_i)$$

and

$$\mathrm{d}u_p(v) = v^i \mathrm{d}u_p(\partial_i) = v^i \frac{\partial \tilde{u}}{\partial x_i} = g_{ij} v^i a^j.$$

It follows with (1.23) that

$$\frac{\partial \tilde{u}}{\partial x_i} = g_{ij} a^j \Rightarrow a^i = g^{ij} \frac{\partial \tilde{u}}{\partial x_j}.$$

and therefore,

$$\nabla u = g^{ij} \frac{\partial \tilde{u}}{\partial x_j} \partial_i. \tag{1.25}$$

The next step is to find a formula for the divergence of a vector field. For this purpose, we use the product rule for a scalar function u and vector field f

$$\mathrm{div}(u \cdot f) = \langle \nabla u, f \rangle + u \cdot \mathrm{div} f$$

and find by Gauss's theorem that

$$\int_{\mathbb{R}^N} u \cdot \mathrm{div} f \mathrm{d}x = - \int_{\mathbb{R}^N} \langle \nabla u, f \rangle \mathrm{d}x$$

for any $u \in C_0^\infty(\mathbb{R}^N)$. This can be transferred to Riemannian manifolds: Considering a manifold M, we have

$$\int_M u \mathrm{div} f \mathrm{d}V = - \int_M g(\nabla u, f) \mathrm{d}V$$

with the volume element $\mathrm{d}V = \sqrt{\mathrm{det} g}\ \mathrm{d}x$. We obtain

$$\begin{aligned} \int_M \tilde{u} \mathrm{div} f \sqrt{\mathrm{det} g}\ \mathrm{d}x &= - \int_M \frac{\partial \tilde{u}}{\partial x_i} f^i \sqrt{\mathrm{det} g}\ \mathrm{d}x \\ &= \int_M \tilde{u} \frac{\partial}{\partial x_i} \left(f^i \sqrt{\mathrm{det} g} \right) \mathrm{d}x. \end{aligned}$$

Since u is chosen arbitrarily, we conclude

$$\mathrm{div} f = \frac{1}{\sqrt{\mathrm{det} g}} \frac{\partial}{\partial x_i} \left(f^i \sqrt{\mathrm{det} g} \right).$$

Knowing how to compute the gradient and the divergence yields the so-called *Laplace-Beltrami operator* applied on a scalar function u:

$$\Delta u = \mathrm{div}\nabla u = \mathrm{div}\left(g^{ij}\frac{\partial \tilde{u}}{\partial x_j}\partial_i\right) = \frac{1}{\sqrt{\det g}}\frac{\partial}{\partial x_i}\left(g^{ij}\sqrt{\det g}\frac{\partial u}{\partial x_j}\right) \tag{1.26}$$

which coincides with the well-known Laplacian for g in the Euclidean case.

1.2.3 Covariant derivative and geodesic equation

In the previous subsection, we discussed how to compute tangent vectors via directional derivatives on a Riemannian manifold. We want to extend this theory to calculate directional derivatives of vector fields. Using this we will be able to find a condition for curves on such a manifold to have a constant velocity.
Let Y be a differentiable tangential vector field defined on an N-dimensional Riemannian manifold (M, g) and let $\xi \in T_pM$ for fixed p. We define the *directional derivative* $D_\xi Y|_p$ of Y in direction ξ by

$$D_\xi Y|_p \coloneqq \frac{\mathrm{d}}{\mathrm{d}\tau} Y(\gamma(\tau))\Big|_{\tau=0} \tag{1.27}$$

where $\gamma\colon (-\epsilon, \epsilon) \to M$ is a curve with tangent vector ξ in $\gamma(0) = p$. As discussed before, the vector $D_\xi Y|_p$ is not necessarily in T_pM. That is why we consider the *covariant derivative* $\nabla_\xi Y$ which is the projection of $D_\xi Y|_p$ on T_pM:

$$\nabla_\xi Y \coloneqq \sum_{m=1}^{N} \langle D_\xi Y, e_m\rangle e_m,$$

where $e_1, \ldots, e_N$ form an orthonormal basis of T_pM.
Let $f\colon \mathbb{R}^N \to M$ be a local parameterization of the N-dimensional manifold M. Then, we can identify the basis vectors $\{\partial_i\}$ by

$$\partial_i \hat{=} \frac{\partial f}{\partial x^i}.$$

Therefore, we obtain for $p = f(u)$

$$D_X Y|_p = DY|_u((Df)^{-1}(X))$$

and, in particular,

$$D_{\frac{\partial f}{\partial x_i}}\frac{\partial f}{\partial x_j} = \frac{\partial^2 f}{\partial x_i \partial x_j}. \tag{1.28}$$

Evaluating this projection for two tangent basis vectors $X = \partial_i$ and $Y = \partial_j$, we obtain with (1.20)

$$\begin{aligned}\nabla_{\partial_i}\partial_j &= \langle D_{\partial_i}\partial_j, e_m\rangle e_m \\ &= \langle D_{\partial_i}\partial_j, \frac{\partial \hat{x}_l}{\partial x_m}\partial_l\rangle \frac{\partial \hat{x}_k}{\partial x_m}\partial_k \\ &= g^{kl}\langle D_{\partial_i}\partial_j, \partial_l\rangle \partial_k. \end{aligned} \tag{1.29}$$

We introduce the Christoffel symbols Γ_{ij}^k as the components of the upper derivative with respect to the basis $\partial_1, \ldots, \partial_N$, i.e.,

$$\nabla_{\partial_i}\partial_j = \Gamma_{ij}^k \partial_k. \tag{1.30}$$

Consequently,

$$\Gamma_{ij}^k = g^{kl}\langle D_{\partial_i}\partial_j, \partial_l\rangle.$$

We verify that in local coordinates this can be written as

$$\Gamma_{ij}^k = \frac{1}{2}\sum_{l=1}^{N} g^{kl}\left(\frac{\partial g_{jl}}{\partial x_i} + \frac{\partial g_{li}}{\partial x_j} - \frac{\partial g_{ij}}{\partial x_l}\right) \qquad \text{for } 1 \le i, j, k \le N. \tag{1.31}$$

To prove this, we compute the terms on the right side:

$$\begin{aligned}\frac{\partial g_{jl}}{\partial x_i} &= \langle D_{\partial_i}\partial_j, \partial_l\rangle + \langle \partial_j, D_{\partial_i}\partial_l\rangle \\ \frac{\partial g_{li}}{\partial x_j} &= \langle D_{\partial_j}\partial_l, \partial_i\rangle + \langle \partial_l, D_{\partial_j}\partial_i\rangle \\ -\frac{\partial g_{ij}}{\partial x_l} &= -\langle D_{\partial_l}\partial_i, \partial_j\rangle - \langle \partial_i, D_{\partial_l}\partial_j\rangle. \end{aligned}$$

Using (1.28), we obtain

$$\Gamma_{ij}^k = \frac{1}{2}\sum_{l=1}^{N} g^{kl}\left(\frac{\partial g_{jl}}{\partial x_i} + \frac{\partial g_{li}}{\partial x_j} - \frac{\partial g_{ij}}{\partial x_l}\right) = g^{kl}\langle D_{\partial_i}\partial_j, \partial_l\rangle$$

and thus, by (1.29),

$$\Gamma_{ij}^k \partial_k = g^{kl}\langle D_{\partial_i}\partial_j, \partial_l\rangle \partial_k = \nabla_{\partial_i}\partial_j.$$

Let γ be a curve on M. Then, in the Euclidean setting, $D_{\dot\gamma}\dot\gamma = \ddot\gamma$ is the accelaration vector of γ within a manifold. We want to consider curves on the manifold for which the tangential component of the acceleration vector, and thus the acceleration within the manifold, vanishes. Thus, we demand that

$$D_{\dot\gamma}\dot\gamma = \nabla_{\dot\gamma}\dot\gamma = 0. \tag{1.32}$$

Let $\dot\gamma = \dot\gamma^i \partial_i$ be written in local coordinates. Then,

$$\begin{aligned}\nabla_{\dot\gamma}\dot\gamma &= \nabla_{\dot\gamma^i\partial_i}(\dot\gamma^j\partial_j)\\ &= \dot\gamma^i \nabla_{\partial_i}(\dot\gamma^j\partial_j)\\ &= \dot\gamma^i\left(\frac{\partial\dot\gamma^j}{\partial\gamma^i}\partial_j + \dot\gamma^j\nabla_{\partial_i}\partial_j\right).\end{aligned}$$

Using (1.30) we obtain

$$\begin{aligned}\nabla_{\dot\gamma}\dot\gamma &= \dot\gamma^i\left(\frac{\partial\dot\gamma^j}{\partial\gamma^i}\partial_j + \dot\gamma^j\Gamma^k_{ij}\partial_k\right)\\ &= \dot\gamma^i\left(\frac{\partial\dot\gamma^k}{\partial\gamma^i} + \dot\gamma^j\Gamma^k_{ij}\right)\partial_k\\ &= \left(\ddot\gamma^k + \Gamma^k_{ij}\dot\gamma^i\dot\gamma^j\right)\partial_k.\end{aligned}$$

Extracting the coefficients results in the following system of differential equation, we get the so-called *geodesic equation*:

$$\ddot\gamma^k + \Gamma^k_{ij}(\gamma)\dot\gamma^i\dot\gamma^j = 0, \qquad k = 1,\dots,N.$$

We note that if $\nabla_{\dot\gamma}\dot\gamma = 0$, then

$$\nabla_{\dot\gamma}\langle\dot\gamma,\dot\gamma\rangle = 2\langle\nabla_{\dot\gamma}\dot\gamma,\dot\gamma\rangle = 0$$

and therefore, $\|\dot\gamma\|$ must be constant with respect to the metric g. The reason why we consider geodesic curves is that all shortest connections between two points in the manifold are geodesics. The opposite is not necessarily true. To explain this statement, the next section is about the fact that a curve satisfies the geodesic equation if it is the shortest connection between two points. For this purpose, we need to introduce the Lagrange formalism.

1.2.4 Lagrange formalism and geodesic equation

This section aims to derive a condition for a curve on a Riemannian manifold being the shortest connection between two points. The derivation is based on [10], [53] and [102]. First, we need an expression for the length of the curve.
Let γ be a curve on a Riemannian manifold (M, g) that is parametrized by the arc length. Let $A = \gamma(s_0)$ be the start point and $B = \gamma(s_1)$ be the end point. Then, the time of propagation is given by

$$T[\gamma] = \int_\gamma \mathrm{d}s = \int_A^B \mathrm{d}s = \int_{s_0}^{s_1} \left\| \frac{\mathrm{d}\gamma}{\mathrm{d}s} \right\| \mathrm{d}s \tag{1.33}$$

with the arc measure $\mathrm{d}s$. Using (1.24), we get

$$\begin{aligned} T[\gamma] &= \int_{s_0}^{s_1} \left\| \frac{\mathrm{d}\gamma}{\mathrm{d}s} \right\| \mathrm{d}s \\ &= \int_{s_0}^{s_1} \sqrt{g_{\gamma(s)} \left(\frac{\mathrm{d}\gamma}{\mathrm{d}s}, \frac{\mathrm{d}\gamma}{\mathrm{d}s} \right)} \mathrm{d}s \\ &= \int_{s_0}^{s_1} \sqrt{g_{ij}(\gamma(s)) \mathrm{d}x^i|_{\gamma(s)} \left(\frac{\mathrm{d}\gamma}{\mathrm{d}s} \right) \mathrm{d}x^j|_{\gamma(s)} \left(\frac{\mathrm{d}\gamma}{\mathrm{d}s} \right)} \mathrm{d}s \\ &= \int_{s_0}^{s_1} \sqrt{g_{ij}(\gamma(s)) \frac{\mathrm{d}\gamma^i}{\mathrm{d}s} \frac{\mathrm{d}\gamma^j}{\mathrm{d}s}} \mathrm{d}s. \end{aligned} \tag{1.34}$$

For simplicity, we define

$$L\left(\gamma(s), \frac{\mathrm{d}\gamma}{\mathrm{d}s}\right) \coloneqq \sqrt{g_{ij}(\gamma(s)) \frac{\mathrm{d}\gamma^i}{\mathrm{d}s} \frac{\mathrm{d}\gamma^j}{\mathrm{d}s}} = 1.$$

The necessary condition for the existence of a local extremum of the functional T for a curve γ can be interpreted as follows:

- The differential of the functional T at the point γ is zero.
- The functional T is stationary at the point γ, that is, it does not change for a function that lies in the infinitesimal neighborhood of the curve γ and coincides with γ at the points A and B.

As a symbol for the type of variation described above, we use δ and can write the differential of L as

$$\delta L\left(\gamma(s), \frac{\mathrm{d}\gamma}{\mathrm{d}s}\right) = \sum_{l=1}^{N} \frac{\partial L}{\partial \gamma^l} \delta\gamma^l + \sum_{l=1}^{N} \frac{\partial L}{\partial \left(\frac{\mathrm{d}\gamma^l}{\mathrm{d}s}\right)} \delta\left(\frac{\mathrm{d}\gamma^l}{\mathrm{d}s}\right).$$

We calculate the variation δT:

$$\begin{aligned}
\delta T[\gamma] &= \delta T\left[\gamma^1(s),\dots,\gamma^N(s),\frac{\mathrm{d}\gamma^1}{\mathrm{d}s}(s),\dots,\frac{\mathrm{d}\gamma^N}{\mathrm{d}s}(s)\right] \\
&= \int_{s_0}^{s_1}\left(\sum_{l=1}^{N}\frac{\partial L}{\partial\gamma^l}\delta\gamma^l+\sum_{l=1}^{N}\frac{\partial L}{\partial\left(\frac{\mathrm{d}\gamma^l}{\mathrm{d}s}\right)}\delta\left(\frac{\mathrm{d}\gamma^l}{\mathrm{d}s}\right)\right)\mathrm{d}s \\
&= \sum_{l=1}^{N}\frac{\partial L}{\partial\left(\frac{\mathrm{d}\gamma^l}{\mathrm{d}s}\right)}\delta\gamma^l\Bigg|_{s_0}^{s_1}+\int_{s_0}^{s_1}\left(\sum_{l=1}^{N}\frac{\partial L}{\partial\gamma^l}\delta\gamma^l-\sum_{l=1}^{N}\frac{\mathrm{d}}{\mathrm{d}s}\frac{\partial L}{\partial\left(\frac{\mathrm{d}\gamma^l}{\mathrm{d}s}\right)}\delta\gamma^l\right)\mathrm{d}s.
\end{aligned}$$

The fact that $\delta\gamma(s_0)=\delta\gamma(s_1)=0$ yields the condition

$$\int_{s_0}^{s_1}\left(\sum_{l=1}^{N}\left(\frac{\partial L}{\partial\gamma^l}-\frac{\mathrm{d}}{\mathrm{d}s}\frac{\partial L}{\partial\left(\frac{\mathrm{d}\gamma^l}{\mathrm{d}s}\right)}\right)\right)\delta\gamma^l\mathrm{d}s=0.$$

Since the variations $\delta\gamma^l$ for $l=1,\dots,N$ are arbitrary we obtain the Euler-Lagrange equations

$$\frac{\partial L}{\partial\gamma^l}-\frac{\mathrm{d}}{\mathrm{d}s}\frac{\partial L}{\partial\left(\frac{\mathrm{d}\gamma^l}{\mathrm{d}s}\right)}=0,\qquad l=1,\dots,N. \tag{1.35}$$

To obtain an explicit equation for γ we compute

$$\begin{aligned}
\frac{\partial L}{\partial\left(\frac{\mathrm{d}\gamma^l}{\mathrm{d}s}\right)} &= \frac{1}{2L}\left(g_{ij}\frac{\partial\left(\frac{\mathrm{d}\gamma^i}{\mathrm{d}s}\right)}{\partial\left(\frac{\mathrm{d}\gamma^l}{\mathrm{d}s}\right)}\left(\frac{\mathrm{d}\gamma^j}{\mathrm{d}s}\right)+g_{ij}\left(\frac{\mathrm{d}\gamma^i}{\mathrm{d}s}\right)\frac{\partial\left(\frac{\mathrm{d}\gamma^j}{\mathrm{d}s}\right)}{\partial\left(\frac{\mathrm{d}\gamma^l}{\mathrm{d}s}\right)}\right) \\
&= \frac{1}{2L}\left(g_{ij}\delta^i_l\left(\frac{\mathrm{d}\gamma^j}{\mathrm{d}s}\right)+g_{ij}\left(\frac{\mathrm{d}\gamma^i}{\mathrm{d}s}\right)\delta^j_l\right) \\
&= \frac{1}{2L}\left(g_{lj}\left(\frac{\mathrm{d}\gamma^j}{\mathrm{d}s}\right)+g_{il}\left(\frac{\mathrm{d}\gamma^i}{\mathrm{d}s}\right)\right) \\
&= \frac{1}{L}g_{lj}\left(\frac{\mathrm{d}\gamma^j}{\mathrm{d}s}\right),
\end{aligned}$$

where we used the symmetry of g. Therefore,

$$\begin{aligned}\frac{\mathrm{d}}{\mathrm{d}s}\left(\frac{\partial L}{\partial\left(\frac{\mathrm{d}\gamma^l}{\mathrm{d}s}\right)}\right) &= -\frac{1}{L^2}\frac{\mathrm{d}L}{\mathrm{d}s}g_{lj}\left(\frac{\mathrm{d}\gamma^j}{\mathrm{d}s}\right)+\frac{1}{L}\frac{\mathrm{d}g_{lj}}{\mathrm{d}s}\left(\frac{\mathrm{d}\gamma^j}{\mathrm{d}s}\right)+\frac{1}{L}g_{lj}\left(\frac{\mathrm{d}^2\gamma^j}{\mathrm{d}s^2}\right)\\ &= -\frac{1}{L^2}\frac{\mathrm{d}L}{\mathrm{d}s}g_{lj}\left(\frac{\mathrm{d}\gamma^j}{\mathrm{d}s}\right)+\frac{1}{L}\frac{\partial g_{lj}}{\partial\gamma^i}\dot{\gamma}^i\left(\frac{\mathrm{d}\gamma^j}{\mathrm{d}s}\right)+\frac{1}{L}g_{lj}\left(\frac{\mathrm{d}^2\gamma^j}{\mathrm{d}s^2}\right)\\ &= \frac{\partial g_{lj}}{\partial\gamma^i}\left(\frac{\mathrm{d}\gamma^i}{\mathrm{d}s}\right)\left(\frac{\mathrm{d}\gamma^j}{\mathrm{d}s}\right)+g_{lj}\left(\frac{\mathrm{d}^2\gamma^j}{\mathrm{d}s^2}\right)\end{aligned}$$

where, in the last step, we applied that $L \equiv 1$. Computing the derivatives of L with respect to γ^l, we get

$$\frac{\partial L}{\partial\gamma^l} = \frac{1}{2L}\frac{\partial g_{ij}}{\partial\gamma^l}\frac{\mathrm{d}\gamma^i}{\mathrm{d}s}\left(\frac{\mathrm{d}\gamma^j}{\mathrm{d}s}\right) = \frac{1}{2}\frac{\partial g_{ij}}{\partial\gamma^l}\left(\frac{\mathrm{d}\gamma^i}{\mathrm{d}s}\right)\left(\frac{\mathrm{d}\gamma^j}{\mathrm{d}s}\right)$$

and hence, (1.35) becomes

$$\begin{aligned}0 &= \frac{\partial g_{lj}}{\partial\gamma^i}\left(\frac{\mathrm{d}\gamma^i}{\mathrm{d}s}\right)\left(\frac{\mathrm{d}\gamma^j}{\mathrm{d}s}\right)+g_{lj}\left(\frac{\mathrm{d}^2\gamma^j}{\mathrm{d}s^2}\right)-\frac{1}{2}\frac{\partial g_{ij}}{\partial\gamma^l}\left(\frac{\mathrm{d}\gamma^i}{\mathrm{d}s}\right)\left(\frac{\mathrm{d}\gamma^j}{\mathrm{d}s}\right)\\ &= g_{lj}\left(\frac{\mathrm{d}^2\gamma^j}{\mathrm{d}s^2}\right)+\left(\frac{\partial g_{lj}}{\partial\gamma^i}-\frac{1}{2}\frac{\partial g_{ij}}{\partial\gamma^l}\right)\left(\frac{\mathrm{d}\gamma^i}{\mathrm{d}s}\right)\left(\frac{\mathrm{d}\gamma^j}{\mathrm{d}s}\right).\end{aligned} \tag{1.36}$$

By using that

$$\begin{aligned}\frac{\partial g_{lj}}{\partial\gamma^i}\left(\frac{\mathrm{d}\gamma^i}{\mathrm{d}s}\right)\left(\frac{\mathrm{d}\gamma^j}{\mathrm{d}s}\right) &= \frac{1}{2}\left(\frac{\partial g_{lj}}{\partial\gamma^i}+\frac{\partial g_{jl}}{\partial\gamma^i}\right)\left(\frac{\mathrm{d}\gamma^i}{\mathrm{d}s}\right)\left(\frac{\mathrm{d}\gamma^j}{\mathrm{d}s}\right)\\ &= \frac{1}{2}\left(\frac{\partial g_{lj}}{\partial\gamma^i}+\frac{\partial g_{il}}{\partial\gamma^j}\right)\left(\frac{\mathrm{d}\gamma^i}{\mathrm{d}s}\right)\left(\frac{\mathrm{d}\gamma^j}{\mathrm{d}s}\right)\end{aligned}$$

we can rewrite (1.36) as

$$g_{lj}\left(\frac{\mathrm{d}^2\gamma^j}{\mathrm{d}s^2}\right)+\frac{1}{2}\left(\frac{\partial g_{lj}}{\partial\gamma^i}+\frac{\partial g_{il}}{\partial\gamma^j}-\frac{\partial g_{ij}}{\partial\gamma^l}\right)\left(\frac{\mathrm{d}\gamma^i}{\mathrm{d}s}\right)\left(\frac{\mathrm{d}\gamma^j}{\mathrm{d}s}\right)=0.$$

Multiplying both sides with g^{kl}, and using that $g^{kl}g_{lj} = \delta^k_j$, we finally arrive at the geodesic equation

$$\frac{\mathrm{d}^2\gamma^k}{\mathrm{d}s^2}+\Gamma^k_{ij}\frac{\mathrm{d}\gamma^i}{\mathrm{d}s}\frac{\mathrm{d}\gamma^j}{\mathrm{d}s}=0, \tag{1.37}$$

where

$$\Gamma_{ij}^{k} = \frac{1}{2} g^{kl} \left(\frac{\partial g_{lj}}{\partial \gamma^{i}} + \frac{\partial g_{il}}{\partial \gamma^{j}} - \frac{\partial g_{ij}}{\partial \gamma^{l}} \right)$$

are the Christoffel symbols from (1.31). From this, it follows that the shortest connections between two points on a manifold correspond to the curves whose acceleration vanishes along their direction.
Using the two preceding derivations of the geodesic differential equations, several things can be established: First, they are solved by curves with a constant velocity vector field along the curve. Thus, a particle moving along such a curve would not experience any acceleration. Second, the equations are solved by curves which locally give the shortest connection between points on the manifold. To speak globally of a shortest connection, certain assumptions must be made on the metric. This is only the case if the equation has exactly one solution, which in turn is directly linked to the metric g by the Christoffel symbols. In the next section, we will see that the metric underlying our applications satisfies the necessary properties.

2 Inverse problem of dynamic tensor tomography

This chapter deals with the inverse problem of dynamic tensor tomography. First, the direct problem from a physical point of view is modeled. It will be shown that there are two ways to describe this direct problem. In particular, we will address the question which conditions must apply so that there is an unambiguous correlation between the investigated quantity and the measurement data. Once this question is clarified, we formulate the inverse problem as an operator equation. We derive the adjoint operator, which, as seen in Chapter 1, is needed for the inversion of the operator, i.e., the solution of the problem.

2.1 Modeling of the direct problem as a ray transform

In this section, we are concerned with modeling the forward operator, i.e., the direct problem. In general, the beam transformation is to be derived for tensors of arbitrary ranks. In the first part, we give some examples of applications for ray transforms for tensor fields of different ranks. Here, we assume that the rays are sent through a homogeneous medium. This means that the propagation is always along straight lines. Although the applications are very different in their dimension, the formulae look quite similar. In the second section, the phenomena of the absorption of the signals and the temporal change of the examined sizes are included. Then it is a question of extending the model found in the first subsection to inhomogeneous media. For this purpose, the theory of Riemannian manifolds and geodesics from Section 1.2 is used.

2.1.1 Applications of ray transforms for different tensor ranks

First, we begin with the simplest case: by the term "tensor" we also mean, in particular, tensors of 0th degree and 1st degree, i.e., scalar functions and vector fields, respectively. We will explain the former with the application example of single photon emission computed tomography (SPECT). It will be shown that the collected data are given as the output of a line integral. It is useful to already include absorption effects here. This will be reflected in a corresponding factor in the integrand. Subsequently, we extend this model to vector fields. As a classical example of vector tomography, we consider tumor detection. By measuring the flow

velocity of blood inside a human body, tumors can be identified. Again, we will consider absorption phenomena. It will turn out that the integral formula obtained here is very similar to that in the scalar case. Therefore, this model can be extended to tensor fields of any level. Some tools from tensor analysis, which will be explained in Chapter 2, will be used for this purpose.

One application of ray transforms, that is not the classical computerized tomography, is SPECT (c.f.[18] and [37]). SPECT stands for single-photon emission computed tomography and is a medical imaging technique used to create 3D images of internal body structures. The idea is to inject a patient's bloodstream with a tracer which is a biochemical molecule that is labeled with radioactive gamma rays. These rays make the body emit photons that propagate through the body until they can be detected from outside the patient's body. For the detection one uses a rotating camera that is equipped with a parallel hole collimator (see Figure 2.1).

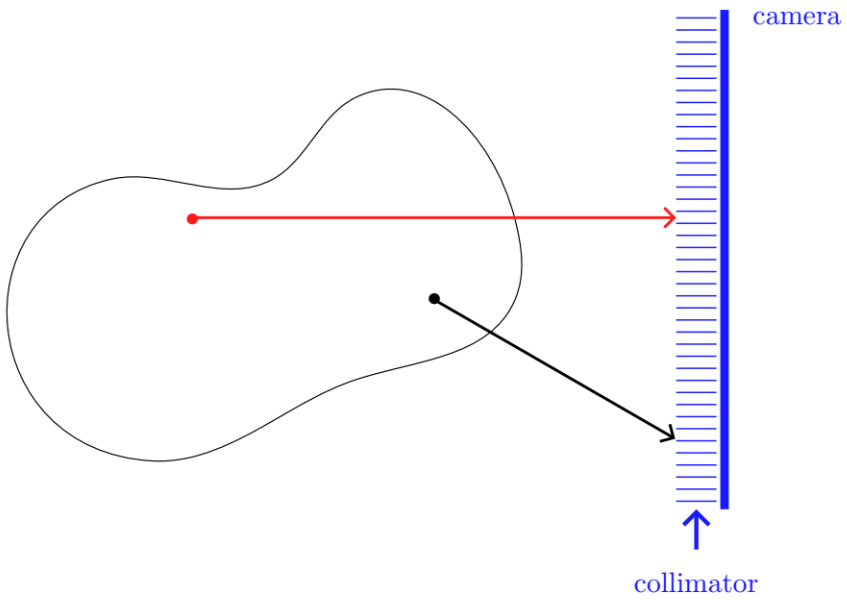

Figure 2.1: Collimator lets photons (red) pass that propagate perpendicular to the camera and filters the others (black).

The reason for this collimator is to only measure photons that come from a specific direction. The smaller the distance between the blue lines the smaller the interval of tolerance gets. In an ideal setting, all the measurements taken for a specific position of the camera are due to emissions from the same direction. Hence, only photons that propagate perpendicular to the camera are recorded. For one detector point, the appropriate emitters in the body are in a straight line. Therefore, the measurement can be seen as the accumulated quantity of photons that move on that line toward the detector. Setting $f(x)$ as the unknown radioactive source at position x and ξ as the directional vector of propagation, the intensity or energy transport at x is given by

$$If(x,\xi) = \int_{-\infty}^{\infty} f(x+\tau\xi)\mathrm{d}\tau.$$

Here, we took into account that, theoretically, every particle in the human body can emit such a photon. To cope with the huge quantity of particles and the very small distances between any two of them, we treat f as a continuous function. The integral limits are due to the assumption that there is no radioactivity outside the body. To be more precise, these limits can be written explicitly as entry time $\tau_-(x,\xi)$ and exit time $\tau_+(x,\xi)$. Hence, the inverse problem consists of recovering the scalar function f from the output of the integral equation

$$If(x,\xi) = \int_{\tau_-(x,\xi)}^{\tau_+(x,\xi)} f(x+\tau\xi)\mathrm{d}\tau. \tag{2.1}$$

In Section 2.2 we will see that in contrast to CT, this application requires further modeling of other physical phenomena.
A similar integral transform as (2.1) can be defined for vector fields as well. As it will be shown in this subsection the so-called Doppler transform computes line integrals of projections of vector fields on the direction of propagation. One application of this transformation is to detect malign tumors in the human body by reconstructing the blood flow in the surroundings. Other applications are, for example, the estimation of gas flows in furnaces (see [93]) or the reconstruction of flow velocities in oceanography (see [81]). In Doppler tomography one uses the Doppler effect describing that a moving fluid or gas in the interior of a medium changes the frequency of an incoming wave. The Doppler transform calculates the total change of frequency along the whole path of propagation inside the medium. This can be seen as follows (see [23]): During a period a signal with velocity c and frequency ν_0 travels the distance $\lambda_0 = \frac{c}{\nu_0}$. If the source of the wave moves with the velocity v_s toward the receiver, the distance between two wavefronts after one period is given by

$$\lambda = \frac{c}{\nu_0} - \frac{v_s}{\nu_0}.$$

Since λ is the wavelength, the receiver measures the frequency

$$\nu = \frac{c}{\lambda} = \frac{\nu_0}{1-\frac{v_s}{c}} > \nu_0. \tag{2.2}$$

Analogously, if the receiver moves in positive x-direction with velocity v_r, it travels the distance $\frac{v_r}{\nu_0}$ during one period. Therefore, the measured frequency is given by

$$\nu = \nu_0\left(1+\frac{v_r}{c}\right) < \nu_0. \tag{2.3}$$

Putting (2.2) and (2.3) together, we obtain

$$\nu = \frac{1 + \frac{v_r}{c}}{1 - \frac{v_s}{c}} \nu_0.$$

Since $v_s \ll c$ we can approximate the denominator by a Taylor expansion and obtain

$$\nu = \nu_0 c \left(1 + \frac{v_r}{c}\right)\left(1 - \frac{v_s}{c}\right) \approx \nu_0 \left(1 + \frac{\Delta v}{c}\right),$$

where $\Delta v = v_s - v_r$. Consequently, there is a shift in the frequency of

$$\Delta\nu = \nu - \nu_0 = \frac{\Delta v}{c}.$$

In our setting, there is a source sending the signal. At some point, the fluid or gas acts like a receiver and changes the frequency once. Afterwards, the signal propagates further to the backside of the object. Hence, the particle of the fluid or gas that caused the first shift can be seen as a new source of a signal with another frequency. Since the source is moving, there is again a Doppler shift. In both processes Δv is the same. That is why the receiver measures a shift of $\frac{2\Delta v}{c}$.
Let us consider the change of velocity in an infinitely small time interval $[\tau, \tau + \Delta\tau]$. We assume the velocity changes linearly in this interval, i.e., Δv is proportional to $\Delta\tau$. Only the length of the projection of $f(x)$ on the integration line has an impact on the frequency. We write

$$\Delta v = \tilde{P}_{\dot\gamma(\tau)}[f(\gamma(\tau))]\Delta\tau,$$

where $\tilde{P}_{\dot\gamma(\tau)}[f(\gamma(\tau))]$ is the acceleration factor given by the projection of f at $\gamma(\tau)$ on the line of propagation with directional vector $\dot\gamma(\tau)$. The tilde above P indicates that we only want information about the length of the projection vector and its sign. Therefore, this term can either increase or decrease the change of velocity. The reason why we keep writing $\dot\gamma(\tau)$ instead of a constant vector ξ is that in the next section, these vectors will not be constant anymore. In the following, we want to compute $\tilde{P}$. Note that the projection vector $P_{\dot\gamma(\tau)}[f(\gamma(\tau))]$ is a multiple of the direction $\dot\gamma(\tau)$, i.e., there is a $\kappa > 0$ such that

$$P_{\dot\gamma(\tau)}[f(\gamma(\tau))] = \kappa\dot\gamma(\tau). \tag{2.4}$$

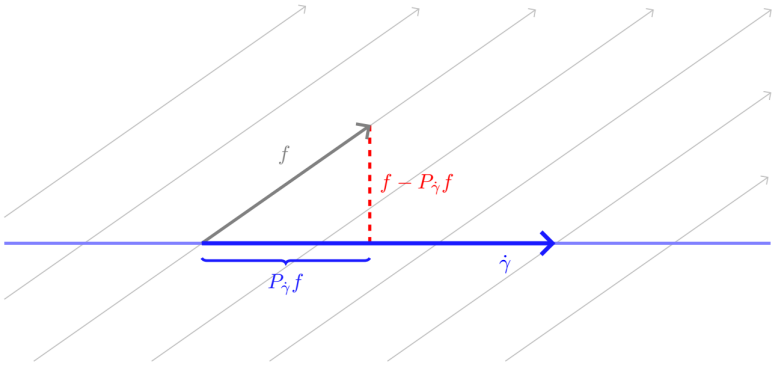

Figure 2.2: Projection $P_{\dot\gamma} f$ (blue) of vector field f (gray) on the line of integration with direction $\dot\gamma$ (blue arrow).

Secondly, the red dashed vector in Figure 2.2 is perpendicular to $\dot\gamma(\tau)$. Therefore, we have

$$\begin{aligned} P_{\dot\gamma(\tau)}[f(\gamma(\tau))] &= \frac{\langle f(\gamma(\tau)), \dot\gamma(\tau)\rangle}{\|\dot\gamma(\tau)\|^2}\dot\gamma(\tau) \\ &= \langle f(\gamma(\tau)), \dot\gamma_0(\tau)\rangle \dot\gamma_0(\tau) \end{aligned}$$

with unit vectors $\dot\gamma_0(\tau)$. Thus,

$$\tilde{P}_{\dot\gamma(\tau)}[f(\gamma(\tau))] = \langle f(\gamma(\tau)), \dot\gamma_0(\tau)\rangle. \tag{2.5}$$

Since $f(\gamma(\tau))$ and $\dot\gamma(\tau)$ are velocity vectors, they have the SI-unit $\frac{m}{s}$, the normalized vector $\dot\gamma_0(\tau)$ has the unit $\frac{1}{s}$, and therefore,

$$\langle f(\gamma(\tau)), \dot\gamma_0(\tau)\rangle$$

describes an acceleration with unit $\frac{m}{s^2}$ and Δv a velocity with unit $\frac{m}{s}$. To compute the total shift, we need to split the whole path of propagation into infinitely many intervals as we used here and end up with an integral as a limit. We obtain

$$\Delta v_{\text{total}} = \int_{\tau_-}^{\tau_+} \langle f(\gamma(\tau)), \dot\gamma_0(\tau)\rangle \mathrm{d}\tau.$$

To make the concept more consistent, we scale the parameterization without loss of generality such that $\dot\gamma(\tau) = \dot\gamma_0(\tau)$. By doing so, the integral only changes by a known constant. In the following, we will only speak of normalized vectors. Therefore, we omit the index 0. This results in the following definition:

Let $f \in C(M, \mathbb{R}^N)$. Then, the Doppler transform $[\mathcal{I}_0 f](x, \xi)$ of a signal that propagates through M with end point $x \in M$ and end direction $\xi \in \mathbb{S}^{N-1}$, is given by

$$[\mathcal{I}_0 f](x, \xi) = \int_{\tau_-(x,\xi)}^{\tau_+(x,\xi)} \langle f(x + \tau\xi), \xi \rangle \mathrm{d}\tau \tag{2.6}$$

$$= \left\langle \int_{\tau_-(x,\xi)}^{\tau_+(x,\xi)} f(x + \tau\xi) \mathrm{d}\tau, \xi \right\rangle \tag{2.7}$$

where $\tau_-(x, \xi)$ and $\tau_+(x, \xi)$ are the time points of entering and exiting the observed object.

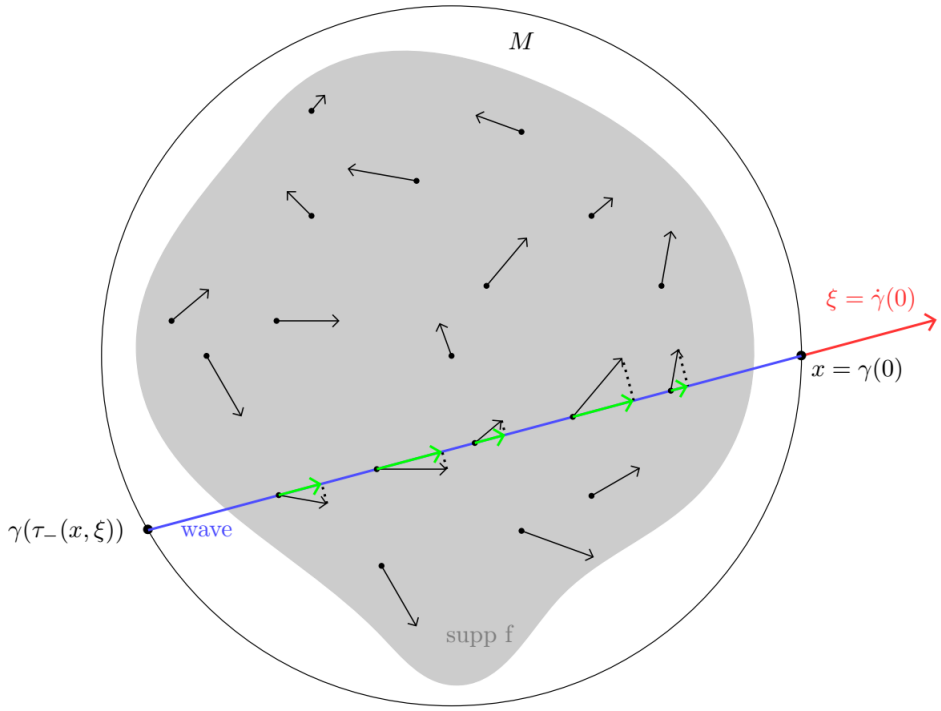

Figure 2.3: 2D-Illustration of data acquisition of vector tomography

We observe that the transform (2.6) is just a special case of the scalar ray transform (2.1), i.e.,

$$[\mathcal{I}_0 f](x, \xi) = I\tilde{f}(x, \xi)$$

where $\tilde{f}(x, \xi) = \langle f(x), \xi \rangle$. There is even a more general case of ray transforms. In fact, (2.6) can be generalized for tensor fields of rank 2 as they occur for example in polarization tomography. Polarization tomography attempts to determine the stress tensor of a material by measuring the polarization, i.e., the direction of transversal oscillation of outgoing light (c.f. [67, 87, 91]). In contrast to the previous application,

the measurements are obtained by integrals along a ray, using the component of the medium that is orthogonal to the ray. Assuming the absence of charges and currents, Maxwell's equations are given by

$$\nabla \times B - \tfrac{1}{c}\tfrac{\partial D}{\partial t} = 0, \quad \mathrm{div} D = 0$$

$$\nabla \times E + \tfrac{1}{c}\tfrac{\partial B}{\partial t} = 0, \quad \mathrm{div} B = 0$$

where B is the magnetic field, E the electric field and $D_j = \epsilon_{ij} E^i$. We assume that the material is quasi-isotropic, i.e., the tensor ϵ_{ij} can be presented as

$$\epsilon_{ij} = n^2 \delta_{ij} + \frac{1}{k} \chi_{ij}$$

where k is the wave number, c the light velocity and n the refractive index. The tensor χ_{ij} describes the anisotropy and has to be reconstructed. By Rytov's law, the polarization vector $\eta = n^{-1} A^{-1} E$ satisfies

$$\nabla_{\dot\gamma} \eta = \pi_{\dot\gamma} f \eta \tag{2.8}$$

where A is the amplitude of the ray and

$$f = \frac{i}{2n^2} \chi.$$

Here, γ denotes again the curve of linear propagation with direction $\dot\gamma = \xi$ and $\pi_{\dot\gamma}$ is the projection operator on the plane $\dot\gamma^\perp$. The inverse problem consists of recovering the anisotropic part of χ, or equivalently, recovering the tensor f. In the literature it is assumed that χ is skew-symmetric and therefore, f is symmetric. The tomographic measurements are of the following type: Given a curve $\gamma\colon [\tau_-, \tau_+] \to M$ between two boundary points, we choose an initial value $\eta_0 = \eta(\tau_-)$ of the polarization vector and measure the final value $\eta_1 = \eta(\tau_+)$. We rewrite (2.8) as an operator equation

$$\frac{\mathrm{d}\tilde U}{\mathrm{d}\tau} = f_{\xi^\perp} \tilde U(\tau)$$

where $f_{\xi^\perp}\colon \xi^\perp \to \xi^\perp$ is the restriction of $\pi_{\xi^\perp} f(\gamma(\tau))$ to the plane $\xi^\perp$ and $\tilde U(\tau)$ is a linear operator satisfying $\tilde U(\tau_-) = \mathbb{1}$. Hence, the measurement data are given by

$$\tilde\Phi[f](\gamma) = \tilde U(\tau_+).$$

Defining $U(\tau)$ such that

$$U(\tau)|_{\xi^\perp} = \tilde{U}(\tau), \qquad U(\tau)\xi = \xi$$

we obtain the initial value problem

$$\frac{\mathrm{d}U}{\mathrm{d}\tau} = (\pi_{\xi^\perp} f \pi_{\xi^\perp})U, \qquad U(\tau_-) = \mathbb{1}.$$

Setting $w = \ln \det U(\tau)$ we get

$$\frac{\mathrm{d}w}{\mathrm{d}\tau} = tr(\pi_{\xi^\perp} f \pi_{\xi^\perp})$$

where the trace $tr(A)$ of an operator A is defined for an orthonormal basis $e_1, \ldots, e_N$ by

$$tr(A) = \sum_{i=1}^{N} \langle Ae_i, e_i \rangle.$$

Hence, one ends up with the fact that the accumulated change w of polarization along the path is an integral over this tensor field f:

$$w[f](x,\xi) = \int_{\tau_-}^{\tau_+} tr(\pi_\xi f(x+\tau\xi)\pi_\xi)\mathrm{d}\tau.$$

Splitting f into

$$f = \tilde{f} + \lambda \mathbb{1}, \qquad tr\,\tilde{f} = 0,$$

where $\mathbb{1}$ is defined by

$$(\mathbb{1}u)_{i_1,\ldots,i_m} = \delta^{j_1}_{i_1} \cdots \delta^{j_m}_{i_m} u_{j_1,\ldots,j_m},$$

is the identity mapping. We complete $\{\xi\}$ to an orthonormal basis by adding basis vectors $\zeta_1, \ldots, \zeta_{N-1}$ we have that

$$
\begin{aligned}
w[\lambda\mathbb{1}](x,\xi) &= \int_{-\infty}^{\infty} tr(\pi_\xi(\lambda(x+\tau\xi)\mathbb{1})\pi_\xi)\mathrm{d}\tau \\
&= \int_{-\infty}^{\infty} \lambda(x+\tau\xi)tr(\pi_\xi^2)\mathrm{d}\tau \\
&= \int_{-\infty}^{\infty} \lambda(x+\tau\xi)tr(\pi_\xi)\mathrm{d}\tau \\
&= \int_{-\infty}^{\infty} \lambda(x+\tau\xi)tr(\mathbb{1}-P_\xi)\mathrm{d}\tau \\
&= \int_{-\infty}^{\infty} \lambda(x+\tau\xi)(tr(\mathbb{1})-tr(P_\xi))\mathrm{d}\tau \\
&= \int_{-\infty}^{\infty} \lambda(x+\tau\xi)\left(N-\langle P_\xi\xi,\xi\rangle - \sum_{k=1}^{N-1}\langle P_\xi\zeta_k,\zeta_k\rangle\right)\mathrm{d}\tau \\
&= \int_{-\infty}^{\infty} \lambda(x+\tau\xi)(N-1)\mathrm{d}\tau \\
&= (N-1)I[\lambda\mathbb{1}](x,\xi).
\end{aligned}
$$

Since

$$
\begin{aligned}
tr(\pi_\xi\tilde{f}\pi_\xi) &= \sum_{k=1}^{N-1}\langle\pi_\xi\tilde{f}\pi_\xi\zeta_k,\zeta_k\rangle + \langle\pi_\xi\tilde{f}\pi_\xi\xi,\xi\rangle \\
&= \sum_{i=1}^{N-1}\langle\tilde{f}\zeta_k,\zeta_k\rangle \\
&= -\langle\tilde{f}\xi,\xi\rangle,
\end{aligned}
$$

it holds that $w[\tilde{f}] = -I[\tilde{f}]$ and, hence,

$$
w[f] = I[(N-1)\lambda\mathbb{1} - \tilde{f}],
$$

where

$$
[If](x,\xi) = \int_{\tau_-(x,\xi)}^{\tau_+(x,\xi)} f_{ij}(x+\tau\xi)\xi^i\xi^j\mathrm{d}t. \tag{2.9}
$$

It can easily be shown that f can be determined by knowing $(N-1)\lambda\mathbb{1} - \tilde{f}$.

In the last examples, it became clear that the integral transformation, known from computerized tomography, can be extended to vector fields and tensor fields of rank 2. The only difference is the degree of multilinear dependence on the direction of propagation of the integrating function. However, it finds a lot of different practical applications. Therefore, we now want to define the generalized ray transform for tensors of any arbitrary rank.
One thing that has been neglected in the application of SPECT is the fact that the material under examination also partially absorbs the energy of tracers and transforms it into heat, for example. Thus, a kind of attenuation of the radiation takes place. This can be compensated by a corresponding exponential term in the integrand. The second problem is that both SPECT and vector tomography take images of the inside of the human body. This means that there can also be slight movements during the measurement, which can of course greatly distort the measurement data. So we also have to look at some kind of temporal dependence of the tensors. The third point is that waves, particularly in the last two examples, do not propagate in a straight line. In the polarization tomography example, the refractive index appears in the formulae. This means that there are places where light propagates faster or slower than in the surrounding material. There are also strong effects on the course when two different media meet. In this case, there is no longer any straight-line propagation.
All these points should be sufficient motivation to derive a general ray transformation that takes these problems into account. These will be modeled step by step in the next subsection. It will be shown that all the points just mentioned can be summarized in one formula.

2.1.2 Attenuated ray transform of dynamic tensor fields in inhomogeneous media

In (2.7) the consequence becomes clear that only the projections on the direction of the wave were measured. This means that all vectors that were perpendicular to the direction of the wave contributed nothing to the integral. Additionally, in this case, only scalar data can be measured. Consequently, a complete reconstruction of any vector field is not possible. This phenomenen can also be observed for tensor fields of any other rank. For this general case one can accurately determine the kernel of $\mathcal{I}_0$. Considering the Euclidean setting, by $S^m(\Omega)$ we denote the symmetric m-tensor fields on Ω. We define the *divergence operator* $\mathfrak{s}\colon C^\infty(S^{m+1}(\Omega)) \to C^\infty(S^m(\Omega))$ in coordinate form by

$$(\mathfrak{s}f)_{i_1\dots i_m} \coloneqq \frac{\partial f_{i_1\dots i_m j}}{\partial x^j}.$$

Moreover, we define the *inner differentiation* $\mathfrak{p}\colon C^\infty(S^m(\Omega)) \to C^\infty(S^{m+1}(\Omega))$ by

$$u_{i_1\dots i_m j} \coloneqq (\mathfrak{p}w)_{i_1\dots i_m j} = \frac{1}{m+1}\left(\frac{\partial w_{i_1\dots i_m}}{\partial x^j} + \sum_{k=1}^{m} \frac{\partial w_{i_1\dots i_{k-1} j i_{k+1}\dots i_m}}{\partial x^{i_k}}\right).$$

Given these definitions, we call a tensor field f *solenoidal* if $\mathfrak{s}f = 0$ and we call it *potential field* if there exists a v such that $f = \mathfrak{p}v$. The next theorem is about the decomposition of tensor fields into solenoidal and potential parts.

Theorem 2.1. *Let Ω be a bounded domain and $m \geq 0$. A tensor field $f \in C^\infty(S^m(\Omega))$ can be uniquely decomposed into a solenoidal and a potential field, i.e., there exist uniquely determined $f_{sol}, f_{pot} \in C^\infty(S^m(\Omega))$ such that*

$$f = f_{sol} + f_{pot},$$

where $\mathfrak{s}f_{sol} = 0$ and $f_{pot} = \mathfrak{p}v$ for a v satisfying $v|_{\partial\Omega} = 0$.

Proof. See Theorem 2.4.2 in [89]. □

Using Theorem 2.1, we obtain

$$\begin{aligned}
[\mathcal{I}_0 f](x,\xi) &= [\mathcal{I}_0 f_{\mathrm{sol}}](x,\xi) + [\mathcal{I}_0 f_{\mathrm{pot}}](x,\xi) \\
&= [\mathcal{I}_0 f_{\mathrm{sol}}](x,\xi) + \int_{\tau_-(x,\xi)}^{\tau_+(x,\xi)} \langle \mathfrak{p}v(x+\tau\xi), \xi^m \rangle \mathrm{d}\tau \\
&= [\mathcal{I}_0 f_{\mathrm{sol}}](x,\xi) + [v(x+\tau\xi)]_{\tau_-(x,\xi)}^{\tau_+(x,\xi)} \\
&= [\mathcal{I}_0 f_{\mathrm{sol}}](x,\xi).
\end{aligned}$$

Consequently, there is only a chance to reconstruct the solenoidal part of a vector field. This changes if the phenomenon of absorption is taken into account. Absorption generally means that part of the energy of a wave is converted into another form of energy. For example, thermal energy loss occurs in sound waves. According to the Lambert-Beer absorption law (see e.g. [22]), the intensity of a wave decreases exponentially with the depth of penetration into a material. More precisely, the following applies to the intensity I after traveling a distance Δz within a medium

$$I = I_0 \cdot \exp^{-\alpha \Delta z},$$

where I_0 is the initial intensity and α denotes the so-called *absorption coefficient*. If we assume that the radiation passes through J different areas of the length Δz_j, $j = 1, \ldots, J$, each with an absorption coefficient α_j, the final intensity results in

$$I = I_0 \cdot \prod_{j=1}^{J} \exp^{-\alpha_j \Delta z_j} = I_0 \cdot \exp\left(- \sum_{j=1}^{J} \alpha_j \Delta z_j \right). \tag{2.10}$$

Letting the distances Δz_i tend to 0, the sum in (2.10) can be approximated by an integral of α over a line segment. Therefore, we define the attenuated ray transform for tensor fields as follows:

For a given bounded domain $\Omega \subset \mathbb{R}^N$ with strictly convex boundary and $\alpha \in C(\Omega \times \mathbb{S}^{N-1})$ with $\alpha \geq \alpha_0 > 0$ for some $\alpha_0 \in \mathbb{R}$, the attenuated ray transform

$$\mathcal{I}_\alpha \colon C(S^m(\Omega)) \to C(\partial\Omega \times \mathbb{S}^{N-1})$$

of a symmetric m-tensor field $f = (f_{i_1,\dots,i_m})$ is given by

$$[\mathcal{I}_\alpha f](x,\xi) = \int_{\tau_-(x,\xi)}^0 \langle f(x+\tau\xi), \xi^m \rangle \exp\left(-\int_\tau^0 \alpha(x+\sigma\xi,\xi)\mathrm{d}\sigma\right)\mathrm{d}\tau. \tag{2.11}$$

By ξ^m we denote the m-fold tensor product, i.e., $\xi^m = \xi \otimes \cdots \otimes \xi$. The fact that we only allow symmetric tensor fields is that symmetric fields are investigated in all tensor tomographic applications. For a rank less than or equal to 1 this makes no difference anyway. We are demanding a lower bound to α. This leads to the fact that the exponential in the integral takes values between 0 and 1 and thus has the impact of an attenuation. Since even atmospheric air has slightly absorbing properties, this is not a constraint. Any positive attenuation coefficient makes the ray transform injective as first has been shown in [35]. One could perhaps get the idea to interpret the exponential term in (2.11) as a new function but we will see in Subsection 2.2 that this form of representation is advantageous.
There have been many achievements in describing the range of the attenuated ray transform in the scalar case in [69]. An explicit inversion formula is derived in [68] and [16] presents numerical results. In [78] it is even shown how to compute f and α simultaneously.

The next goal is to adapt (2.11) for time-dependent fields. Especially in the two examples of SPECT and Doppler-tomography, it is obvious that the examined object and thus also the size to be reconstructed can change over time. If we assume that the object is not compressed or stretched, we can take the change as a rigid-body deformation. This would mean that we would only include rotations and translations in our model. Accordingly, there exist suitable rotation matrices A_t and translation vectors b_t, so that the model for the function to be reconstructed could be

$$f(t,x) = f^{\mathrm{ref}}(A_t x + b_t), \qquad t \in [0,T].$$

Another point would be that f varies in time even without external action. For example, the blood flow in (2.3) could change simply due to blood circulation to the extent that measurement inaccuracies occur. Thus, to keep the formulation as general as possible, we allow arbitrary temporal changes. This leads to the definition of the dynamic attenuated ray transform of time-dependent tensor fields.

For a given bounded domain $\Omega \subset \mathbb{R}^N$ with strictly convex boundary and $\alpha \in C(\Omega \times \mathbb{S}^{N-1})$ with $\alpha \geq \alpha_0 > 0$ for some $\alpha_0 \in \mathbb{R}$, the dynamic attenuated ray transform

$$\mathcal{I}_\alpha^d \colon C(0,T;S^m(\Omega)) \to C(0,T;\partial\Omega \times \mathbb{S}^{N-1})$$

of a symmetric m-tensor field $f = (f_{i_1,\dots,i_m})$ is given by

$$[\mathcal{I}_\alpha^d f](t,x,\xi) = \int_{\tau_-(x,\xi)}^0 \langle f(t+\tau, x+\tau\xi), \xi^m \rangle \exp\left(-\int_\tau^0 \alpha(x+\sigma\xi,\xi)\mathrm{d}\sigma\right)\mathrm{d}\tau. \quad (2.12)$$

A more complex phenomenon that should not be neglected is the directional deflection of signals in inhomogeneous media. These deviations from straight lines occur when the signal does not propagate at the same speed everywhere in the object of consideration. This can be because the object does not have the same temperature everywhere or is exposed to the same pressure. Here, even small deviations can lead to measurable changes in velocity. Above all, however, the deflections occur when the signal passes through more than one medium. To stay with the example of vector tomography from the last section, the sound waves do not only hit blood but also other substances such as tissue, muscles, etc. For all these, one can give a typical range for the so-called *refractive index*. This number denoted by n gives the ratio of the speed of propagation v_0 of the wave in a reference medium and the speed v_{medium} in the observed medium, i.e.,

$$n = \frac{v_0}{v_{\text{medium}}}. \quad (2.13)$$

For mechanical waves such as ultrasound waves, one uses v_0 for the velocity in air, and for electromagnetic waves, one uses the velocity in vacuum. Note, that for a fixed frequency the refractive index is a positive number greater than or equal to 1. Now what happens when a wave hits the interface between two media, is that it splits into two partial waves.

As seen in Figure (2.4) one part of the wave is reflected at the interface, i.e., it changes its direction and propagates further in the first medium. The second part, the so-called *transmitted wave*, penetrates the second medium and is deflected in the process. Depending on the ratio of the two refractive indices, a larger part can be reflected or transmitted.

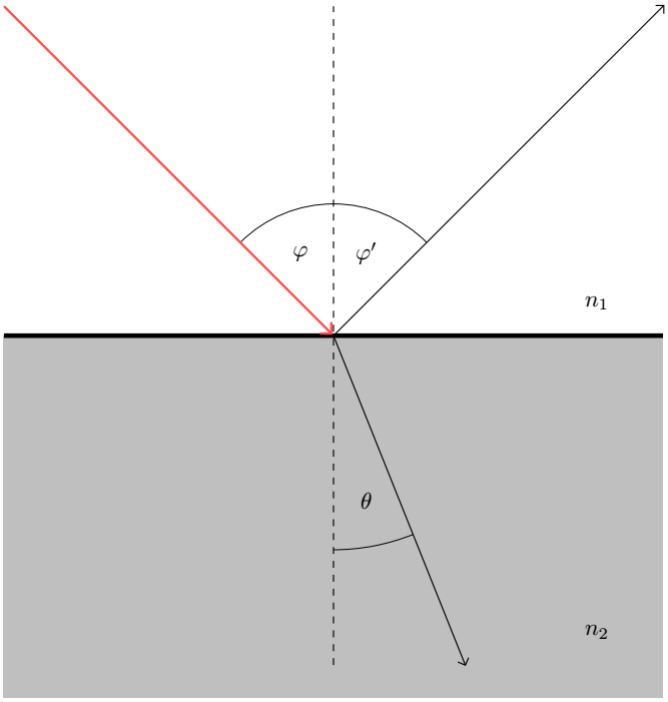

Figure 2.4: Incoming wave (red) hits boundary with incident angle φ, gets split into reflected part with angle φ' and refracted/transmitted part with an angle θ.

In the following, we will now examine how exactly this refraction is to be understood. The refraction of the transmitted wave is not random but can be specified explicitly for given refractive indices. This requires the principle of Pierre de Fermat:

Fermat's principle states that an optical or mechanical signal in a medium takes paths between two points on which its travel time does not change with small variations of the path. In particular, the optical path length is extremal, i.e., the longest or shortest.

This therefore means that the acceleration of the path curve along the path vanishes (c.f. (1.32)), which means that these curves are the minimizers of (1.34).
As discussed in Chapter 1, it is necessary to define an appropriate metric on M which describes the phenomenon of refraction. The metric tensor is defined via the tangent basis vectors $\partial_1, \dots, \partial_N$ at each point $x \in M$. Since cotangent vectors describe the derivative into some direction which is nothing else than the velocity of a curve passing through $x \in M$, we rewrite (2.13) as

$$v(x) = \frac{v_0}{n(x)}$$

and therefore, define the local coordinate system by

$$\hat{x}_i = \frac{x_i}{n(x)}, \qquad i = 1, \dots, N.$$

Hence,

$$\partial_i = \frac{\partial x_k}{\partial \hat{x}_i} e_k = n(x) e_i$$

and the metric tensor is given by

$$g_{ij}(x) = \langle \partial_i, \partial_j \rangle = n^2(x) \delta_{ij}. \tag{2.14}$$

We observe that g is a diagonal matrix with positive entries that satisfies the conditions of a Riemannian metric for a smooth enough n. In particular, in the homogeneous case of the previous section, this metric becomes a multiple of the identity matrix. As a simple example, we consider what happens if $M = M_1 \cup M_2$ consists of only two different media M_1 and M_2 separated by a straight boundary between them. Let $A \in M_1$ with $n = n_1$ and $B \in M_2$ with $n = n_2$. To find the path that a signal takes from A to B we minimize the optical arc length.

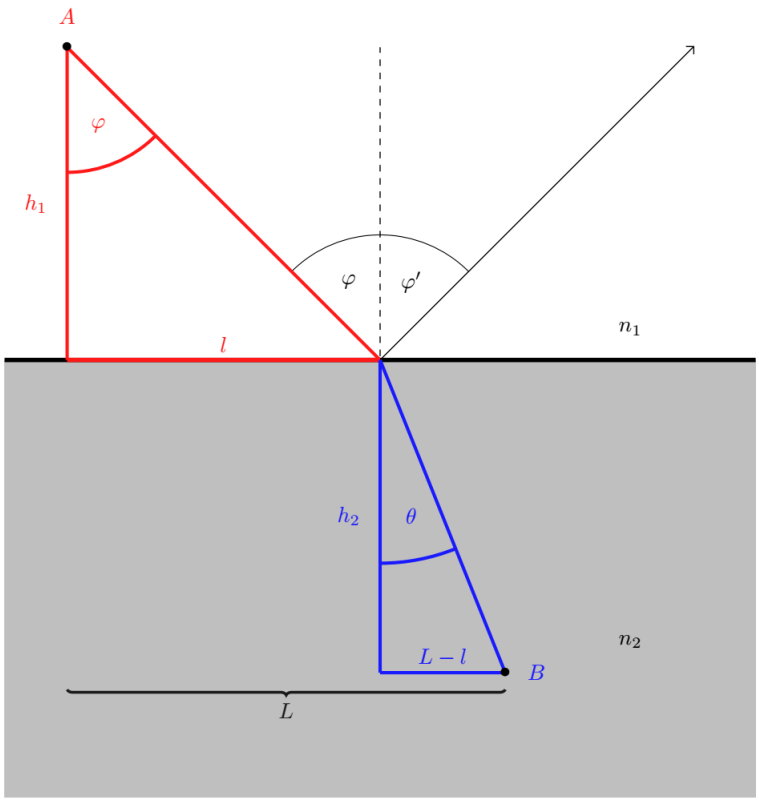

Figure 2.5: Sketch for proving Snellius' law

Let A and B be the starting and ending points of the wave. By construction, the angle φ appears again in the red triangle of Figure (2.5). Let h_1 and h_2 be the distances the wave travels perpendicular to the plane of refraction in each medium. We split the distance L parallel to this plane into the part l in medium 1 and the part $L - l$ in medium 2. By (1.34), the length of propagation with respect to the metric g becomes:

$$T(l) = n_1\sqrt{h_1^2 + l^2} + n_2\sqrt{h_2^2 + (L-l)^2}. \tag{2.15}$$

Minimizing this function means to choose l such that $T'(l) = 0$. Differentiating yields

$$\begin{aligned} T'(l) &= n_1 \frac{l}{\sqrt{h_1^2 + l^2}} - n_2 \frac{L-l}{\sqrt{h_2^2 + (L-l)^2}} \\ &= n_1 \sin\varphi - n_2 \sin\theta. \end{aligned}$$

Hence, we obtain the following condition which is called Snellius' law:

$$\frac{\sin\varphi}{\sin\theta} = \frac{n_2}{n_1}.$$

The second part of his law states that the angle of incidence φ and the angle of reflection φ' are equal. This can be derived similarly by using Fermat's principle.
So you can see that for $n_1 \approx n_2$ the angle barely changes. The transmitted wave has a different wavelength, but still the same frequency. We do not consider the propagation of the reflected wave any further in the following. We include the loss of energy in the absorption coefficient from (2.11).
At the moment, we know how to calculate the paths for piecewise constant refractive indices. It is different if we assume that the refractive index changes continuously or is differentiable. We justify this assumption by the fact that we can numerically approximate any discontinuity arbitrarily well by continuous functions. The advantage now is that we can use the geodesic equation from (1.37) instead of many small minimization problems. Analogous to the homogeneous case, we define a curve

$$\gamma_{x,\xi} \colon \mathbb{R} \to M$$

as a solution to the initial value problem

$$\frac{\mathrm{d}^2\gamma^k}{\mathrm{d}s^2} + \Gamma_{ij}^k \frac{\mathrm{d}\gamma^i}{\mathrm{d}s}\frac{\mathrm{d}\gamma^j}{\mathrm{d}s} = 0$$

with $\gamma(0) = x$ and $\dot\gamma(0) = \xi$.

Thus, the illustration from Figure 2.3 is no longer correct but looks as in Figure 2.6. It is noticeable that the same wave that was sent through the object in Figure 2.3 with the same direction of propagation now emerges at a completely different location. Due to the changed propagation, other projections of the field also contribute to the integral.

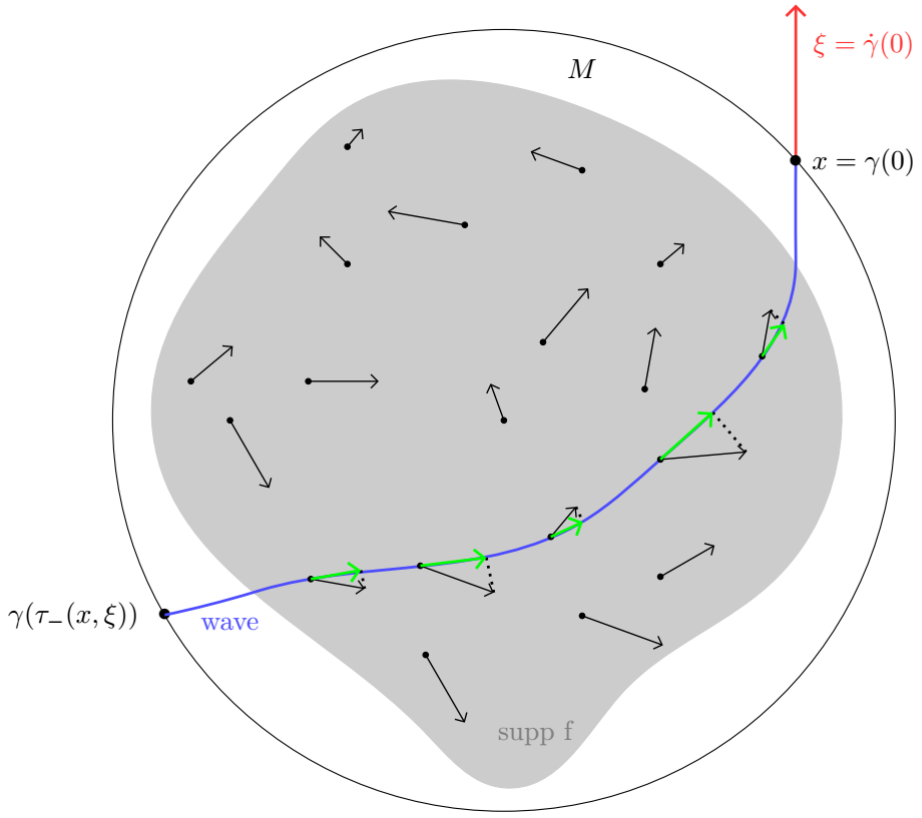

Figure 2.6: 2D-Illustration of the principle of RTT

In contrast to the modeling in the homogeneous case, this curve is parameterized with respect to time instead of arc length. Keeping in mind that one goal of this modeling is to reconstruct fields that change by time, we are interested in a geodesic equation that is parameterized by time instead of the arc length. Unfortunately, (1.37) does not necessarily remain correct if we choose any arbitrary parameterization. To see this, let $\tilde{\gamma}(\tau) = \gamma(s(\tau))$ be any other parameterization of a geodesic curve. Then, it holds for $k = 1, \dots, N$ that

$$\begin{aligned} \frac{\mathrm{d}\tilde{\gamma}^k(\tau)}{\mathrm{d}\tau} &= \frac{\mathrm{d}\gamma^k(s)}{\mathrm{d}s} \cdot \frac{\mathrm{d}s}{\mathrm{d}\tau} \\ \frac{\mathrm{d}^2\tilde{\gamma}^k(\tau)}{\mathrm{d}\tau^2} &= \frac{\mathrm{d}^2\gamma^k(s)}{\mathrm{d}s^2} \cdot \left(\frac{\mathrm{d}s}{\mathrm{d}\tau}\right)^2 + \frac{\mathrm{d}\gamma^k(s)}{\mathrm{d}s} \cdot \frac{\mathrm{d}^2 s}{\mathrm{d}\tau^2}. \end{aligned}$$

The Christoffel symbols depend only on the partial derivatives of the metric and not on the parameter representation of the curve. Therefore, they remain unchanged.

Hence,

$$\frac{\mathrm{d}^2\tilde{\gamma}^k(\tau)}{\mathrm{d}\tau^2} + \Gamma^k_{ij}(\tilde{\gamma})\frac{\mathrm{d}\tilde{\gamma}^i(\tau)}{\mathrm{d}\tau}\frac{\mathrm{d}\tilde{\gamma}^j(\tau)}{\mathrm{d}\tau} = \frac{\mathrm{d}\gamma^k(s)}{\mathrm{d}s}\frac{\mathrm{d}^2 s}{\mathrm{d}\tau^2}.$$

The last expression vanishes only if s depends linearly on τ. In the case that we parameterize by time, this is true. Observing that (1.34) can be derived similarly for the time variable τ, we obtain for $g_{ij}(x) = n^2(x)\delta_{ij}$

$$\mathrm{d}s = n(\gamma(\tau))\left\|\frac{\mathrm{d}\gamma}{\mathrm{d}\tau}\right\|_{euclid}\mathrm{d}\tau$$

and thus

$$\frac{\mathrm{d}s}{\mathrm{d}\tau} = n(\gamma(\tau))\left\|\frac{\mathrm{d}\gamma}{\mathrm{d}\tau}\right\|_{euclid} = c_0,$$

where c_0 is the vacuum velocity of the propagating signal. Hence, the second derivative is zero as required and we obtain

$$\ddot{\gamma}^k(\tau) + \Gamma^k_{ij}(\gamma(\tau))\dot{\gamma}^i(\tau)\dot{\gamma}^j(\tau) = 0 \tag{2.16}$$

with initial conditions $\gamma(0) = x$ and $\dot{\gamma}(0) = \xi$. This leads us finally to the definition of the stationary and dynamic ray transform taking refraction into account:

Let (M, g) be a Riemannian manifold where M is a N-dimensional manifold with strictly convex boundary and $g_{ij}(x) = n^2(x)\delta_{ij}$. Given the tangent bundle

$$TM = \{(x, \xi) | x \in M, \xi \in T_x M\},$$

we define the following submanifold:

$$\Omega M \coloneqq \{(x, \xi) \in TM |\ \|\xi\| = 1\}.$$

Its boundary can be splitted into an *inflow boundary* and an *outflow boundary*:

$$\partial_- \Omega M \coloneqq \{(x, \xi) \in \Omega M | x \in \partial M, \langle \nu(x), \xi \rangle \leq 0\},$$
$$\partial_+ \Omega M \coloneqq \{(x, \xi) \in \Omega M | x \in \partial M, \langle \nu(x), \xi \rangle > 0\}.$$

Since the measurement data is taken when a signal exits the object M, we restrict the set of possible pairs (x, ξ) to $\partial_+ \Omega M$. Therefore, we substitute the integral limit $\tau_+(x, \xi)$ by 0. For a given $\alpha \in C(\Omega M)$ with $\alpha \geq \alpha_0 > 0$ for some $\alpha_0 \in \mathbb{R}$, we define

- the stationary attenuated ray transform of a m-tensor field $f = (f_{i_1,\dots,i_m})$ by the function $\mathcal{I}_\alpha f \colon C(S^m \tau'_M) \to C(\partial_+ \Omega M)$ where

$$[\mathcal{I}_\alpha f](x, \xi) = \int_{\tau_-(x,\xi)}^0 \langle f(\gamma_{x,\xi}(\tau)), \dot{\gamma}^m_{x,\xi}(\tau) \rangle \exp\left(- \int_\tau^0 \alpha(\gamma_{x,\xi}(\sigma), \dot{\gamma}_{x,\xi}(\sigma)) \mathrm{d}\sigma \right) \mathrm{d}\tau. \tag{2.17}$$

- the dynamic attenuated ray transform of a m-tensor field $f = (f_{i_1,\dots,i_m})$ by the function $\mathcal{I}^d_\alpha f \colon C(0, T; C(S^m \tau'_M)) \to C(0, T; C(\partial_+ \Omega M))$ where

$$[\mathcal{I}^d_\alpha f](t, x, \xi) = \int_{\tau_-(x,\xi)}^0 \langle f(t + \tau, \gamma_{x,\xi}(\tau)), \dot{\gamma}^m_{x,\xi}(\tau) \rangle \exp\left(- \int_\tau^0 \alpha(\gamma_{x,\xi}(\sigma), \dot{\gamma}_{x,\xi}(\sigma)) \mathrm{d}\sigma \right) \mathrm{d}\tau. \tag{2.18}$$

It is noteworthy that there exist similar decompositions of tensor fields on Riemannian manifolds as in Theorem 2.1. Therefore, for $\alpha = 0$, potential fields do not contribute to the integrals in (2.17) and (2.18). For more details, we refer to [89].

The next question is whether this operator is well defined, i.e., the path of integration is uniquely determined. Furthermore, we want to investigate if this transform is continuous for appropriate spaces.

2.1.3 Well-definedness and continuity of the ray transform

First, we investigate under which conditions this equation is uniquely solvable. For this purpose, we compute the Christoffel symbols for the metric g from (2.14).

Lemma 2.2. *Let (M, g) be a Riemannian manifold with $M \subset \mathbb{R}^3$ and $g_{ij}(x) = n^2(x)\delta_{ij}$ the metric tensor. The Christoffel symbols are given by*

$$(\Gamma^1_{ij}(x))_{ij} = n^{-1}(x) \begin{pmatrix} \partial_1 n(x) & \partial_2 n(x) & \partial_3 n(x) \\ \partial_2 n(x) & -\partial_1 n(x) & 0 \\ \partial_3 n(x) & 0 & -\partial_1 n(x) \end{pmatrix}, \tag{2.19}$$

$$(\Gamma^2_{ij}(x))_{ij} = n^{-1}(x) \begin{pmatrix} -\partial_2 n(x) & \partial_1 n(x) & 0 \\ \partial_1 n(x) & \partial_2 n(x) & \partial_3 n(x) \\ 0 & \partial_3 n(x) & -\partial_2 n(x) \end{pmatrix} \tag{2.20}$$

and

$$(\Gamma^3_{ij}(x))_{ij} = n^{-1}(x) \begin{pmatrix} -\partial_3 n(x) & 0 & \partial_1 n(x) \\ 0 & -\partial_3 n(x) & \partial_2 n(x) \\ \partial_1 n(x) & \partial_2 n(x) & \partial_3 n(x) \end{pmatrix} \tag{2.21}$$

for all $x \in M$.

Proof. The Christoffel symbols are defined by

$$\begin{aligned} \Gamma^k_{ij}(x) &= \frac{1}{2} g^{kl}(x) \left(\frac{\partial g_{jl}(x)}{\partial x^i} + \frac{\partial g_{il}}{\partial x^j}(x) - \frac{\partial g_{ij}}{\partial x^l}(x) \right) \\ &= \frac{1}{2} g^{kl}(x)(\partial_i g_{jl}(x) + \partial_j g_{il}(x) - \partial_l g_{ij}(x)), \end{aligned}$$

where $g^{ij}(x)$ are the entries of the inverse of $g_{ij}(x)$ and given by

$$g^{ij}(x) = n^{-2}(x)\delta^{ij}.$$

Using that

$$\partial_k g_{ij}(x) = \partial_k n^2(x)\delta_{ij} = 2n(x)\partial_k n(x)\delta_{ij}$$

we obtain for $k = 1$

$$\Gamma^1_{ij}(x) = n(x)^{-1}\Big(\partial_j n(x)\delta_{ik} + \partial_i n(x)\delta_{jk} - \partial_k n(x)\delta_{ij}\Big)$$

and hence, by (2.19),

$$\begin{aligned}
\Gamma^1_{11}(x) &= n(x)^{-1}\partial_1 n(x)\\
\Gamma^1_{22}(x) &= -n(x)^{-1}\partial_1 n(x)\\
\Gamma^1_{33}(x) &= n(x)^{-1}\partial_1 n(x)\\
\Gamma^1_{12}(x) &= \Gamma^1_{21}(x) = n(x)^{-1}\partial_1 n(x)\\
\Gamma^1_{13}(x) &= \Gamma^1_{31}(x) = n(x)^{-1}\partial_3 n(x)\\
\Gamma^1_{23}(x) &= \Gamma^1_{32}(x) = 0.
\end{aligned}$$

In the same way, we get (2.20) and (2.21).

□

Corollary 2.3. *Let (M, g) be a Riemannian manifold as in Lemma 2.2 but with $M \subset \mathbb{R}^2$. Then, the Christoffel symbols are given by*

$$(\Gamma^1_{ij}(x))_{ij} = n^{-1}(x)\begin{pmatrix}\partial_1 n(x) & \partial_2 n(x)\\ \partial_2 n(x) & -\partial_1 n(x)\end{pmatrix}, \tag{2.22}$$

and

$$(\Gamma^2_{ij}(x))_{ij} = n^{-1}(x)\begin{pmatrix}-\partial_2 n(x) & \partial_1 n(x)\\ \partial_1 n(x) & \partial_2 n(x)\end{pmatrix}. \tag{2.23}$$

Proof. The equations (2.22) and (2.23) can be derived as in (2.19) and (2.20). □

In the next theorem, we present the uniqueness result. To this end, it is necessary to know how to compute the scalar product of two tangent vectors, the norm of a tangent vector, and the gradient of a vector in M. By construction, g_x defines a scalar product on T_xM for every point $x \in M$. Therefore, we define for $\xi, \eta \in T_xM$

$$\langle \xi, \eta\rangle \coloneqq g_x(\xi,\eta) = g_{ij}(x)\xi^i\eta^j = n^2(x)\xi^i\eta^j = n^2(x)\langle\xi,\eta\rangle_{\text{euclid}}.$$

Accordingly, the norm of $\xi \in T_xM$ is defined as

$$\|\xi\| \coloneqq \sqrt{g_x(\xi,\xi)} = n(x)\|\xi\|_{\text{euclid}} \tag{2.24}$$

Using (1.25), the gradient of a given function $u\colon M \to \mathbb{R}$ is given by

$$\nabla u = g^{ij}\partial_i u \partial_j = n^{-2}(x)\nabla_{\text{euclid}}.$$

Hence, the following expression is independent of the refractive index:

$$\langle \nabla u, \xi \rangle = \langle \nabla u, \xi \rangle_{\text{euclid}}.$$

We will use that to prove the next theorem.

Theorem 2.4. *Let (M, g) be a compact Riemannian manifold in $\mathbb{R}^N$, $N = 2, 3$ and $n \in C^2(M)$. Then, the following initial value system has a unique solution:*

$$\ddot{\gamma}^k + \Gamma^k_{ij}(n(\gamma))\dot{\gamma}^i\dot{\gamma}^j = 0, \qquad \gamma(0) = x, \dot{\gamma}(0) = \xi. \tag{2.25}$$

Proof. In [86] the proof has been done for two dimensions. For $N = 3$ we refer to the proof in [101]. First, we write the second-order ordinary differential equation into a system of first-order equations. Setting $\Gamma_{ij}(x) = (\Gamma^1_{ij}(x), \dots, \Gamma^N_{ij}(x))$ we obtain

$$\begin{cases} \frac{\mathrm{d}}{\mathrm{d}t}\gamma(t) & = \dot{\gamma}(t) \\ \frac{\mathrm{d}}{\mathrm{d}t}\dot{\gamma}(t) & = -\Gamma_{ij}(\gamma(t))\dot{\gamma}^i(t)\dot{\gamma}^j(t) \\ \gamma(0) & = x \\ \dot{\gamma}(0) & = \xi \end{cases}. \tag{2.26}$$

According to Picard-Lindelöf's theorem (c.f. [103]) it suffices to show that for

$$z(t) = (z_{(1)}(t), z_{(2)}(t)) \coloneqq (\gamma(t), \dot{\gamma}(t))$$

the function

$$f(z(t)) \coloneqq \begin{pmatrix} z_{(2)}(t) \\ -\Gamma_{ij}(z_{(1)}(t))z^i_{(2)}z^j_{(2)} \end{pmatrix}$$

satisfies a Lipschitz condition

$$\|f(\zeta_1(t)) - f(\zeta_2(t))\| \leq L\|\zeta_1(t) - \zeta_2(t))\|,$$

where ζ_1, ζ_2 are in a small neighborhood of z and $L > 0$. Due to the mean value theorem, it remains to show that the Jacobian $\nabla_z f(z(t))$ is bounded for all t.

First, we remark that, in local coordinates, we have

$$\frac{\partial \dot{\gamma}^k}{\partial \gamma^l} = 0, \qquad \frac{\partial \dot{\gamma}^k}{\partial \dot{\gamma}^l} = \delta_l^k, \qquad k, l = 1, \dots, N.$$

We obtain for $k = 1, \dots, N$

$$\begin{aligned}
&- \Gamma_{ij}^k(\gamma)\dot{\gamma}^i\dot{\gamma}^j \\
&= -n^{-1}(\gamma)\left(\frac{\partial n}{\partial x_k}(\gamma)(\dot{\gamma}^k)^2 + \sum_{i=k\neq j}\frac{\partial n}{\partial x_j}(\gamma)\dot{\gamma}^i\dot{\gamma}^j + \sum_{i\neq k=j}\left(-\frac{\partial n}{\partial x_k}(\gamma)\right)(\dot{\gamma}^i)^2 + \sum_{i\neq j=k}\frac{\partial n}{\partial x_i}(\gamma)\dot{\gamma}^i\dot{\gamma}^j\right) \\
&= -n^{-1}(\gamma)\left(2\frac{\partial n}{\partial x_k}(\gamma)(\dot{\gamma}^k)^2 + 2\sum_{i=k\neq j}\frac{\partial n}{\partial x_j}(\gamma)\dot{\gamma}^i\dot{\gamma}^j + \sum_{i}\left(-\frac{\partial n}{\partial x_k}(\gamma)\right)(\dot{\gamma}^i)^2\right) \\
&= n^{-1}(\gamma)\left(n^{-2}(x)\frac{\partial n}{\partial x_k}(\gamma)\|\dot{\gamma}\|^2 - 2\frac{\partial n}{\partial x_k}(\gamma)(\dot{\gamma}^k)^2 - 2\sum_{j\neq k}\frac{\partial n}{\partial x_j}(\gamma)\dot{\gamma}^j\dot{\gamma}^k\right) \\
&= n^{-1}(\gamma)\left(n^{-2}(x)\frac{\partial n}{\partial x_k}(\gamma)\|\dot{\gamma}\|^2 - 2\sum_{j}\frac{\partial n}{\partial x_j}(\gamma)\dot{\gamma}^j\dot{\gamma}^k\right) \\
&= n^{-1}(\gamma)\left(n^{-2}(\gamma)\frac{\partial n}{\partial x_k}(\gamma)\|\dot{\gamma}\|^2 - 2\dot{\gamma}^k\langle\nabla n(\gamma), \dot{\gamma}\rangle\right). \qquad (2.27)
\end{aligned}$$

Thus,

$$\begin{aligned}
\frac{\partial}{\partial \dot{\gamma}^l}(-\Gamma_{ij}^k(\gamma)\dot{\gamma}^i\dot{\gamma}^j) &= n^{-1}(\gamma)\left(2n^{-2}(\gamma)\frac{\partial n}{\partial x_k}(\gamma)\dot{\gamma}^l - 2\dot{\gamma}^k\frac{\partial n}{\partial x_l}(\gamma) - 2\delta_l^k\langle\nabla n(\gamma), \dot{\gamma}\rangle\right) \\
\frac{\partial}{\partial \gamma^l}(-\Gamma_{ij}^k(\gamma)\dot{\gamma}^i\dot{\gamma}^j) &= -\frac{\partial n}{\partial x_l}(\gamma)n^{-2}(\gamma)\left(3n^{-2}(x)\frac{\partial n}{\partial x_k}(\gamma)\|\dot{\gamma}\|^2 - 2\dot{\gamma}^k\langle\nabla n(\gamma), \dot{\gamma}\rangle\right) \\
&\quad + n^{-1}(\gamma)\left(n^{-2}(x)\frac{\partial^2 n}{\partial x_k \partial x_l}(\gamma)\|\dot{\gamma}\|^2 - 2\dot{\gamma}^k\langle\nabla\left(\frac{\partial n}{\partial x_l}(\gamma)\right), \dot{\gamma}\rangle\right).
\end{aligned}$$

Since $n \in C^2(M)$ and $n > 0$ by definition, all the derivatives are bounded and the asserted statement follows. □

In particular, the solution z depends continuously on the initial values according to [103]. This means that (2.17) and (2.18) are well-defined operators. In the next theorem, it will be shown that they are even continuous operators. We will mainly focus on Sobolev spaces. That is why it is necessary to consider different volume and angle measures.

Let $(V, \mathcal{A}, \mu)$ be a measure space, i.e., a non-empty set V, a σ-algebra $\mathcal{A}$ on V and a measure μ on $(V, \mathcal{A})$. For a real number $1 \leq p < \infty$ we define the following vector space

$$L^p(V) = \left\{ f \colon V \to \mathbb{R} \middle| \int_V f^p \mathrm{d}\mu < \infty \right\}.$$

On $L^p(V)$ we can define the norm

$$\|f\|_{L^p(V)} \coloneqq \left(\int_V |f|^p \mathrm{d}\mu \right)^{\frac{1}{p}}.$$

We will only use the case where $p = 2$. Then, on $L^2(V)$ we define a scalar product by

$$\langle f, g \rangle_{L^2(V)} = \int_V fg \mathrm{d}\mu.$$

for $f, g \in L^2(V)$. To write these L^2-spaces explicitly for some spaces V of interest we need to find the corresponding volume forms. Keeping in mind that, for every point $x \in M$, the tangent space T_xM is equipped with the structure of an Euclidean vector space induced by the Riemannian metric. As proven in [87], the Euclidean volume form on T_xM in a local coordinate system is expressed by

$$\mathrm{d}V_x^N(\xi) = \sqrt{\det g}\ \mathrm{d}\xi^1 \wedge \cdots \wedge \mathrm{d}\xi^N = \sqrt{\det g}\ \mathrm{d}\xi.$$

The angular measure $\mathrm{d}\omega_x(\xi)$ on the unit sphere $\Omega_x M \coloneqq \{\xi \in T_xM |\ \|\xi\|^2 = 1\}$ of the tangent space T_xM can be written as

$$\mathrm{d}\omega_x^N(\xi) = \sqrt{\det g} \sum_{i=1}^{N} (-1)^{i-1} \xi^i \mathrm{d}\xi^1 \wedge \cdots \wedge \widehat{\mathrm{d}\xi^i} \wedge \cdots \wedge \mathrm{d}\xi^N,$$

where the $\widehat{\mathrm{d}\xi^i}$ means that this index will be skipped in the summation. Therefore, the volume forms on ΩM and on $\partial_+ \Omega M$ ($\partial \Omega M$) are

$$\begin{aligned} \mathrm{d}\Sigma^N &= \mathrm{d}\omega_x(\xi) \wedge \mathrm{d}V^N(x), \\ \mathrm{d}\sigma^N &= (-1)^N \mathrm{d}\omega_x(\xi) \wedge \mathrm{d}V^{N-1}(x), \end{aligned}$$

where $\mathrm{d}V^N(x) = \sqrt{\det g}\ \mathrm{d}x = n^N(x)\mathrm{d}x$ is the Riemannian volume form on M and $\mathrm{d}V^{N-1}(x)$ is the one on ∂M.

For $N = 2$ and $N = 3$ we want to compute $\mathrm{d}\omega_x^N(\xi)$ and $\mathrm{d}\Sigma^N$. For $N = 2$, ξ reads in polar coordinates as

$$\xi = \begin{pmatrix} \xi^1 \\ \xi^2 \end{pmatrix} = n^{-1}(x) \begin{pmatrix} \cos\varphi \\ \sin\varphi \end{pmatrix}.$$

It holds that

$$\begin{aligned} \mathrm{d}\xi^1 &= -n^{-1}(x)\sin\varphi \mathrm{d}\varphi \\ \mathrm{d}\xi^2 &= n^{-1}(x)\cos\varphi \mathrm{d}\varphi. \end{aligned}$$

Hence,

$$\begin{aligned} \mathrm{d}\omega_x^2(\xi) &= \sqrt{\det g} \sum_{i=1}^{2} (-1)^{i-1} \xi^i \mathrm{d}\xi^1 \wedge \cdots \wedge \widehat{\mathrm{d}\xi^i} \wedge \cdots \wedge \mathrm{d}\xi^2 \\ &= n^2(x)(\xi^1 \mathrm{d}\xi^2 - \xi^2 \mathrm{d}\xi^1) \\ &= n^2(x)(n^{-2}(x)\cos^2\varphi \mathrm{d}\varphi + n^{-2}(x)\sin^2\varphi \mathrm{d}\varphi) \\ &= \mathrm{d}\varphi \end{aligned} \tag{2.28}$$

and

$$\mathrm{d}\Sigma^2 = \mathrm{d}\omega_x^2(\xi) \wedge \mathrm{d}V^2(x) = n^2(x)\mathrm{d}\varphi \mathrm{d}x.$$

Analogously, for $N = 3$, we write ξ in spherical coordinates

$$\xi = \begin{pmatrix} \xi^1 \\ \xi^2 \\ \xi^3 \end{pmatrix} = n^{-1}(x) \begin{pmatrix} \cos\varphi\sin\theta \\ \sin\varphi\sin\theta \\ \cos\theta \end{pmatrix}.$$

Therefore,

$$\begin{aligned} \mathrm{d}\xi^1 &= n^{-1}(x)(-\sin\varphi\sin\theta \mathrm{d}\varphi + \cos\varphi\cos\theta \mathrm{d}\theta) \\ \mathrm{d}\xi^2 &= n^{-1}(x)(\cos\varphi\sin\theta \mathrm{d}\varphi + \sin\varphi\cos\theta \mathrm{d}\theta) \\ \mathrm{d}\xi^3 &= n^{-1}(x)(-\sin\theta \mathrm{d}\theta), \end{aligned}$$

$$\begin{aligned} \mathrm{d}\omega_x^3(\xi) &= \sqrt{\det g} \sum_{i=1}^{3} (-1)^{i-1} \xi^i \mathrm{d}\xi^1 \wedge \cdots \wedge \widehat{\mathrm{d}\xi^i} \wedge \cdots \wedge \mathrm{d}\xi^2 \\ &= n^3(x)(\xi^1 \mathrm{d}\xi^2 \wedge \mathrm{d}\xi^3 - \xi^2 \mathrm{d}\xi^1 \wedge \mathrm{d}\xi^3 + \xi^3 \mathrm{d}\xi^1 \wedge \mathrm{d}\xi^2) \\ &= \cos\varphi\sin\theta(\cos\varphi\sin\theta \mathrm{d}\varphi + \sin\varphi\cos\theta \mathrm{d}\theta)(-\sin\theta \mathrm{d}\theta) \\ &\quad - \sin\varphi\sin\theta(-\sin\varphi\sin\theta \mathrm{d}\varphi + \cos\varphi\cos\theta \mathrm{d}\theta)(-\sin\theta \mathrm{d}\theta) \\ &\quad + \cos\theta(-\sin\varphi\sin\theta \mathrm{d}\varphi + \cos\varphi\cos\theta \mathrm{d}\theta)(\cos\varphi\sin\theta \mathrm{d}\varphi + \sin\varphi\cos\theta \mathrm{d}\theta) \\ &= \sin\theta \mathrm{d}\theta \mathrm{d}\varphi \end{aligned} \tag{2.29}$$

and

$$\mathrm{d}\Sigma^3 = \mathrm{d}\omega_x^3(\xi) \wedge \mathrm{d}V^3(x) = n^3(x) \sin\theta \mathrm{d}\theta \wedge \mathrm{d}\varphi \wedge \mathrm{d}x.$$

Given all these measures above leads to the following norms for scalar functions u and tensor fields f of rank m:

$$\|u\|_{L^2(M)} = \left(\int_M u^2 \mathrm{d}V\right)^{\frac{1}{2}} \tag{2.30}$$

$$\|u\|_{L^2(\Omega M)} = \left(\int_{\Omega M} u^2 \mathrm{d}\Sigma\right)^{\frac{1}{2}} \tag{2.31}$$

$$\|u\|_{L^2(\partial_+\Omega M)} = \left(\int_{\partial_+\Omega M} u^2 \mathrm{d}\sigma_+\right)^{\frac{1}{2}} \tag{2.32}$$

$$\|u\|_{L^2(\Omega_x M)} = \left(\int_{\Omega_x M} u^2 \mathrm{d}\omega_x(\xi)\right)^{\frac{1}{2}} \tag{2.33}$$

$$\|f\|_{L^2(S^m\tau'_M)} = \left(\int_M f_{i_1,\ldots,i_m} f^{i_1,\ldots,i_m} \mathrm{d}V\right)^{\frac{1}{2}}. \tag{2.34}$$

For $V \subset \mathbb{R}^N$, let $L^1_{\mathrm{loc}}(V)$ be the space of local integrable functions on V, i.e.,

$$L^1_{\mathrm{loc}}(V) \coloneqq \left\{ f \colon V \to \mathbb{R} \middle| \int_K |f(x)| \mathrm{d}x < \infty \ \forall \text{ compact } K \subset V \right\}.$$

Given that space, it is possible to define weak derivatives: Let $f, g \in L^1_{\mathrm{loc}}(V)$. We call g the α-th weak derivative of f if for all test functions ϕ it holds

$$\int_V g(x)\phi(x)\mathrm{d}x = (-1)^{|\alpha|} \int_V f(x) D^\alpha \phi(x) \mathrm{d}x$$

where $\alpha = (\alpha_1, \ldots, \alpha_N)$ is a multi-index with $\alpha_i \in \mathbb{N}_0$ and

$$|\alpha| = \sum_{i=1}^N \alpha_i \qquad \text{and} \qquad D^\alpha = \frac{\partial^{|\alpha|}}{\partial^{\alpha_1} x_1 \ldots \partial^{\alpha_N} x_N}.$$

All functions that are α-times strongly differentiable are also α-times weakly differentiable. Generalizing the understanding of differentiability leads to the fact that there are Hilbert spaces of weakly differentiable functions by demanding that the weak derivatives are L^2-integrable.

The so-called *Sobolev spaces* $H^k(V)$ are defined by the norm

$$\|u\|_{H^k(V)} = \left(\sum_{|\alpha| \leq k} \|D^\alpha u\|^2_{L^2(V)} \right)^{\frac{1}{2}}$$

being induced by the scalar product

$$\langle u, v \rangle_{H^k(V)} = \sum_{|\alpha| \leq k} \langle D^\alpha u, D^\alpha v \rangle_{L^2(V)}.$$

In (2.18) we considered functions which are additionally time dependent. For this class of functions, we introduce the so-called *Bochner spaces*, see [85]. Assuming that a function is known on a finite interval $[0, T]$, we define

$$L^2(0, T; H^k(V)) = \left\{ u \colon [0, T] \times V \to \mathbb{R} \middle| \|u\|_{L^2(0,T;H^k(V))} < \infty \right\},$$

where

$$\|u\|_{L^2(0,T;H^k(V))} = \left(\int_0^T \|u(t)\|^2_{H^k(V)} \mathrm{d}t \right)^{\frac{1}{2}}.$$

Similarly, we can define

$$H^l(0, T; H^k(V)) = \left\{ u \colon [0, T] \times V \to \mathbb{R} \middle| \|u\|_{H^l(0,T;H^k(V))} < \infty \right\},$$

where

$$\|u\|_{H^l(0,T;H^k(V))} = \left(\sum_{i=1}^{l} \|\partial_t^i u\|^2_{L^2(0,T;H^k(V))} \right)^{\frac{1}{2}}.$$

Given these norms, it is possible to prove a continuity estimate of (2.17) and (2.18) for tensor fields that are weakly smooth in time and space.

Theorem 2.5. *Let (M, g) be a Riemannian manifold with $g_{ij} = n^2(x)\delta_{ij}$ and $n \geq 1$. Further, let $\alpha \in H^k(\Omega M)$ with $\alpha \geq \alpha_0 > 0$. Then, $\mathcal{I}^d_\alpha$ from (2.18) is bounded, i.e., for all $l \in \mathbb{N}_0$ there is a constant $C = C(T, \alpha, \Omega M) > 0$, such that*

$$\|\mathcal{I}^d_\alpha f\|_{H^l(0,T;H^k(\partial_+ \Omega M))} \leq C \|f\|_{H^l(0,T;H^k(S^m \tau'_M))}. \tag{2.35}$$

Proof. In this proof, we follow Sharafutdinov's approach as outlined in [87], which provides the continuity for the stationary case with $\alpha = 0$.
Let $f \in C^\infty(0,T;S^m\tau'_M)$. For further simplifications we put

$$F(t,x,\xi) = f_{i_1\cdots i_m}(t,x)\xi^{i_1}\cdots\xi^{i_m}.$$

Using (2.24), we have that

$$\begin{aligned}|F(t,x,\xi)|^2 &= |\langle f(t,x),\xi^m\rangle|^2\\ &\le \langle f(t,x),f(t,x)\rangle\cdot\langle \xi_m,\xi^m\rangle\\ &= \langle f(t,x),f(t,x)\rangle\cdot\left(\sum_{i=1}^N \xi_i^2\right)^m\\ &= \langle f(t,x),f(t,x)\rangle\cdot n^{-2m}\\ &\le |f(t,x)|^2.\end{aligned}$$

Hence,

$$\|F\|_{H^l(0,T;H^k(\Omega M))} \le \|f\|_{H^l(0,T;H^k(S^m\tau'_M))}. \tag{2.36}$$

We can rewrite $\mathcal{I}^d_\alpha f$ as

$$\mathcal{I}^d_\alpha f(t,x,\xi) = \int_{\tau_-(x,\xi)}^0 F(t+\tau,\gamma_{x,\xi}(\tau),\dot\gamma_{x,\xi}(\tau))\exp\left(-\int_\tau^0 \alpha(\gamma_{x,\xi}(\sigma),\dot\gamma_{x,\xi}(\sigma))\mathrm{d}\sigma\right)\mathrm{d}\tau. \tag{2.37}$$

By (2.36), it is sufficient to prove

$$\|\mathcal{I}^d_\alpha f\|_{H^l(0,T;H^k(\partial_+\Omega M))} \le \tilde C\|F\|_{H^l(0,T;H^k(\Omega M))}. \tag{2.38}$$

Let $U \subset \Omega M$ and $V \subset \partial_+\Omega M$ be domains with local coordinates $(y^1,...,y^{2N-1})$ and $(z^1,\dots,z^{2N-2})$, respectively. If we take a smooth function φ with supp $\varphi \subset V$, the linearity of the operator $\mathcal{I}^d_\alpha$ implies the sufficiency of showing that

$$\|\varphi\cdot\mathcal{I}^d_\alpha f\|_{H^l(0,T;H^k(V))} \le \tilde C\|F\|_{H^l(0,T;H^k(U))}.$$

For $|\kappa| \le k$ and fixed t we obtain by using the product rule

$$
\begin{aligned}
&\partial_z^\kappa \left(\varphi(x,\xi)\mathcal{I}_\alpha^d f(t,x,\xi)\right)\\
&= \sum_{\beta+\gamma+\delta=\kappa} (\partial_z^\gamma \varphi)(x,\xi) \int_{\tau_-(x,\xi)}^0 \partial_z^\beta \left(F(t+\tau,\gamma_{x,\xi}(\tau),\dot\gamma_{x,\xi}(\tau))\right) \partial_z^\delta \exp\left(-\int_\tau^0 \alpha(\gamma_{x,\xi}(\sigma),\dot\gamma_{x,\xi}(\sigma))\mathrm{d}\sigma\right)\mathrm{d}\tau\\
&+ \sum_{\substack{\beta+\gamma+\delta=\kappa\\ \delta<\kappa}} C^\kappa_{\beta\gamma\delta} (\partial_z^\beta \varphi)(x,\xi)(\partial_z^\gamma \tau_-)(x,\xi)\times\\
&\times \partial_z^\delta \left(F(t+\tau_-(x,\xi),\gamma_{x,\xi}(\tau_-(x,\xi)),\dot\gamma_{x,\xi}(\tau_-(x,\xi)) \exp\left(-\int_{\tau_-(x,\xi)}^0 \alpha(\gamma_{x,\xi}(\sigma),\dot\gamma_{x,\xi}(\sigma))\mathrm{d}\sigma\right)\right).
\end{aligned}
\tag{2.39}
$$

According to [89], the function τ_- is smooth and thus all derivatives are locally bounded. In particular, we can define a diffeomorphism $p\colon \partial_+\Omega M \to \partial_-\Omega M$ by

$$
p(x,\xi) \coloneqq (v,\eta) \coloneqq (\gamma_{x,\xi}(\tau_-(x,\xi)),\dot\gamma_{x,\xi}(\tau_-(x,\xi))
$$

Using this transformation, we have that $\tau_-(p^{-1}(v,\eta)) = 0$. Therefore, we can write for $\delta < \kappa$

$$
\begin{aligned}
&\int_V \left|\partial_z^\delta \left(F(t+\tau_-(x,\xi),\gamma_{x,\xi}(\tau_-(x,\xi)),\dot\gamma_{x,\xi}(\tau_-(x,\xi)) \exp\left(-\int_{\tau_-(x,\xi)}^0 \alpha(\gamma_{x,\xi}(\sigma),\dot\gamma_{x,\xi}(\sigma))\mathrm{d}\sigma\right)\right)\right|^2 \mathrm{d}\sigma_+\\
&= \int_{\tilde V} |\partial_{\tilde z}^\delta F(t,\gamma_{v,\eta}(0),\dot\gamma_{v,\eta}(0))|^2 \ |\mathrm{det} Dp(v,\eta)|^{-1} \mathrm{d}\sigma_-
\end{aligned}
$$

with local coordinates $(\tilde z^1,\dots,\tilde z^{2N-2})$ of $\tilde V \subset \partial_-\Omega M$ and surface measure $\mathrm{d}\sigma_-$ of $\tilde V$.
Considering the smoothness of p, the $L^2(V)$-norm of the second sum in (2.39) can be majorized by $\tilde c\|F(t,\cdot,\cdot)\|_{H^{k-1}(\partial_-\Omega M)}$ for $\tilde c = \tilde c(\Omega M)$ and all $t \in [0,T]$.
Since the trace operator

$$
\gamma_-\colon H^l(0,T;H^k(\Omega M)) \to H^l(0,T;H^{k-1}(\partial_-\Omega M)), \qquad F \mapsto F|_{\partial_-\Omega M}
$$

is bounded, we can even estimate the second sum in (2.39) by $\tilde c\|F(t,\cdot,\cdot)\|_{H^k(V)}$. The integral on the right-hand side of (2.39) can be estimated using Cauchy-Schwarz:

$$
\begin{aligned}
&\left|\int_{\tau_-(x,\xi)}^0 \partial_z^\beta \left(F(t+\tau,\gamma_{x,\xi}(\tau),\dot\gamma_{x,\xi}(\tau))\right) \partial_z^\delta \exp\left(-\int_\tau^0 \alpha(\gamma_{x,\xi}(\sigma),\dot\gamma_{x,\xi}(\sigma))\mathrm{d}\sigma\right)\mathrm{d}\tau\right|^2\\
&\le \int_{\tau_-(x,\xi)}^0 1\mathrm{d}\tau \cdot \int_{\tau_-(x,\xi)}^0 \left|\partial_z^\beta \left(F(t+\tau,\gamma_{x,\xi}(\tau),\dot\gamma_{x,\xi}(\tau))\right) \partial_z^\delta \exp\left(-\int_\tau^0 \alpha(\gamma_{x,\xi}(\sigma),\dot\gamma_{x,\xi}(\sigma))\mathrm{d}\sigma\right)\right|^2 \mathrm{d}\tau\\
&= -\tau_-(x,\xi) \int_{\tau_-(x,\xi)}^0 \left|\partial_z^\beta \left(F(t+\tau,\gamma_{x,\xi}(\tau),\dot\gamma_{x,\xi}(\tau))\right) \partial_z^\delta \exp\left(-\int_\tau^0 \alpha(\gamma_{x,\xi}(\sigma),\dot\gamma_{x,\xi}(\sigma))\mathrm{d}\sigma\right)\right|^2 \mathrm{d}\tau\\
&= -\tau_-(x,\xi) \int_{\tau_-(x,\xi)}^0 \sum_{\gamma\le\beta} C^\alpha_{\beta\gamma}(t,x,\xi) \left|\partial_y^\gamma \left(F(t+\tau,\gamma_{x,\xi}(\tau),\dot\gamma_{x,\xi}(\tau))\right)\right|^2 \mathrm{d}\tau.
\end{aligned}
$$

The factors $C^{\alpha}_{\beta\gamma}(t,x,\xi)$ are smooth functions. Integrating both sides of the last inequality leads to

$$\begin{aligned}&\Big|\Big|\int_{\tau_-(x,\xi)}^{0}\partial_z^{\beta}\left(F(t+\tau,\gamma_{x,\xi}(\tau),\dot\gamma_{x,\xi}(\tau))\right)\partial_z^{\delta}\exp\Big(-\int_{\tau}^{0}\alpha(\gamma_{x,\xi}(\sigma),\dot\gamma_{x,\xi}(\sigma))\mathrm{d}\sigma\Big)\,\mathrm{d}\tau\Big|\Big|^2_{L^2(V)}\\ &\leq\int_V\sum_{\gamma\leq\beta}C^{\alpha}_{\beta\gamma}\int_{\tau_-(x,\xi)}^{0}|\tau_-(x,\xi)|\cdot|\partial_z^{\gamma}\left(F(t+\tau,\gamma_{x,\xi}(\tau),\dot\gamma_{x,\xi}(\tau))\right)|^2\mathrm{d}\tau\mathrm{d}z.\end{aligned}$$

We substitute all arguments of F by $G(t,x,\xi;\tau)$, i.e.,

$$G(t,x,\xi;\tau)=(t+\tau,\gamma_{x,\xi}(\tau),\dot\gamma_{x,\xi}(\tau)),$$

similarly to the mapping constructed in Corollary 3.3.3 of [89]. Therefore, we can adapt Santaló's formula (c.f. Lemma 3.3.2 of [89]), which becomes

$$\int_{\Omega M}\psi(t,x,\xi)\mathrm{d}\Sigma=\int_{\partial_+(\Omega M)}\int_{\tau_-(x,\xi)}^{0}\psi(t+\tau,\gamma_{x,\xi}(\tau),\dot\gamma_{x,\xi}(\tau))\langle\nu(x),\xi\rangle\mathrm{d}\tau\mathrm{d}\sigma_+$$

for any $\psi\in C(\Omega M)$, and obtain

$$\begin{aligned}&\Big|\Big|\int_{\tau_-(x,\xi)}^{0}\partial_z^{\beta}\left(F(t+\tau,\gamma_{x,\xi}(\tau),\dot\gamma_{x,\xi}(\tau))\right)\partial_z^{\delta}\exp\Big(-\int_{\tau}^{0}\alpha(\gamma_{x,\xi}(\sigma),\dot\gamma_{x,\xi}(\sigma))\mathrm{d}\sigma\Big)\,\mathrm{d}\tau\Big|\Big|^2_{L^2(V)}\\ &\leq\int_U\sum_{\gamma\leq\beta}C^{\beta}_{\gamma}\Big|\frac{\tau_-(x,\xi)}{\langle\xi,\nu(x)\rangle}\Big|\partial_y^{\gamma}\left(F(t,y)\right)|^2\mathrm{d}y.\end{aligned}$$

By Lemma 4.1.1 in [87], the function $\tau_-:\partial_+\Omega M\to\mathbb{R}$ is smooth. Since $\tau_-(x,\xi)=0$ for (x,ξ) with $\langle\nu(x),\xi\rangle=0$, the function $\tau_-(x,\xi)/\langle\nu(x),\xi\rangle$ is bounded. This leads to the final estimation

$$\begin{aligned}&\Big|\Big|\int_{\tau_-(x,\xi)}^{0}\partial_z^{\beta}\left(F(t+\tau,\gamma_{x,\xi}(\tau),\dot\gamma_{x,\xi}(\tau))\right)\partial_z^{\delta}\exp\Big(-\int_{\tau}^{0}\alpha(\gamma_{x,\xi}(\sigma),\dot\gamma_{x,\xi}(\sigma))\mathrm{d}\sigma\Big)\,\mathrm{d}\tau\Big|\Big|^2_{L^2(V)}\\ &\leq\tilde c_t\|F(t,\cdot,\cdot)\|_{H^k(U)}.\end{aligned}$$

Computing strong derivatives of F, we proved that for fixed t

$$\|\mathcal{I}^d_\alpha f(t,\cdot,\cdot)\|_{H^k(\partial_+\Omega M)}\leq c_t\|f(t,\cdot)\|_{H^k(S^m\tau'_M)}\tag{2.40}$$

for $f(t,\cdot)\in H^k(S^m\tau'_M)$, where c_t depends continuously on t. Hence,

$$\begin{aligned}\|\mathcal{I}_\alpha^d f\|^2_{L^2(0,T;H^k(\partial_+\Omega M))} &= \int_0^T \|\mathcal{I}_\alpha^d f(t,\cdot,\cdot)\|^2_{H^k(\partial_+\Omega M)}\mathrm{d}t \\ &\leq \int_0^T c_t^2 \|f(t,\cdot,\cdot)\|^2_{H^k(S^m\tau'_M)}\mathrm{d}t \\ &\leq \sup_{t\in[0,T]} c_t^2 \cdot \int_0^T \|f(t,\cdot,\cdot)\|^2_{H^k(S^m\tau'_M)}\mathrm{d}t \\ &= C^2\|f\|^2_{L^2(0,T;H^k(S^m\tau'_M))}\end{aligned}$$

where $C \coloneqq \sup_{t\in[0,T]} c_t < \infty$. This proves (2.35) for arbitrary $k \in \mathbb{N}$ and $l = 0$. Let now $l \geq 0$. By Hölder's inequality, the integrand of (2.18) is L^1-integrable. Thus, one can interchange the integration over τ and the differentiation concerning the time variable t yielding

$$\begin{aligned}\|\partial_t^l \mathcal{I}_\alpha^d f\|_{L^2(0,T;H^k(\partial_+(\Omega M))} &= \|\mathcal{I}_\alpha^d \partial_t^l f\|_{L^2(0,T;H^k(\partial_+(\Omega M))} \\ &\leq C\|\partial_t^l f\|_{L^2(0,T;H^k(S^m\tau'_M))}\end{aligned}$$

and therefore,

$$\begin{aligned}\|\mathcal{I}_\alpha^d f\|^2_{H^l(0,T;H^k(\partial_+\Omega M))} &= \sum_{i=1}^{l} \|\partial_t^i \mathcal{I}_\alpha^d f\|^2_{L^2(0,T;H^k(\partial_+\Omega M))} \\ &\leq \sum_{i=1}^{l} C^2\|\partial_t^i f\|^2_{L^2(0,T;H^k(S^m\tau'_M))} \\ &\leq C^2\|f\|^2_{H^l(0,T;H^k(S^m\tau'_M))}.\end{aligned}$$

The proof now follows by a standard density argument. □

The inverse problem consists of recovering f from given measurement data $\mathcal{I}_\alpha f$, respectively $\mathcal{I}_\alpha^d f$. Instead of inverting the integral transforms we can consider an inverse source problem for a corresponding transport equation. This is subject of the next section.

2.2 Modelling of the direct problem as a solution of a transport equation

This section consists of two parts. In the first part, it is demonstrated that the extensions of $\mathcal{I}_\alpha f$ and $\mathcal{I}_\alpha^d f$ solve a boundary value problem on the entire domain ΩM. Subsequently, the unique solvability of this problem is investigated. Without loss of generality, we assume that M is the strictly convex N-dimensional unit ball. This assumption enables the establishment of a unique outward normal on ∂M. This assumption is justified by the practical application of M being a bounded N-dimensional connected set, capable of being scaled and translated into a corresponding unit ball.

2.2.1 Derivation of the transport equation

It suffices to derive the transport equation for the dynamic case which directly implies the equation for static tensor fields. We primarily rely on the explanations of [101]. Let (M, g) be the Riemannian manifold with $g_{ij}(x) = n^2(x)\delta_{ij}$ and $n \in C^2(M)$,

$$T^0M := \{(x, \xi) \in TM | \xi \neq 0\},$$

$\alpha \in L^\infty(\Omega M)$, $\alpha \geq 0$, and $f = (f_{i_1,\dots,i_m}) \in L^2(0, T; L^2(S^m\tau'_M))$. As an extension of $\mathcal{I}_\alpha^d f$ to T^0M we define the function $u\colon [0, T] \times T^0M \to \mathbb{R}$ by

$$\begin{aligned} u(t, x, \xi) = \int_{\tau_-(x,\xi)}^0 & f_{i_1,\dots,i_m}(t + \tau, \gamma_{x,\xi}(\tau))\dot\gamma_{x,\xi}^{i_1}(\tau) \cdots \dot\gamma_{x,\xi}^{i_m}(\tau) \times \\ & \times \exp\left(-\int_\tau^0 \alpha(\gamma_{x,\xi}(\sigma), \dot\gamma_{x,\xi}(\sigma))\mathrm{d}\sigma\right) \mathrm{d}\tau. \end{aligned} \tag{2.41}$$

It can be observed that for $(x, \xi) \in \partial_+\Omega M$ this integral coincides with $\mathcal{I}_\alpha^d f$ and for $(x, \xi) \in \partial_-\Omega M$ that the integral vanishes since τ_- is zero. Next, we show that (2.41) is a solution of a transport equation. Similar results have been obtained in [87] for static fields without absorption and constant refractive index n in [25]. Let $(x, \xi) \in T^0M \backslash T(\partial M)$ and $\gamma = \gamma_{x,\xi} : [\tau_-(x, \xi), \tau_+(x, \xi)] \to M$ be a geodesic uniqueley determined by the initial conditions $\gamma_{x,\xi}(0) = x$, and $\dot\gamma_{x,\xi}(0) = \xi$. According to the definition and the smoothness of γ, its length is finite. We assume that the interval of definition cannot be further extended. Therefore, the interval boundaries can also be characterized by

$$\begin{aligned} \tau_-(x, \xi) &= \max\{\tau \in (-\infty, 0] : \gamma_{x,\xi}(t) \cap \partial M \neq \emptyset\}, \\ \tau_+(x, \xi) &= \min\{\tau \in [0, \infty) : \gamma_{x,\xi}(t) \cap \partial M \neq \emptyset\}. \end{aligned}$$

Choosing a sufficiently small $s \in \mathbb{R}$, we set $t_s = t + s$, $x_s = \gamma(s)$ and $\xi_s = \dot\gamma(s)$.

Then, $\gamma_{x_s,\xi_s}(\tau) = \gamma(\tau + s)$ and $\tau_-(x_s, \xi_s) = \tau_-(x, \xi) - s$ yield

$$\begin{aligned} u(t+s, x_s, \xi_s) &= \int_{\tau_-(x_s,\xi_s)}^{0} f_{i_1,\dots,i_m}(t_s + \tau, \gamma_{x_s,\xi_s}(\tau))\dot{\gamma}^{i_1}_{x_s,\xi_s}(\tau)\cdots\dot{\gamma}^{i_m}_{x_s,\xi_s}(\tau)\times \\ &\qquad \times \exp\left(-\int_\tau^0 \alpha(\gamma_{x_s,\xi_s}(\sigma), \dot{\gamma}_{x_s,\xi_s}(\sigma))\mathrm{d}\sigma\right)\mathrm{d}\tau \\ &= \int_{\tau_-(x,\xi)}^{s} f_{i_1,\dots,i_m}(t+\tau, \gamma_{x,\xi}(\tau))\dot{\gamma}_{x,\xi}(\tau)^{i_1}\cdots\dot{\gamma}_{x,\xi}(\tau)^{i_m}\times \\ &\qquad \times \exp\left(-\int_\tau^s \alpha(\gamma_{x,\xi}(\sigma), \dot{\gamma}_{x,\xi}(\sigma))\mathrm{d}\sigma\right)\mathrm{d}\tau. \end{aligned} \tag{2.42}$$

The next step is to differentiate this equation with respect to s and to evaluate it at $s = 0$. For the left-hand side, we get

$$\begin{aligned} \frac{\partial u}{\partial t} + \dot{\gamma}^k(0)\frac{\partial u}{\partial x_k} + \ddot{\gamma}^k(0)\frac{\partial u}{\partial \xi^k} &= \frac{\partial u}{\partial t} + \dot{\gamma}^k(0)\frac{\partial u}{\partial x_k} - \Gamma^k_{ij}(\gamma(0))\dot{\gamma}^i(0)\dot{\gamma}^j(0)\frac{\partial u}{\partial \xi^k} \\ &= \frac{\partial u}{\partial t} + \langle \nabla_x u, \xi\rangle - \Gamma^k_{ij}(x)\xi^i\xi^j\frac{\partial u}{\partial \xi^k} \\ &= \frac{\partial u}{\partial t} + \mathcal{H}u, \end{aligned}$$

where $\mathcal{H}$ denotes the *geodesic vector field* defined by

$$\mathcal{H}u := \langle \nabla_x u, \xi\rangle - \Gamma^k_{ij}(x)\xi^i\xi^j\frac{\partial u}{\partial \xi^k}.$$

For brevity, we write

$$\begin{aligned} U(\tau) &= f_{i_1,\dots,i_m}(t+\tau, \gamma_{x,\xi}(\tau))\dot{\gamma}^{i_1}_{x,\xi}(\tau)\cdots\dot{\gamma}^{i_m}_{x,\xi}(\tau), \\ V(\tau, s) &= \exp\left(-\int_\tau^s \alpha(\gamma_{x,\xi}(\sigma), \dot{\gamma}_{x,\xi}(\sigma))\mathrm{d}\sigma\right). \end{aligned}$$

Then, the right hand side of (2.42) reads as

$$\int_{\tau_-(x,\xi)}^{s} U(\tau)V(\tau, s)\mathrm{d}\tau.$$

Let us define $W(\tau, s)$ as an antiderivative of $U(\tau)V(\tau, s)$ with respect to t, i.e.,

$$W(\tau, s) = \int U(\tau)V(\tau, s)\mathrm{d}\tau.$$

The function is only uniquely defined up to a constant, which can be neglected since we are only interested in its derivatives. Note that $[\tau_-(x, \xi), s]$ is bounded.

The fact that $\alpha \geq 0$ leads to the boundedness of the function V, i.e., $V(\tau, s) \leq 1$, and we obtain

$$\frac{\partial}{\partial s} W(\tau, s) = \int U(\tau) \frac{\partial V}{\partial s}(\tau, s) \mathrm{d}\tau.$$

Therefore,

$$\begin{aligned}
\frac{\mathrm{d}}{\mathrm{d}s} \int_{\tau_-(x,\xi)}^{s} U(\tau) V(\tau, s) \mathrm{d}\tau &= \frac{\mathrm{d}}{\mathrm{d}s} W(s, s) - \frac{\partial}{\partial s} W(\tau, s) \\
&= \frac{\partial W}{\partial \tau}(\tau, s)\Big|_{\tau=s} + \frac{\partial W}{\partial s}(\tau, s)\Big|_{\tau=s} - \frac{\partial}{\partial s} W(\tau, s) \\
&= U(s) \underbrace{V(s, s)}_{=1} + \int_{\tau_-(x,\xi)}^{s} U(\tau) \frac{\partial V}{\partial s}(\tau, s) \mathrm{d}\tau \\
&= U(s) + \int_{\tau_-(x,\xi)}^{s} U(\tau) \frac{\partial V}{\partial s}(\tau, s) \mathrm{d}\tau.
\end{aligned}$$

Using that

$$\frac{\partial V}{\partial s}(\tau, s) = -\alpha(\gamma_{x,\xi}(s), \dot{\gamma}_{x,\xi}(s)) V(\tau, s),$$

we obtain

$$\begin{aligned}
\lim_{s \to 0} \frac{\mathrm{d}}{\mathrm{d}s} \int_{\tau_-(x,\xi)}^{s} U(\tau) V(\tau, s) \mathrm{d}\tau &= f_{i_1,\ldots,i_m}(t, \gamma_{x,\xi}(0)) \dot{\gamma}_{x,\xi}^{i_1}(0) \cdots \dot{\gamma}_{x,\xi}^{i_m}(0) \\
&\quad - \alpha(x, \xi) \int_{\tau_-(x,\xi)}^{0} U(\tau) V(\tau, 0) \mathrm{d}\tau \\
&= f_{i_1,\ldots,i_m}(t, x) \xi^{i_1} \cdots \xi^{i_m} - \alpha(x, \xi) u(t, x, \xi).
\end{aligned}$$

Finally, we conclude that

$$\left(\frac{\partial}{\partial t} + \mathcal{H} + \alpha(x, \xi) \right) u(t, x, \xi) = f_{i_1,\ldots,i_m}(t, x) \xi^{i_1} \cdots \xi^{i_m}. \tag{2.43}$$

Note that furthermore, u satisfies the boundary conditions

$$u(t, x, \xi) = \begin{cases} \mathcal{I}_\alpha^d f(t, x, \xi) =: \phi(t, x, \xi), & (x, \xi) \in \partial_+ \Omega M, t \in [0, T] \\ 0, & (x, \xi) \in \partial_- \Omega M, t \in [0, T] \end{cases}. \tag{2.44}$$

Because of (2.41) a natural initial value for u is given by

$$u(0, x, \xi) = 0, \tag{2.45}$$

assuming that there is no flow f for $t < 0$. For static tensor fields f, (2.43) and (2.44) turn into

$$(\mathcal{H} + \alpha(x, \xi))\, u(x, \xi) = f_{i_1,\ldots,i_m}(x)\xi^{i_1} \cdots \xi^{i_m} \tag{2.46}$$

and

$$u(x, \xi) = \begin{cases} \phi(x, \xi), & (x, \xi) \in \partial_+ \Omega M \\ 0, & (x, \xi) \in \partial_- \Omega M \end{cases} \tag{2.47}$$

for given $\phi = \mathcal{I}_\alpha f$, see [87]. Instead of computing f from $\mathcal{I}_\alpha^d f$, $\mathcal{I}_\alpha f$, respectively, the inverse problem can now be re-formulated as inverse source problems for (2.43), (2.46): Given the constraints (2.43) and (2.44), (2.46) and (2.47), respectively, compute f from ϕ. Along with this, it is very important that the initial- and boundary-value problems have unique solutions which leads to a well-defined parameter-to-solution map $f \mapsto u$. As it has been shown in [31] for the Euclidean case, it turns out that indeed this is not satisfied in general. As a remedy, we consider viscosity solutions. This is the subject of the following subsection.

2.2.2 Uniqueness of viscosity solutions

We focus on the existence and uniqueness of weak solutions for (2.43) given the boundary conditions (2.44) and the initial condition (2.45). First, we consider static fields f. To derive the weak formulation of (2.46) we multiply both sides by a test function $v \in H_0^1(\Omega M)$ and integrate over ΩM. Let

$$\gamma_+ : H^1(\Omega M) \to L^2(\partial_+ \Omega M)$$

be the trace operator restricting a function from ΩM to $\partial_+ \Omega M$. This results in the following weak formulation:

Find $u \in H^1(\Omega M)$ such that

$$a(u,v) = b(v), \qquad v \in H_0^1(\Omega M)$$

where the bilinear form $a : H^1(\Omega M) \times H^1(\Omega M) \to \mathbb{R}$ is given as

$$a(u,v) := \int_{\Omega M} \left(\langle \nabla_x u, \xi \rangle v - \Gamma_{ij}^k(x) \xi^i \xi^j \frac{\partial u}{\partial \xi^k} v + \alpha u v \right) \mathrm{d}\Sigma \tag{2.48}$$

and the linear functional $b : H^1(\Omega M) \to \mathbb{R}$ as

$$b(v) := \int_{\Omega M} f_{i_1,\dots,i_m} \xi^{i_1} \cdots \xi^{i_m} v \mathrm{d}\Sigma.$$

According to standard results such as [57, Theorem 2.1], the bilinear form a must be H^1-coercive to prove the uniqueness of a weak solution, which is not fulfilled. As a remedy, we turn over to *viscosity solutions* as investigated in [19]. By adding a small multiple of the Laplace-Beltrami operator to the first-order differential operator of the original equation we transform the transport equation into an elliptic equation. For the arising elliptic problem, we want to prove the coercivity and thus the unique solvability by using the Lax-Milgram Theorem.

Remark 2.6. *One reason the term "viscosity solution" is used for perturbated PDEs, despite it being a misuse of notation, is the convergence that these solutions exhibit. As $\varepsilon \to 0$, the solutions u_ε often converge to a viscosity solution of the unperturbed equation.*

To arrange the following computations more clearly, we split the Laplacian from (A.11) into $\Delta = \Delta_x + \Delta_\xi$, where

$$\Delta_x := n^{-2}(x) \sum_i \frac{\partial^2}{\partial x_i^2} + (N-2) n^{-3}(x) \sum_i \frac{\partial n}{\partial x_i} \frac{\partial}{\partial x_i},$$
$$\Delta_\xi := n^{-2}(x) \sum_i \frac{\partial^2}{\partial (\xi^i)^2}.$$

The following propositions are useful to prove the uniqueness of viscosity solutions.

Lemma 2.7. *Let $u, v \in H^1(\Omega M)$. Then, we have*

$$-\int_{\Omega M} \Delta_x u v \mathrm{d}\Sigma = \int_{\Omega M} \langle \nabla_x u, \nabla_x v \rangle \, \mathrm{d}\Sigma - \int_{\partial_+ \Omega M} v \nabla_\nu u \mathrm{d}\sigma_+, \tag{2.49}$$

as well as

$$-\int_{\Omega M} \Delta_\xi u v \mathrm{d}\Sigma = \int_{\Omega M} \langle \nabla_\xi u, \nabla_\xi v \rangle \, \mathrm{d}\Sigma. \tag{2.50}$$

Particularly, we get for $u \in H_0^1(\Omega M)$

$$-\int_{\Omega M} \Delta_x u u \mathrm{d}\Sigma = \int_{\Omega M} \langle \nabla_x u, \nabla_x u \rangle \, \mathrm{d}\Sigma. \tag{2.51}$$

The two statements follow directly from Green's formula. For the second part, one uses that $\partial(\Omega_x M) = \emptyset$. The following lemma is useful to rewrite the bilinear form.

Lemma 2.8. *Let $N = 2, 3$ and $u, v \in H^1(\Omega M)$. Then, the following identities hold:*

$$-\int_{\Omega_x M} \Gamma_{ij}^k \xi^i \xi^j \frac{\partial u}{\partial \xi^k} w \mathrm{d}\omega_x(\xi) = \int_{\Omega_x M} \Gamma_{ij}^k \xi^i \xi^j \frac{\partial w}{\partial \xi^k} u + n^{-1}(x) \langle \nabla n, \xi \rangle u w \mathrm{d}\omega_x(\xi), \quad N = 2, \tag{2.52}$$

$$-\int_{\Omega_x M} \Gamma_{ij}^k \xi^i \xi^j \frac{\partial u}{\partial \xi^k} w \mathrm{d}\omega_x(\xi) = \int_{\Omega_x M} \Gamma_{ij}^k \xi^i \xi^j \frac{\partial w}{\partial \xi^k} u + 2n^{-1}(x) \langle \nabla n, \xi \rangle u w \mathrm{d}\omega_x(\xi), \quad N = 3. \tag{2.53}$$

Proof. See Appendix (A.1). □

From Lemma 2.8, one directly gets the following corollary.

Corollary 2.9. *Let $N = 2, 3$ and $u, v \in H^1(\Omega M)$. Then, the following identities hold:*

$$-\int_{\Omega_x M} \Gamma_{ij}^k \xi^i \xi^j \frac{\partial u}{\partial \xi^k} u \mathrm{d}\omega_x(\xi) = \frac{1}{2} \int_{\Omega_x M} n^{-1}(x) \langle \nabla n, \xi \rangle u^2 \mathrm{d}\omega_x(\xi), \quad N = 2, \tag{2.54}$$

$$-\int_{\Omega_x M} \Gamma_{ij}^k \xi^i \xi^j \frac{\partial u}{\partial \xi^k} u \mathrm{d}\omega_x(\xi) = \int_{\Omega_x M} n^{-1}(x) \langle \nabla n, \xi \rangle u^2 \mathrm{d}\omega_x(\xi), \quad N = 3. \tag{2.55}$$

Proof. Set $u = w$ in (2.52) and (2.53). □

The next theorem is used for proving the uniqueness of solutions in general elliptic PDEs.

Theorem 2.10. *(Lax-Milgram Theorem)*
Let V be a Hilbert space, $a(\cdot,\cdot) : V \times V \to \mathbb{R}$ a coercive and continuous coercive bilinear form, i.e., there exist $c_1, c_2 > 0$ such that

$$\begin{aligned} a(u,u) &\geq c_1 \|u\|_V^2 \quad \forall u \in V \\ |a(u,v)| &\leq c_2 \|u\|_V \|v\|_V \quad \forall u, v \in V, \end{aligned}$$

and $b \in V'$ be a linear bounded functional, i.e., there exists $c_3 > 0$ such that

$$|b(v)| \leq c_3 \|v\|.$$

Then, the solution u of the variational problem

$$a(u,v) = b(v) \quad \forall v \in V$$

exists and is unique.

Proof. See Theorem 1.1 in [57]. □

By definition, a viscosity solution to (2.46) solves the equation

$$-\varepsilon \Delta u + \langle \nabla_x u, \xi \rangle + \alpha u - \Gamma_{ij}^k \xi^i \xi^j \frac{\partial u}{\partial \xi^k} = f_{i_1,\dots,i_m}(x) \xi^{i_1} \cdots \xi^{i_m}, \tag{2.56}$$

for $\varepsilon > 0$. Multiplying both sides with a test function $v \in H^1(\Omega M)$ and integrating over ΩM leads to

$$\int_{\Omega M} -\varepsilon \Delta u v + \langle \nabla_x u, \xi \rangle v + \alpha u v - \Gamma_{ij}^k \xi_i \xi_j \frac{\partial u}{\partial \xi_k} v \mathrm{d}\Sigma = \int_{\Omega M} f_{i_1,\dots,i_m}(x) \xi^{i_1} \cdots \xi^{i_m} v \mathrm{d}\Sigma.$$

We derive the variational formulation of the boundary value problem by setting

$$\begin{aligned} a_\varepsilon(u,v) &= \int_{\Omega M} -\varepsilon \Delta u v \mathrm{d}\Sigma + a(u,v) \\ &= \int_{\Omega M} \varepsilon \langle \nabla u, \nabla v \rangle \mathrm{d}\Sigma - \int_{\partial_+ \Omega M} \varepsilon v \nabla_\nu u \mathrm{d}\sigma_+ + a(u,v) \qquad (2.57) \\ b^\varepsilon(v) &= \int_{\Omega M} f_{i_1,\dots,i_m}(x) \xi^{i_1} \cdots \xi^{i_m} v \mathrm{d}\Sigma. \qquad (2.58) \end{aligned}$$

Since $u|_{\partial_+ \Omega M} \neq 0$, to prove coercivity, we split u into two parts. We assume that there is a $H^1(\Omega M)$-extension $\hat{\phi}$ of ϕ, i.e., $\hat{\phi}|_{\partial_+ \Omega M} = \phi$. Then, the function $\tilde{u} = u - \hat{\phi}$ lies in $V = H_0^1(\Omega M)$ and solves

$$
\begin{aligned}
(-\varepsilon\Delta + \mathcal{H} + \alpha)\tilde{u} &= (-\varepsilon\Delta + \mathcal{H} + \alpha)u - (-\varepsilon\Delta + \mathcal{H} + \alpha)\hat{\phi} \\
&= \langle f, \xi^m \rangle - (-\varepsilon\Delta + \mathcal{H} + \alpha)\hat{\phi}
\end{aligned}
$$

and $\tilde{u} = 0$ on $\partial_+\Omega M$. Consequently, the final weak formulation of (2.56) along with the boundary condition (2.47) is given by:

Find $\hat{\phi} \in H^1(\Omega M)$ such that $\gamma_+\hat{\phi} = \phi$ and $u_\varepsilon \in H_0^1(\Omega M)$ such that

$$
a_\varepsilon(u_\varepsilon, v) = b_\phi^\varepsilon(v), \qquad \forall v \in H_0^1(\Omega M), \tag{2.59}
$$

where

$$
\begin{aligned}
a_\varepsilon(u, v) &= \int_{\Omega M} \varepsilon\langle \nabla u, \nabla v\rangle \mathrm{d}\Sigma - \int_{\partial_+\Omega M} \varepsilon v \nabla_\nu u \mathrm{d}\sigma_+ + a(u, v) \\
b_\phi^\varepsilon(v) &= b_\varepsilon(v) - a_\varepsilon(\hat{\phi}, v)
\end{aligned}
$$

and set $u_{\phi,\varepsilon} = u_\varepsilon + \hat{\phi} \in H^1(\Omega M)$.

The variational problem (2.59) has a unique solution under certain conditions.

Theorem 2.11. *Let $\varepsilon > 0$, $\alpha \in L^\infty(\Omega M)$ for $N = 2, 3$ with $\alpha(x, \xi) \geq \alpha_0 > 0$ for all $(x, \xi) \in \Omega M$, $n \in C^1(M)$ and $f \in L^2(S^m\tau_M')$ a m-tensor field. If*

$$
\sup_{x\in M} \frac{\|\nabla n(x)\|}{2n(x)} < \alpha_0, \qquad N = 2 \tag{2.60}
$$

$$
\sup_{x\in M} \frac{\|\nabla n(x)\|}{n(x)} < \alpha_0, \qquad N = 3 \tag{2.61}
$$

then the solution $u_\varepsilon \in H^1(\Omega M)$ of the variational problem (2.59) exists and is unique.

Proof. It is possible to prove this theorem for $N = 2$ and $N = 3$ simultaneously. The only difference comes from the fact that the equations (2.54) and (2.55) differ by a factor $\frac{1}{2}$. We define

$$
\Xi_n(x, \xi) \coloneqq \begin{cases} \frac{1}{2}n^{-1}(x)\langle \nabla n(x), \xi\rangle, & N = 2 \\ n^{-1}(x)\langle \nabla n(x), \xi\rangle, & N = 3. \end{cases} \tag{2.62}
$$

The proof consists of an application of the Lax-Milgram Theorem. To this end, we have to show

- the coercivity of a_ε,
- the continuity of a_ε and
- the continuity of b_ϕ^ε

on $H_0^1(\Omega M)$. Let $0 < \delta < 1$ be sufficiently small such that for $N = 2$,

$$\sup_{x\in M} \frac{\|\nabla n(x)\|}{2n(x)} \leq (1-\delta)\alpha_0, \tag{2.63}$$

and for $N = 3$

$$\sup_{x\in M} \frac{\|\nabla n(x)\|}{n(x)} \leq (1-\delta)\alpha_0, \tag{2.64}$$

is satisfied. Since $v = 0$ on $\partial\Omega M$, the boundary integral in (2.57) vanishes. We split $a_\varepsilon = a_\varepsilon^{(1)} + a_\varepsilon^{(2)}$, where

$$a_\varepsilon^{(1)}(u,v) = \int_{\Omega M} \varepsilon\langle\nabla_x u, \nabla_x v\rangle + \langle\nabla_x u, \xi\rangle v + \delta\alpha uv \mathrm{d}\Sigma$$

$$a_\varepsilon^{(2)}(u,v) = \int_{\Omega M} \varepsilon\langle\nabla_\xi u, \nabla_\xi v\rangle - \Gamma_{ij}^k(x)\xi^i\xi^j\frac{\partial u}{\partial \xi^k}v + (1-\delta)\alpha uv \mathrm{d}\Sigma.$$

One verifies that

$$\begin{aligned}\int_{\Omega M}\langle\nabla_x u, \xi\rangle u \mathrm{d}\Sigma &= \int_{\partial_+\Omega M} u^2\langle\xi,\nu\rangle \mathrm{d}\sigma - \int_{\Omega M}\langle\nabla_x u,\xi\rangle u\mathrm{d}\Sigma,\\ &= -\int_{\Omega M}\langle\nabla_x u,\xi\rangle u\mathrm{d}\Sigma,\end{aligned}$$

where $\mathrm{d}\sigma$ is the measure on $\partial\Omega M$. Hence,

$$\int_{\Omega M}\langle\nabla_x u,\xi\rangle u\mathrm{d}\Sigma = 0, \tag{2.65}$$

and, consequently,

$$a_\varepsilon^{(1)}(u,u) = \int_{\Omega M}\varepsilon\|\nabla_x u\|^2 + \delta\alpha u^2 \mathrm{d}\Sigma.$$

Using equations (2.54)-(2.55) and (2.60)-(2.62) we estimate the second part by

$$\begin{aligned} a_\varepsilon^{(2)}(u,u) &= \int_{\Omega M} \varepsilon \|\nabla_\xi u\|^2 + ((1-\delta)\alpha + \Xi_n(x,\xi))\, u^2 \mathrm{d}\Sigma \\ &\geq \int_{\Omega M} \varepsilon \|\nabla_\xi u\|^2 \mathrm{d}\Sigma. \end{aligned}$$

Adding both parts, we have the coercivity condition

$$\begin{aligned} a_\varepsilon(u,u) &\geq \int_{\Omega M} \varepsilon(\|\nabla_x u\|^2 + \|\nabla_\xi u\|^2) + \delta\alpha u^2 \mathrm{d}\Sigma \\ &\geq \min(\varepsilon, \delta\alpha_0)\, \|u\|^2_{H^1(\Omega M)}. \end{aligned} \tag{2.66}$$

Next, we prove the continuity of a. Using the triangle inequality and (2.57), gives

$$\begin{aligned} |a_\varepsilon(u,v)| \leq & \left| \int_{\Omega M} \varepsilon \left(\langle \nabla_x u, \nabla_x v \rangle + \langle \nabla_\xi u, \nabla_\xi v \rangle \right) \mathrm{d}\Sigma \right| + \left| \int_{\Omega M} \xi^k \frac{\partial u}{\partial x_k} v \mathrm{d}\Sigma \right| \\ & + \left| \int_{\Omega M} \alpha u v \mathrm{d}\Sigma \right| + \left| \int_{\Omega M} \Gamma^k_{ij} \xi^i \xi^j \frac{\partial u}{\partial \xi^k} v \mathrm{d}\Sigma \right|. \end{aligned} \tag{2.67}$$

The first summand can be estimated by using the Cauchy-Schwarz inequality

$$\left| \int_{\Omega M} \varepsilon \left(\langle \nabla_x u, \nabla_x v \rangle + \langle \nabla_\xi u, \nabla_\xi v \rangle \right) \mathrm{d}\Sigma \right| \leq \varepsilon \|u\|_{H^1(\Omega M)} \|v\|_{H^1(\Omega M)}. \tag{2.68}$$

In the same manner, we obtain for the second summand

$$\begin{aligned} \left| \int_{\Omega M} \langle \nabla_x, \xi \rangle v \mathrm{d}\Sigma \right| &= \left| \int_{\Omega M} \langle \nabla_x u, v\xi \rangle \mathrm{d}\Sigma \right| \\ &\leq \left(\int_{\Omega M} \langle \nabla_x u, \nabla_x u \rangle \mathrm{d}\Sigma \right)^{\frac{1}{2}} \cdot \left(\int_{\Omega M} v^2 \mathrm{d}\Sigma \right)^{\frac{1}{2}} \\ &\leq \|u\|_{H^1(\Omega M)} \|v\|_{H^1(\Omega M)}. \end{aligned} \tag{2.69}$$

Moreover,

$$\left| \int_{\Omega M} \alpha u v \mathrm{d}\Sigma \right| \leq \|\alpha\|_{L^\infty(\Omega M)} \|u\|_{L^2(\Omega M)} \|v\|_{L^2(\Omega M)} \tag{2.70}$$

$$\leq \|\alpha\|_{L^\infty(\Omega M)} \|u\|_{H^1(\Omega M)} \|v\|_{H^1(\Omega M)}. \tag{2.71}$$

We use (2.27) for the last part in (2.67) and obtain

$$\begin{aligned}
\left|\int_{\Omega M} -\Gamma_{ij}^k(x)\xi^i\xi^j\frac{\partial u}{\partial \xi^k}v\mathrm{d}\Sigma\right| &= \left|\int_{\Omega M}\left(n^{-3}(x)\frac{\partial n(x)}{\partial x_k} - 2n^{-1}(x)\xi^k\langle\nabla n,\xi\rangle\right)\frac{\partial u}{\partial \xi^k}v\mathrm{d}\Sigma\right| \\
&= \int_{\Omega M} n^{-1}(x)\langle\nabla n,\nabla_\xi u\rangle|v| - 2n^{-1}(x)\langle\nabla n,\xi\rangle\langle\xi,\nabla_\xi u\rangle|v|\mathrm{d}\Sigma \\
&= \int_{\Omega M} n^{-1}(x)\left(\langle\nabla n,\nabla_\xi u\rangle - 2\langle\nabla n,\xi\rangle\langle\xi,\nabla_\xi u\rangle\right)|v|\mathrm{d}\Sigma \\
&\leq \int_{\Omega M} n^{-1}(x)\left(\|\nabla n(x)\|\|\nabla_\xi u\| + 2\|\nabla n(x)\|\|\nabla_\xi u\|\right)|v|\mathrm{d}\Sigma \\
&\leq \int_{\Omega M} 3\frac{\|\nabla n(x)\|}{n(x)}\|\nabla_\xi u\||v|\mathrm{d}\Sigma \\
&\leq 6\|\alpha\|_{L^\infty(\Omega M)}\|\nabla_\xi u\|_{L^2(\Omega M)}\|v\|_{L^2(\Omega M)} \\
&\leq 6\|\alpha\|_{L^\infty(\Omega M)}\|u\|_{H^1(\Omega M)}\|v\|_{H^1(\Omega M)}. \qquad (2.72)
\end{aligned}$$

Finally, with (2.68) - (2.72) we arrive at

$$|a_\varepsilon(u,v)| \leq (\varepsilon + 1 + 7\|\alpha\|_{L^\infty(\Omega M)})\|u\|_{H^1(\Omega M)}\|v\|_{H^1(\Omega M)}.$$

The last step is to prove the continuity of b_ϕ^ε. We compute

$$\begin{aligned}
\left|\int_{\Omega M} f_{i_1,\dots i_m}(x)\xi^{i_1}\cdots\xi^{i_m}v\mathrm{d}\Sigma\right| &\leq \left(\int_{\Omega M}\langle f(x),\xi^m\rangle^2\mathrm{d}\Sigma\right)^{\frac{1}{2}}\cdot\left(\int_{\Omega M}v^2\mathrm{d}\Sigma\right)^{\frac{1}{2}} \\
&\leq c(n)\|f\|_{L^2(S^m\tau_M')}\|v\|_{H^1(\Omega M)}
\end{aligned}$$

for a positive constant $c(n)$ depending on the refractive index n. The continuity of b_ϕ^ε then follows from this estimate and the continuity of a_ε. This completes the proof. □

The continuity conditions for a_ε and b_ϕ^ε hold true also for $\varepsilon = 0$, whereas the coercivity only holds for $\varepsilon > 0$. Theorem (2.11) guarantees that there exists a unique, weak viscous solution if n varies only slowly. Especially in the Euclidean geometry ($n = 1$) conditions (2.60) and (2.61) are valid for any positive α_0. These results are in accordance with those presented in [25]. It is consistent with the observation that in the absence of absorption, the integral transform (2.17) exhibits a non-trivial kernel, encompassing, at least, all potential fields.

Based on the results obtained for static fields, we will now proceed analogously for the dynamic case. Let V be a reflexive and separable Banach space with norm $\|\cdot\|_V$ and V^* its dual space with norm $\|\cdot\|_{V^*}$. The dual pairing is denoted by $\langle\cdot,\cdot\rangle_{V\times V^*}$. Furthermore, let

$$W^{1,1,2}(V,V^*) = \{u \in L^2(0,T;V) : \mathrm{d}_t u \in L^2(0,T;V^*)\},$$

where $\mathrm{d}_t u$ represents the distributional derivative of u. Throughout, we consistently assume $V = H_0^1(\Omega M)$, yielding $V^* = H^{-1}(\Omega M)$. We interpret (2.59) as an abstract operator equation (c.f. [60],[92]) in which

$$A_\varepsilon(u) = f_{i_1,\dots,i_m}\xi^{i_1}\cdots\xi^{i_m} \quad \text{in } V^*,$$

where $A_\varepsilon : V \to V^*$ defined by $A_\varepsilon(u) = a_\varepsilon(u,\cdot)$ constitues a monotone operator. The monotonicity is evident since for all $u_1, u_2 \in V$, we have

$$\begin{aligned}\langle A_\varepsilon(u_1) - A_\varepsilon(u_2), u_1 - u_2\rangle &= \langle A_\varepsilon(u_1 - u_2), u_1 - u_2\rangle \\ &= a_\varepsilon(u_1 - u_2, u_1 - u_2) \\ &\geq 0.\end{aligned}$$

This finding is also applicable to the dynamic equation, as discussed in [80] and [105]. As illustrated in (2.43), the extension u of $\mathcal{I}_\alpha^d f$ satisfies

$$\frac{\partial u}{\partial t} + (\mathcal{H} + \alpha)u = f_{i_1,\dots,i_m}(t,x)\xi^{i_1}\cdots\xi^{i_m}.$$

The corresponding viscosity solution is characterized by

$$\frac{\partial u}{\partial t} - \varepsilon\Delta u + (\mathcal{H} + \alpha)u = f_{i_1,\dots,i_m}(t,x)\xi^{i_1}\cdots\xi^{i_m}$$

and the associated variational formulation reads as:

Find $u_\varepsilon \in W^{1,1,2}(0,T;V,V^*)$ such that

$$\begin{aligned}\langle \mathrm{d}_t u_\varepsilon(t), v\rangle_{V^*,V} + a_\varepsilon(t; u_\varepsilon(t), v) &= \langle b_\phi^\varepsilon(t), v\rangle_{V^*,V}, \\ u_\varepsilon(0) &= 0,\end{aligned} \tag{2.73}$$

for all $v \in V$ and for a.e. $t \in (0,T)$ and set $u_{\phi,\varepsilon}^d = u_\varepsilon + \hat{\phi}$.

Analogously to equation (2.57), the bilinear form a_ε is defined by

$$\begin{aligned}a_\varepsilon(t;u,v) = \int_{\Omega M} &\varepsilon\langle\nabla u(t), \nabla v(t)\rangle + \langle\nabla_x u(t), \xi\rangle v(t) - \Gamma_{ij}^k\xi^i\xi^j\frac{\partial u(t)}{\partial \xi^k}v(t) + \alpha u(t)v(t)\mathrm{d}\Sigma \\ &- \int_{\partial_+\Omega M}\varepsilon\nabla_\nu u(t)v(t)\mathrm{d}\sigma_+\end{aligned}$$

and the linear form b_ϕ^ε is specified by

$$\langle b_\phi^\varepsilon(t), v\rangle = \int_{\Omega M} f_{i_1,\dots,i_m}(t,x)\xi^{i_1}\cdots\xi^{i_m}v(t)\mathrm{d}\Sigma - a_\varepsilon(t,\hat{\phi}(t),v(t)).$$

Due to the Aubin-Lions Lemma, $W^{1,1,2}(V,V^*)\subset C(0,T;L^2(\Omega M))$ holds, ensuring that the point evaluation $u_\varepsilon(0)$ in (2.73) is well-defined. The subsequent theorem represents a standard tool employed to ensure unique solutions of time-dependent differential equations.

Theorem 2.12 (Theorem 3.6 in [4])**.** *Let V be a reflexive Banach space. Assume $b\in V^*$ and that the bilinear form $a(t;\cdot,\cdot): V\times V\to\mathbb{R}$ satisfies the following properties:*

- *The mapping $t\mapsto a(t;u,v)$ is measurable for all $u,v\in V$.*
- *There exists a $c_1>0$: $a(t,u,v)\geq c_1\|u\|_V^2$ for all $t\in(0,T)$.*
- *There exists a $c_2>0$: $|a(t,u,v)|\leq c_2\|u\|_V\|v\|_V$ for all $t\in(0,T)$.*

Then, the equation

$$\langle \mathrm{d}_t u(t), v\rangle_{V^*,V} + a(t,u(t),v) = \langle b, v\rangle_{V^*,V} \qquad \forall v\in V$$

has a unique solution $u\in W^{1,1,2}(0,T;V,V^*)$ satisfying

$$\|u\|_{W^{1,1,2}(V,V^*)}\leq \frac{1}{c_1}\|b\|_{V^*}.$$

Using Theorem 2.12 we get:

Theorem 2.13. *Let $\varepsilon>0$, $\alpha\in L^\infty(\Omega M)$ for $N=2,3$ with $\alpha(x,\xi)\geq\alpha_0>0$ for all $(x,\xi)\in\Omega M$, $n\in C^1(M)$ and $f\in L^2(0,T;S^m\tau_M')$ a m-tensor field. If*

$$\sup_{x\in M}\frac{\|\nabla n(x)\|}{2n(x)}<\alpha_0, \qquad N=2$$

$$\sup_{x\in M}\frac{\|\nabla n(x)\|}{n(x)}<\alpha_0, \qquad N=3$$

then the variational problem (2.73) has a unique solution u_ε.

Proof. The assumption follows directly from Theorem 2.11, Theorem 2.12 and the fact that the bilinear form a_ε is continuous and hence measurable. □

In summary, based on Theorems 2.11 and 2.13, static and dynamic tensor field tomography in a medium with absorption and refraction can be mathematically represented by the linear equations

$$\mathcal{S}_\alpha^\varepsilon f = \phi, \qquad \mathcal{S}_\alpha^{\varepsilon,d} f = \phi$$

for given data ϕ, where

$$\begin{aligned} \mathcal{S}_\alpha^\varepsilon &: L^2(S^m\tau_M') \to L^2(\partial_+\Omega M), \\ \mathcal{S}_\alpha^{\varepsilon,d} &: W^{1,1,2}(0,T;V,V^*) \to L^2(0,T;\partial_+\Omega M) \end{aligned}$$

can be decomposed as

$$\begin{aligned} \mathcal{S}_\alpha^\varepsilon &= \gamma_+ \circ \mathcal{F}_\alpha^\varepsilon, \\ \mathcal{S}_\alpha^{\varepsilon,d} &= \gamma_+ \circ \mathcal{F}_\alpha^{\varepsilon,d} \end{aligned}$$

with parameter-to-solution mappings

$$\begin{aligned} \mathcal{F}_\alpha^\varepsilon &: L^2(S^m\tau_M') \to L^2(\partial\Omega M), && f \mapsto u_{\phi,\varepsilon}, \\ \mathcal{F}_\alpha^{\varepsilon,d} &: W^{1,1,2}(0,T;V,V^*) \to L^2(0,T;\partial\Omega M), && f \mapsto u_{\phi,\varepsilon}^d. \end{aligned}$$

Theorems 2.11 and 2.13 then guarantee that all mappings are well-defined.

2.3 The inverse problem of refractive dynamic tensor tomography (RDTT)

There exist representations of the adjoint operator $\mathcal{I}_\alpha^*$ of the integral transform in a non-Euclidean static setting but only for $\alpha = 0$. Using Santaló's formula it is shown in [20] that

$$[\mathcal{I}_0^*\psi](x) = \int_{\Omega_x M} \psi^\#(x,\xi)\xi^i\xi^j\langle\nu_x,\xi\rangle \mathrm{d}\sigma_x(\xi), \tag{2.74}$$

where $\psi^\#(x,\xi)$ is defined as a function that equals $\psi(x,\xi)$ on $\partial_+\Omega M$ and that is constant along $\gamma_{x,\xi}$. Note that (2.74) looks quite similar to the backprojection operator $\mathcal{R}^*$ used in computerized tomography. In this section, the adjoint operator via transport equations is derived for the attenuated and dynamic case.

Theorem 2.14. *Let $f \in L^2(0,T;L^2(S^m\tau_M'))$ and $\phi = \mathcal{S}_\alpha^d(f)$. Assuming that for any $h \in L^2(0,T;L^2(\partial_+\Omega M))$ there is a unique solution $w \in H^1(0,T;H^1(\Omega M))$ of the adjoint problem*

$$-\frac{\partial w}{\partial t} - \langle\nabla w,\xi\rangle + \Gamma_{ij}^k\xi^i\xi^j\frac{\partial w}{\partial\xi^k} + (\alpha + \Xi_n(x,\xi))\, w = 0, \qquad t\in[0,T], (x,\xi)\in\Omega M \tag{2.75}$$

with boundary and end conditions

$$w(T,x,\xi) = 0, \qquad (x,\xi)\in\Omega M \tag{2.76}$$

$$w(t,x,\xi) = \frac{h(t,x,\xi)}{\langle\nu_x,\xi\rangle}, \qquad t\in[0,T],\ (x,\xi)\in\partial_+\Omega M \tag{2.77}$$

$$w(t,x,\xi) = k_h(t,x,\xi)\exp\left(-\int_0^{\tau_+(x,\xi)}\Big(\alpha+\Xi_n\Big)(\gamma_{x,\xi}(\tilde\tau),\dot\gamma_{x,\xi}(\tilde\tau))\mathrm{d}\tilde\tau\right), \tag{2.78}$$
$$t\in[0,T],\ (x,\xi)\in\partial_-\Omega M$$

where

$$k_h(t,x,\xi) = \frac{h(t,\gamma_{x,\xi}(\tau_+(x,\xi)),\dot\gamma_{x,\xi}(\tau_+(x,\xi)))}{\langle\nu_{\gamma_{x,\xi}(\tau_+(x,\xi)},\dot\gamma_{x,\xi}(\tau_+(x,\xi)\rangle}, \tag{2.79}$$

the adjoint operator can be computed explicitly by

$$[(\mathcal{S}_\alpha^d)^*h](t,x) = \int_{\Omega_x M} w(t,x,\xi)\xi^m \mathrm{d}\sigma_x(\xi) \in L^2(0,T;L^2(S^m\tau_M')).$$

Proof. We consider (2.56) and multiply both sides by a test function $w \in H^1(\Omega M)$ and integrate over $[0,T] \times \Omega M$. Then, the equation becomes

$$\begin{aligned}&\int_0^T \int_{\Omega M} \frac{\partial u}{\partial t} w + \langle \nabla_x u, \xi \rangle w - \Gamma_{ij}^k \xi^i \xi^j \frac{\partial u}{\partial \xi^k} + \alpha u w \, \mathrm{d}\Sigma \mathrm{d}t \\ &= \int_0^T \int_{\Omega M} f_{i_1,\dots,i_m}(t,x) \xi^{i_1} \cdots \xi^{i_m} w \mathrm{d}\Sigma \mathrm{d}t. \end{aligned} \tag{2.80}$$

To rewrite the left side of (2.80), we compute

$$\begin{aligned}\int_0^T \frac{\partial u}{\partial t} w \mathrm{d}t &= u(T)w(T) - u(0)w(0) - \int_0^T u \frac{\partial w}{\partial t} \mathrm{d}t \\ &= u(T)w(T) - \int_0^T u \frac{\partial w}{\partial t} \mathrm{d}t. \end{aligned} \tag{2.81}$$

Next,

$$\int_{\Omega M} \langle \nabla_x u, \xi \rangle w \mathrm{d}\Sigma = \int_{\partial_+ \Omega M} \phi w \langle \xi, \nu_x \rangle \mathrm{d}\sigma - \int_{\Omega M} \langle \nabla_x w, \xi \rangle u \mathrm{d}\Sigma, \tag{2.82}$$

and by (2.52),

$$-\int_{\Omega_x M} \Gamma_{ij}^k \xi^i \xi^j \frac{\partial u}{\partial \xi^k} w \mathrm{d}\Sigma = \int_{\Omega_x M} \Gamma_{ij}^k \xi^i \xi^j \frac{\partial w}{\partial \xi^k} u + \Xi_n(x,\xi) u w \, \mathrm{d}\Sigma. \tag{2.83}$$

Inserting (2.81)-(2.83) into (2.80) yields

$$\int_0^T \int_{\Omega M} u \Big(-\frac{\partial w}{\partial t} - \langle \nabla_x w, \xi \rangle + \Gamma_{ij}^k \xi^i \xi^j \frac{\partial w}{\partial \xi^k} + (\alpha + \Xi_n(x,\xi)) w \Big) \mathrm{d}\Sigma \tag{2.84}$$

$$+ \int_0^T \int_{\partial_+ \Omega M} \phi \Big(w \langle \nu_x, \xi \rangle \Big) \mathrm{d}\sigma \mathrm{d}t \tag{2.85}$$

$$+ \int_{\Omega M} u(T,x,\xi) w(T,x,\xi) \mathrm{d}\Sigma \tag{2.86}$$

$$= \int_0^T \int_{\Omega M} \langle f, w \xi^m \rangle \mathrm{d}\Sigma \mathrm{d}t \tag{2.87}$$

$$= \langle f, (\mathcal{S}_\alpha^d)^* h \rangle_{L^2(0,T;L^2(S^m \tau_M'))}. \tag{2.88}$$

If w solves (2.75)-(2.76), the integrals (2.84) and (2.86) vanish and (2.85) becomes

$$\int_0^T \int_{\Omega M} \phi h \mathrm{d}\Sigma = \langle \mathcal{S}_\alpha^d f, h \rangle_{L^2(0,T;L^2(\Omega M))}.$$

Since u vanishes on $\partial_-\Omega M$, there is so far no information about w on that part of the boundary. To obtain them, we restrict w to a geodesic $\gamma_{x,\xi}$ for some $(x,\xi) \in \Omega M$. Then, we get for $\tilde{w}(\tau) \coloneqq w(t+\tau, \gamma_{x,\xi}(\tau), \dot{\gamma}_{x,\xi}(\tau))$ that

$$\frac{\mathrm{d}\tilde{w}(\tau)}{\mathrm{d}\tau} = \mathcal{H}\tilde{w}(\tau) = (\alpha + \Xi_n)w(\tau) \tag{2.89}$$

and

$$\tilde{w}(\tau_+(x,\xi)) = \frac{h(t+\tau_+(x,\xi), \gamma_{x,\xi}(\tau_+(x,\xi)), \dot{\gamma}_{x,\xi}(\tau_+(x,\xi)))}{\langle \nu_{\gamma_{x,\xi}(\tau_+(x,\xi))}, \dot{\gamma}_{x,\xi}(\tau_+(x,\xi))\rangle} =: k_h(t,x,\xi). \tag{2.90}$$

Solving the first order ODE (2.89) for given final condition (2.90) by separation of variables, results in

$$\tilde{w}(\tau) = k_h(t,x,\xi) \exp\left(- \int_\tau^{\tau_+(x,\xi)} (\alpha + \Xi_n)(\gamma_{x,\xi}(\tilde{\tau}), \dot{\gamma}_{x,\xi}(\tilde{\tau}))\mathrm{d}\tilde{\tau} \right).$$

Therefore,

$$\tilde{w}(0) = w(t,x,\xi) = k_h(t,x,\xi) \exp\left(- \int_0^{\tau_+(x,\xi)} (\alpha + \Xi_n)(\gamma_{x,\xi}(\tilde{\tau}), \dot{\gamma}_{x,\xi}(\tilde{\tau}))\mathrm{d}\tilde{\tau} \right) \tag{2.91}$$

on ΩM and, in particular, on $\partial_-\Omega M$. This shows the assertion.

□

Corollary 2.15. *In the case of static tensor fields, i.e., $f \in L^2(S^m\tau_M')$ and $\phi = \mathcal{S}_\alpha(f)$, the adjoint problem is to find the unique solution $w \in H^1(\Omega M)$ of*

$$-\langle \nabla w, \xi\rangle + \Gamma_{ij}^k \xi^i \xi^j \frac{\partial w}{\partial \xi^k} + \Big(\alpha + n^{-1}(x)\langle \nabla n(x), \xi\rangle\Big) w = 0, \qquad (x,\xi) \in \Omega M \tag{2.92}$$

with boundary conditions

$$w(x,\xi) = \frac{h(x,\xi)}{\langle \nu_x, \xi\rangle}, \qquad (x,\xi) \in \partial_+\Omega M \tag{2.93}$$

$$w(x,\xi) = k_h(x,\xi) \exp\left(- \int_0^{\tau_+(x,\xi)} \Big(\alpha + \Xi_n\Big)(\gamma_{x,\xi}(\sigma), \dot{\gamma}_{x,\xi}(\sigma))\mathrm{d}\sigma \right), \quad (x,\xi) \in \partial_-\Omega M \tag{2.94}$$

where

$$k_h(x,\xi) = \frac{h(\gamma_{x,\xi}(\tau_+(x,\xi)), \dot{\gamma}_{x,\xi}(\tau_+(x,\xi)))}{\langle \nu_{\gamma_{x,\xi}(\tau_+(x,\xi))}, \dot{\gamma}_{x,\xi}(\tau_+(x,\xi))\rangle} \tag{2.95}$$

for any $h \in L^2(\partial\Omega M)$*. Then, the adjoint operator is given by*

$$[\mathcal{S}_\alpha^* h](x) = \int_{\Omega_x M} w(x,\xi)\xi^m \mathrm{d}\sigma_x(\xi) \in L^2(S^m\tau_M'). \tag{2.96}$$

Remark 2.16. *Note that* w *is well-definied on the boundary since* $h(x,\xi) = 0$ *for* $\langle \nu_x, \xi\rangle = 0$*. It can be observed that* (2.96) *coincides with* (2.74) *for* $\alpha = 0$*.*

Regarding the well-definedness of the adjoint operators, which is equivalent to the unique solvability of the adjoint problem, the same approach as for the forward problem can be used. Adding the viscosity term $-\varepsilon\Delta w$ to the left side of (2.92), deriving the variational formulation by identifying the bilinear form a^* analogously to (2.48)

$$a^*(w,v) = \int_{\Omega M} -\langle \nabla_x w, \xi\rangle v + \Gamma_{ij}^k(x)\xi^i\xi^j \frac{\partial w}{\partial \xi^k} v + \alpha w v \mathrm{d}\Sigma, \qquad w, v \in H^1(\Omega M) \tag{2.97}$$

and setting

$$a_\varepsilon^*(w,v) = \int_{\Omega M} \varepsilon\langle \nabla w, \nabla v\rangle \mathrm{d}\Sigma - \int_{\partial_+\Omega M} v\nabla_\nu w \mathrm{d}\sigma_+ + a^*(w,v) \tag{2.98}$$

$$b_{h,\varepsilon}^*(v) = -a^*(\hat{h}, v). \tag{2.99}$$

we arrive at the following weak formulation:

Find $w_{h,\varepsilon} = w_\varepsilon + \hat{h} \in H^1(\Omega M)$ such that

$$a_\varepsilon^*(w_\varepsilon, v) = b_{h,\varepsilon}^*(v), \qquad \forall v \in H_0^1(\Omega M), \tag{2.100}$$

where $w_\varepsilon \in H_0^1(\Omega M)$ and $\gamma_+\hat{h} = h$.

The variational problem (2.100) has a unique solution under certain conditions:

Theorem 2.17. *Let $\varepsilon > 0$, $\alpha \in L^\infty(\Omega M)$ for $N = 2, 3$ with $\alpha(x, \xi) \geq \alpha_0 > 0$ for all $(x, \xi) \in \Omega M$ and $n \in C^1(M)$. If*

$$\sup_{x \in M} \frac{\|\nabla n(x)\|}{2n(x)} < \alpha_0, \qquad N = 2$$

$$\sup_{x \in M} \frac{\|\nabla n(x)\|}{n(x)} < \alpha_0, \qquad N = 3$$

then the solution $w_\varepsilon \in H^1(\Omega M)$ of the variational problem (2.100) exists and is unique.

Proof. The proof works similarly to the one of (2.11) by applying the Lax-Milgram theorem. □

We have observed that the adjoint operator can be represented using the solution of a transport equation. However, an alternative approach exists for representing this operator. To explore this, let us revisit equation (2.91). The introduction of $\tilde{w}$ was intended to provide us with the complete boundary data of the function w. Notably, we observe here that we can explicitly specify w along the entire geodesic γ as a result of a curve integral. In the dynamic case, we derive the following alternative representation:

For a given function $h \in L^2(0, T; L^2(\partial_+ \Omega M))$ we define the adjoint operator

$$(\mathcal{I}_\alpha^d)^* \colon L^2(0, T; L^2(\partial_+ \Omega M)) \to L^2(0, T; L^2(S^m \tau_M'))$$

of the generalized dynamic attenuated ray transform $\mathcal{I}_\alpha^d$ by

$$[(\mathcal{I}_\alpha^d)^* h](t, x) = \int_{\Omega_x M} w(t, x, \xi) \xi^m \mathrm{d}\sigma_x(\xi),$$

where

$$w(t, x, \xi) = k_h(t, x, \xi) \exp\left(- \int_0^{\tau_+(x,\xi)} \Big(\alpha + \Xi_n\Big)(\gamma_{x,\xi}(\tilde{\tau}), \dot{\gamma}_{x,\xi}(\tilde{\tau})) \mathrm{d}\tilde{\tau} \right),$$
$$t \in [0, T], \ (x, \xi) \in \Omega M$$

and

$$k_h(t, x, \xi) = \frac{h(t, \gamma_{x,\xi}(\tau_+(x, \xi)), \dot{\gamma}_{x,\xi}(\tau_+(x, \xi)))}{\langle \nu_{\gamma_{x,\xi}(\tau_+(x,\xi))}, \dot{\gamma}_{x,\xi}(\tau_+(x, \xi)) \rangle}.$$

At this point, one might ask the reasons to study partial differential equations when they can be equivalently understood as ordinary differential equations through integral transformations or along geodesics. In the former scenario, involving the forward operator, employing the integral formula is logical, as it necessitates solving the geodesic differential equation once for each evaluation, followed by the application of a quadrature formula. However, the advantage of partial differential equations becomes apparent in the context of the adjoint operator: If one would solve these equations using the characteristics method, determining $\mathcal{S}_\alpha^* h(x)$ or $(\mathcal{S}_\alpha^d)^* h(x)$ for a point x would require solving an ordinary differential equation for all possible directions ξ in the corresponding discretization to evaluate the integral over $\Omega_x M$. Instead, solving one system of linear equations per iterate proves to be more efficient.

3 Numerical results

In this Chapter, the theory of the previous ones is applied to some numerical experiments. In all examples we let M be the 2-dimensional unit circle and $m = 1$. The attenuation coefficient α is assumed to be constant equal to α_0. First, we will restrict ourselves to the Euclidean case and evaluate the accuracy of the two representations of the adjoint operator for synthetic data. Afterward, we test different regularization methods to reconstruct the vector fields. Once we find the optimal parameters of the grid and the best type of regularization, we extend the examples to variable metrics.

All subsequent computations were implemented in Matlab. We utilized an Intel(R) Core(TM) processor operating at 3.7 GHz with 64 GB of RAM. In cases where we parallelized the code, we utilized ten cores.

3.1 Numerical results for the Euclidean case

First, we compute the line integrals of the forward operator. Because of the radial symmetry, we choose polar coordinates for all variables. Since we only need to consider vectors x on ∂M, it is sufficient to parameterize as follows:

$$x_p = \begin{pmatrix} \cos \mu_p \\ \sin \mu_p \end{pmatrix}, \qquad \mu_p = \frac{2\pi p}{P}, \qquad p = 1, \dots, P.$$

For ξ we write this accordingly:

$$\xi_q = \begin{pmatrix} \cos \varphi_q \\ \sin \varphi_q \end{pmatrix}, \qquad \varphi_q = \frac{2\pi q}{Q}, \qquad q = 1, \dots, Q.$$

For $(x, \xi) \in \partial_+ \Omega M$, the integral limit $\tau_-(x, \xi)$ of (2.17) can be computed explicitly by

$$\begin{aligned} \tau_-(x,\xi) &= \min\{\tau \in \mathbb{R} |\ \|x + \tau\xi\|^2_{euclid} = 1\} \\ &= -\langle x, \xi\rangle - \sqrt{\langle x, \xi\rangle^2 + 1 - \langle x, x\rangle} \\ &= -2\langle x, \xi\rangle. \end{aligned}$$

Hence, $\mathcal{I}_{\alpha_0}$ becomes

$$[\mathcal{I}_{\alpha_0} f](x,\xi) = \int_{-2\langle x,\xi\rangle}^{0} \langle f(x+\tau\xi),\xi\rangle \exp(-2\alpha_0\langle x,\xi\rangle)\mathrm{d}\tau.$$

To approximate this integral numerically, we use the trapezoidal sum. That is why we need an approximation for f on some points on the integration line. There we have to distinguish two cases: The first one is that the point $\tilde{x}$ is located between two concentric grid lines, see Figure 3.1.

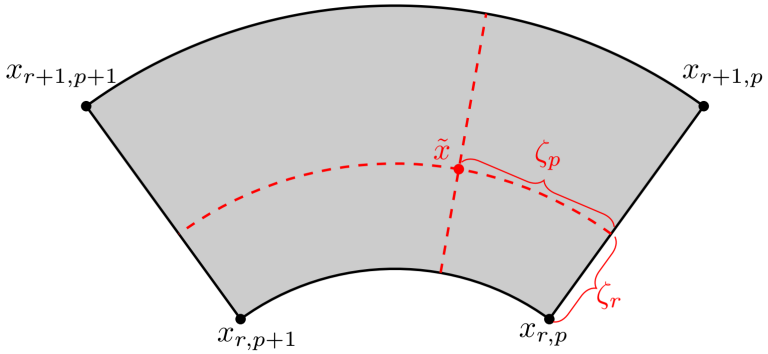

Figure 3.1: Segment between two concentrical circles

Without loss of generality $\tilde{x}$ is in the mesh with grid points $x_{r,p}$, $x_{r+1,p}$, $x_{r,p+1}$ and $x_{r+1,p+1}$. Let $0 \le \zeta_r \le 1$ be the radial difference to the inner circle and $0 \le \zeta_p \le 1$ the angular one of the lower index. Then,

$$\begin{aligned} f(x_{r+\zeta_r,p}) &\approx \zeta_r f(x_{r,p}) + (1-\zeta_r) f(x_{r+1,p}) \\ f(x_{r+\zeta_r,p+1}) &\approx \zeta_r f(x_{r,p+1}) + (1-\zeta_r) f(x_{r+1,p+1}). \end{aligned}$$

Hence,

$$\begin{aligned} f(\tilde{x}) &\approx \zeta_p f(x_{r+\zeta_r,p}) + (1-\zeta_p) f(x_{r+\zeta_r,p+1}) \\ &= \zeta_r\zeta_p f(x_{r,p}) + (1-\zeta_r)\zeta_p f(x_{r+1,p}) \\ &+ \zeta_r(1-\zeta_p) f(x_{r,p+1}) + (1-\zeta_r)(1-\zeta_p) f(x_{r+1,p+1}). \end{aligned}$$

The second case is where $\tilde{x}$ lies in the inside of the inner circle. As mentioned above, 0 is not part of the grid. We assign it a value by taking the average of all grid points on the inner circle, i.e.

$$f(0) \coloneqq \frac{1}{P}\sum_{p=1}^{P} f(x_{1,p}).$$

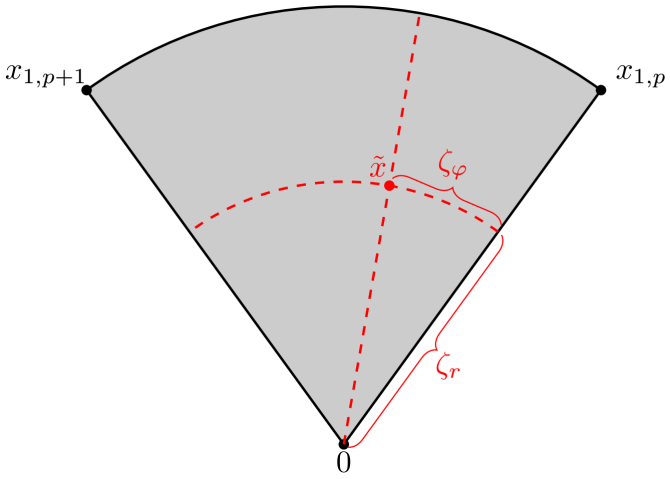

Figure 3.2: Segment inside the inner circle

For any $\tilde{x} \neq 0$ there is a segment containing $\tilde{x}$ that is given by two grid points $x_{1,p}$ and $x_{1,p+1}$ and 0, see Figure 3.2.
Analogously, we define ζ_r and ζ_p and set

$$f(\tilde{x}) \approx \zeta_r f(0) + (1-\zeta_r)(\zeta_p f(x_{1,P}) + (1-\zeta_p) f(x_{1,p+1})).$$

Since the line of integration is given analytically we can choose the grid points for the integration equidistantly. Therefore, splitting $[\tau_-(x,\xi), 0]$ into T intervals of length $\Delta\tau = \frac{-\tau_-(x,\xi)}{T}$, we get the step sizes

$$\tau_t = \tau_-(x,\xi) + t\Delta\tau, \qquad t = 0, \dots, T$$

and set

$$H_{p,q} := [\mathcal{I}_{\alpha_0} f](x_p, \xi_q) = \frac{1}{T+1} \sum_{t=0}^{T} \langle f(x_p + \tau_t \xi_q), \xi_q \rangle \exp(\alpha_0 \tau_t).$$

3.1.1 Implementation of the adjoint operator via integration

Next, we turn over to the adjoint operator. In the Euclidean case and with constant absorption, this is given for $h \in L^2(\partial_+ \Omega M)$ by

$$[\mathcal{I}^*_{\alpha_0} h](x) = \int_0^{2\pi} w(x, \xi(\varphi)) \xi(\varphi) \mathrm{d}\varphi$$

where

$$w(x,\xi) = \frac{h(\gamma_{x,\xi}(\tau_+(x,\xi)), \dot{\gamma}_{x,\xi}(\tau_+(x,\xi)))}{\langle x + \tau_+(x,\xi)\xi, \xi\rangle} \exp(-\alpha_0 \tau_+(x,\xi))$$
$$= \frac{h(x + \tau_+(x,\xi)\xi, \xi)}{\langle x,\xi\rangle + \tau_+(x,\xi)} \exp(-\alpha_0 \tau_+(x,\xi)). \tag{3.1}$$

For $(x,\xi) \in \Omega M$ we can compute $\tau_+(x,\xi)$ explicitly by

$$\tau_+(x,\xi) = \max\{\tau \in \mathbb{R} |\ \|x + \tau\xi\|^2_{euclid} = 1\}$$
$$= -\langle x,\xi\rangle + \sqrt{\langle x,\xi\rangle^2 + 1 - \langle x,x\rangle}.$$

This means that a large part of (3.1) can be calculated analytically. Only the evaluation of h requires interpolation. It is possible to precisely calculate the location where h needs to be evaluated. We parameterize $x \in M$ as follows:

$$x_{r,p} = \rho_r \begin{pmatrix} \cos\mu_p \\ \sin\mu_p \end{pmatrix}, \qquad \rho_r = \frac{r}{R}, \qquad r = 1,\dots,R$$

Let x_p and x_{p+1} be these points points with polar angles μ_p and μ_{p+1} and let $\xi = \xi_q$ be constant. We write

$$\tilde{x}_{r,p,q} \coloneqq x_{r,p} + \tau_+(x_{r,p},\xi_q)\xi_q \in \partial M$$

for the endpoint of the integration line. Then, there is exists a $\tilde{\mu}$, such that

$$\tilde{x}_{r,p,q} = \begin{pmatrix} \cos\tilde{\mu} \\ \sin\tilde{\mu} \end{pmatrix}. \tag{3.2}$$

This point in ∂M has the neighboring points

$$\left(\left\lfloor \frac{\mu P}{2\pi} \right\rfloor, q\right) \qquad \text{and} \qquad \left(\left\lfloor \frac{\mu P}{2\pi} \right\rfloor + 1, q\right).$$

where the indices are taken modulo P. This results in linear interpolation

$$h(\tilde{x}_{r,p,q},\xi_q) \approx \left(1 - \left(\frac{\mu P}{2\pi} - \left\lfloor \frac{\mu P}{2\pi} \right\rfloor\right)\right) H_{\lfloor \frac{\mu P}{2\pi} \rfloor, q} + \left(\frac{\mu P}{2\pi} - \left\lfloor \frac{\mu P}{2\pi} \right\rfloor\right) H_{\lfloor \frac{\mu P}{2\pi} \rfloor + 1, q}.$$

The total adjoint operator is then calculated using the trapezoidal sum as follows:

$$[\mathcal{I}_{\alpha_0}^* h](x_{r,p}) = \frac{2\pi}{Q} \sum_{q=1}^{Q} w(x_{r,p}, \xi_q)\xi_q.$$

Given the forward and adjoint operators, we can implement the Landweber iteration. Let us discuss the ratio between the number of angles and radii. In the Cartesian case, it is obvious that both grid sizes should be chosen equally. The resulting squares correspond to the rectangles that minimize the area of the grid meshes with a constant perimeter. We want to proceed similarly here: We want to select the grid sizes in such a way that the straight side pieces for a grid segment are approximately as long as the curved sections. Note that the length of the straight sides is the same for all segments for a given number of radii, whereas the curved sides naturally become larger towards the outside. We therefore consider how long the curved sides are on average. If R is the number of concentric rings in the grid, these have the radii

$$r_i = \frac{i}{R}, \qquad i = 0, \dots, R.$$

If you add up the outer and inner radii, you get an average of

$$\frac{1}{2R}\left(\sum_{i=0}^{R-1} r_i + \sum_{i=1}^{R} r_i\right) = \frac{1}{2R}\left(\frac{1}{2}(R-1) + \frac{1}{2}(R+1)\right) = \frac{1}{2}.$$

Thus, for a grid with P angles, the meshes have an average arc length of $\frac{\pi}{P}$. This should correspond to the lengths of the straight sides of a mesh, i.e.

$$\frac{\pi}{P} = \frac{1}{R}$$

and thus

$$P \approx \pi R. \tag{3.3}$$

We check this hypothesis using two examples for solenoidal vector fields. Setting a fixed amount of $R \cdot P = 3600$ grid points, we consider different combinations of R and $P = Q$ and compare the relative errors after reconstruction where we used Landweber's method with relaxation parameter 0.1. Additionally, we include the pair $(R, P) = (34, 106)$ which is the closest combination for satisfying (3.3) and having approximately 3600 grid points. For both vector fields, we choose $\alpha \in \{0, 0.1, 0.2, 0.3, 0.4\}$.

(R, P)	α 0	0.1	0.2	0.3	0.4
(20, 180)	0.0579	0.1432	0.4580	0.9739	1.1155
(30, 120)	0.0637	0.1457	0.4599	0.9703	1.1156
(34, 106)	0.0233	0.1190	0.4403	0.9568	1.1094
(40, 90)	0.0313	0.1209	0.4407	0.9567	1.1108
(60, 60)	0.1190	0.1762	0.4672	0.9540	1.1371
(90, 40)	1.6989	1.7108	1.7675	1.9603	2.2919
(120, 30)	0.3920	0.4228	0.6306	1.0871	1.3950
(180, 20)	2.9775	3.0166	3.0895	3.2521	3.5495

Table 3.1: Relative L^2-error (%) between reconstruction and true vector field $f^{(1)}(x) = (x_1 + x_2, x_1 - x_2)^\top$ for the same number of pixels but in different proportions of R and $P = Q$.

(R, P)	α 0	0.1	0.2	0.3	0.4
(20, 180)	0.1323	0.1862	0.4330	0.8553	1.4147
(30, 120)	0.1401	0.1991	0.4437	0.8613	1.4173
(34, 106)	0.0549	0.1292	0.3951	0.8228	1.3827
(40, 90)	0.0715	0.1403	0.4012	0.8284	1.3871
(60, 60)	0.2635	0.3108	0.5226	0.9155	1.4462
(90, 40)	2.9140	2.9588	3.0184	3.1318	3.3409
(120, 30)	1.0319	1.0537	1.1794	1.4641	1.9150
(180, 20)	5.4409	5.5277	5.6187	5.7324	5.7936

Table 3.2: Relative L^2-error (%) between reconstruction and true vector field $f^{(2)}(x) = (x_1^2 - 2x_2^2, -2x_1x_2)^\top$ for the same number of pixels but in different proportions R and $P = Q$.

In both examples, we observe that, regardless of the choice of α, the combination $(R, P) = (34, 106)$, c.f. Equation (3.3), consistently yields the smallest errors in reconstruction. Therefore, this combination will be retained for the subsequent numerical experiments.

Subsequently, we investigate the optimal number of directions Q. In the aforementioned tables, we maintained $P = Q$. Now, with $R = 34$ and $P = 106$ held constant, we vary Q and present the results in the following two tables.

Q	α 0	0.1	0.2	0.3	0.4
10	0.2330	0.2639	0.5030	0.9684	1.1268
20	1.1849	1.2326	1.3388	1.6129	2.1131
30	0.1741	0.2146	0.4851	0.9668	1.1090
40	0.5509	0.5682	0.7118	1.1090	1.5050
50	0.1260	0.1801	0.4745	0.9580	1.1090
60	0.3371	0.3585	0.5583	1.0103	1.1270
70	0.1514	0.1950	0.4713	0.9671	1.1090
80	0.1878	0.2229	0.4839	0.9720	1.1067
90	0.0506	0.1268	0.4415	0.9548	1.1056
100	0.1858	0.2202	0.4776	0.9714	1.1135
106	0.0233	0.1190	0.4403	0.9568	1.1094

Table 3.3: Relative error (%) between reconstruction and true vector field $f^{(1)}$ for $(R, P) = (34, 106)$ and different number of directions Q.

Q	α 0	0.1	0.2	0.3	0.4
10	0.3445	0.3652	0.5251	0.8934	1.4230
20	0.2914	0.3122	0.4886	0.8723	1.4051
30	0.2390	0.2709	0.4749	0.8673	1.3937
40	0.2204	0.2479	0.4501	0.8480	1.3812
50	0.1459	0.1933	0.4346	0.8461	1.3880
60	0.1846	0.2206	0.4458	0.8490	1.3783
70	0.2201	0.2490	0.4515	0.8492	1.3910
80	0.1202	0.1611	0.4005	0.8190	1.3739
90	0.0850	0.1352	0.3877	0.8124	1.3716
100	0.0485	0.1175	0.3830	0.8116	1.3735
106	0.0549	0.1292	0.3951	0.8228	1.3827

Table 3.4: Relative error (%) between reconstruction and true vector field $f^{(2)}$ for $(R, P) = (34, 106)$ and different number of directions Q.

According to Table 3.3 and 3.4 we have the best reconstruction for $Q = 106$ independent of α. However, we also observe in both examples that for $\alpha = 0.2$ the error for $Q = 106$ is hardly better than for $Q = 30$. However, the first case mentioned is significantly more complex, as the number of arithmetic operations is proportional to Q in both the forward and the adjoint problem. For this reason, we decide the following in favor of $P = Q$ for small absorptions and then for a significantly smaller number for larger ones.

We test the optimal grid sizes on

$$f^{(2)}(x) = (x_1^2 - 2x_2^2, -2x_1x_2)^\top$$

for noisy data, see Figure 3.3. We observe even for high noise levels very stable reconstructions.

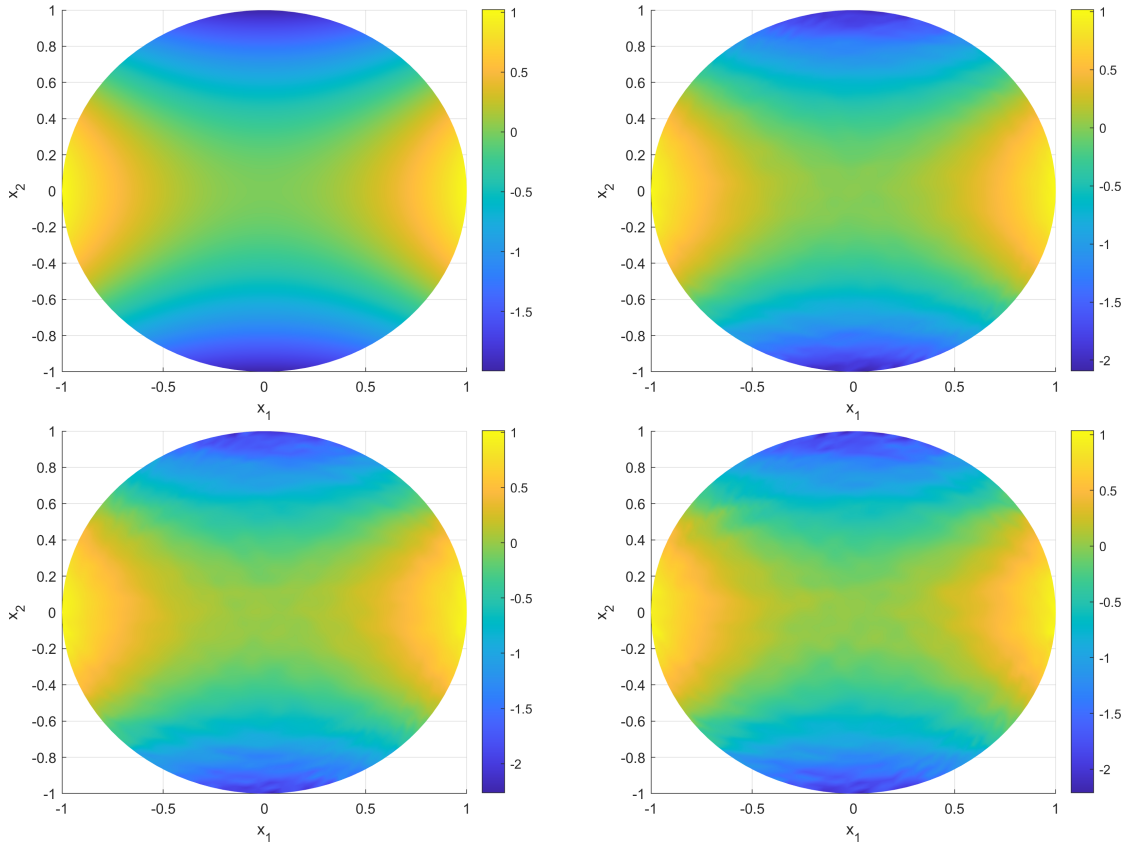

Figure 3.3: Reconstruction of $f_1^{(2)}$ for $\delta \in \{0, 0.1, 0.15, 0.2\}$

An example will be used to demonstrate the influence of α on the quality of the reconstruction. For various noise levels δ, the forward operator with the corresponding α will be initially applied. Subsequently, using the undamped integral transformation model, a reconstruction will be performed using the Landweber method. In this process, ω has been set to 0.1.

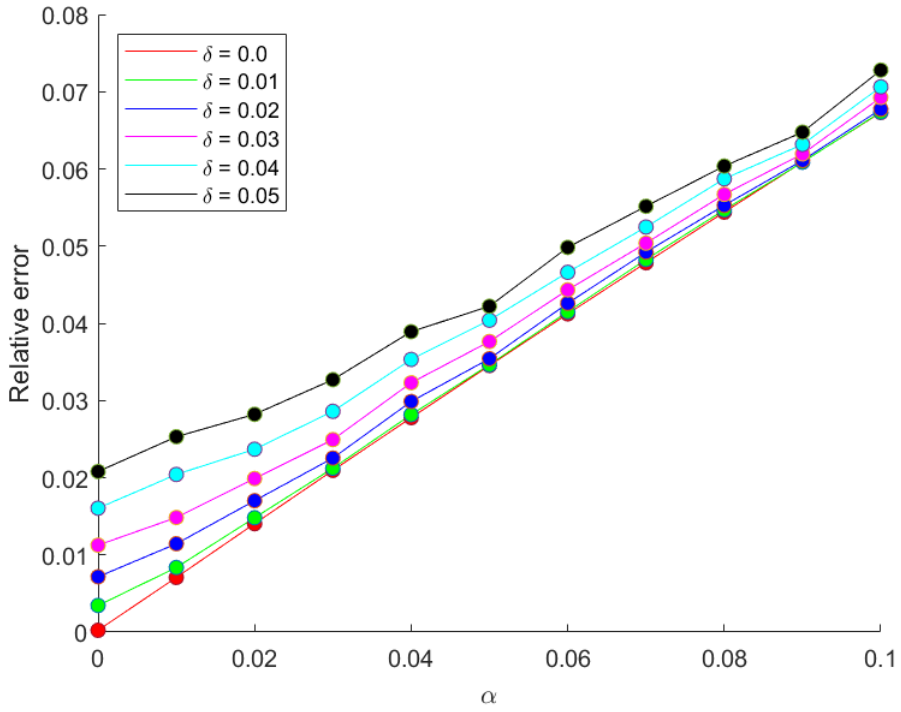

Figure 3.4: Influence of α on the relative error in reconstruction

We see that, as expected, the relative error becomes greater as δ increases. Moreover, it can be observed that for all choices δ, there is an asymptotical linear increasing behavior.

3.1.2 Implementation of adjoint operator via PDE

In this subsection, we examine the alternative approach of solving the adjoint operator using $\mathcal{S}_\alpha^*$ instead of $\mathcal{I}_\alpha^*$. We consider the Euclidean case and a constant damping α_0. In this case, we can evaluate the quality of the approximation using analytical representations.

Let $h \in L^2(\partial_+\Omega M)$. Then, $\mathcal{S}_{\alpha_0}^* : L^2(\partial_+\Omega M) \to L^2(S^1\tau_M')$ is given by

$$[\mathcal{S}_{\alpha_0}^* h](x) = \int_{\Omega_x M} w(x,\xi)\xi \mathrm{d}\sigma_x(\xi),$$

where w solves the following boundary value problem:

$$\begin{aligned} -\langle \nabla w(x,\xi), \xi\rangle + \alpha_0 w &= 0, && (x,\xi) \in \Omega M \\ w &= \frac{h(x+\tau_+(x,\xi)\xi,\xi)}{\sqrt{\langle x,\xi\rangle^2 + 1 - |x|^2}}, && (x,\xi) \in \partial\Omega M. \end{aligned}$$

For stabilization, we add the term $-\varepsilon\Delta w$ for $\varepsilon > 0$ to the left-hand side of the PDE and obtain

$$\begin{aligned} -\varepsilon\Delta w - \langle \nabla w(x,\xi), \xi\rangle + \alpha_0 w = 0, \qquad & (x,\xi) \in \Omega M \\ w = \frac{h(x + \tau_+(x,\xi)\xi, \xi)}{\sqrt{\langle x,\xi\rangle^2 + 1 - |x|^2}}, \qquad & (x,\xi) \in \partial\Omega M. \end{aligned}$$

We use again polar coordinates for parameterizing x and ξ. We calculate the boundary values for $r = R$ analytically via $\mathcal{I}_{\alpha_0}$. For the inner points, we first convert the PDE into polar coordinates:

$$\begin{aligned} & -\varepsilon\Delta w - \langle \nabla w(x,\xi), \xi\rangle + \alpha_0 w = 0 \\ \Leftrightarrow\ & -\varepsilon\left(\frac{1}{\rho}\frac{\partial w}{\partial \rho} + \frac{\partial^2 w}{\partial \rho^2} + \frac{1}{\rho^2}\frac{\partial^2 w}{\partial \mu^2}\right) - \frac{\partial w}{\partial \rho}\cos(\varphi - \mu) - \frac{1}{\rho}\frac{\partial w}{\partial \mu}\sin(\varphi - \mu) + \alpha_0 w = 0 \end{aligned} \tag{3.4}$$

We use difference quotients for the approximations of the partial derivatives. In the case of the radial derivative, we use the forward differences so that a derivative can also be assigned to the points on the innermost ring. The second derivative is approximated using central differential quotients. For the azimuthal derivative, we use central differences, i.e.,

$$\begin{aligned} \frac{\partial w}{\partial \rho}(x_{r,p}, \xi_q) \quad &\approx \frac{w_{r+1,p,q} - w_{r,p,q}}{\Delta\rho}, && r = 1, \dots, R-1 \\ \frac{\partial^2 w}{\partial \rho^2}(x_{r,p}, \xi_q) \quad &\approx \frac{w_{r+1,p,q} - 2w_{r,p,q} + w_{r-1,p,q}}{(\Delta\rho)^2}, && r = 2, \dots, R-1 \\ \frac{\partial w}{\partial \mu}(x_{r,p}, \xi_q) \quad &\approx \frac{w_{r,p+1,q} - w_{r,p-1,q}}{2\Delta\mu}, && p = 1, \dots, P \\ \frac{\partial^2 w}{\partial \mu^2}(x_{r,p}, \xi_q) \quad &\approx \frac{w_{r,p+1,q} - 2w_{r,p,q} + w_{r,p-1,q}}{(\Delta\mu)^2}, && p = 1, \dots, P. \end{aligned}$$

The indices for specifying the polar angle are again to be understood modulo P. For $r = 1$ we have the special case that the second radial derivative cannot be calculated in this way. To this end, we assume that P is even. Then the grid point $x_{1,p+\frac{P}{2}}$ lies at a distance of $2\Delta\rho$ on the line through $x_{1,p}$ and $x_{2,p}$ beyond $x_{1,p}$. We choose a linear combination of these three points so that they approximate the second derivative in $x_{1,p}$. For simplicity, we write $w(x_{r,p}) \coloneqq w(x_{r,p}, \xi_q)$.

A Taylor expansion leads to

$$\begin{aligned}\frac{\partial^2 w}{\partial \rho^2}(x_{1,p}) &= Aw(x_{2,p}) + Bw(x_{1,p}) + Cw(x_{1,p+\frac{P}{2}}) \\ &= A\left(w(x_{1,p}) + \Delta\rho\frac{\partial w}{\partial \rho}(x_{1,p}) + \frac{(\Delta\rho)^2}{2}\frac{\partial^2 w}{\partial \rho^2}(x_{1,p}) + \mathcal{O}((\Delta\rho)^3)\right) \\ &+ Bw(x_{1,p}) \\ &+ C\left(w(x_{1,p}) - 2\Delta\rho\frac{\partial w}{\partial \rho}(x_{1,p}) + 2(\Delta\rho)^2\frac{\partial^2 w}{\partial \rho^2}(x_{1,p}) + \mathcal{O}((\Delta\rho)^3)\right).\end{aligned}$$

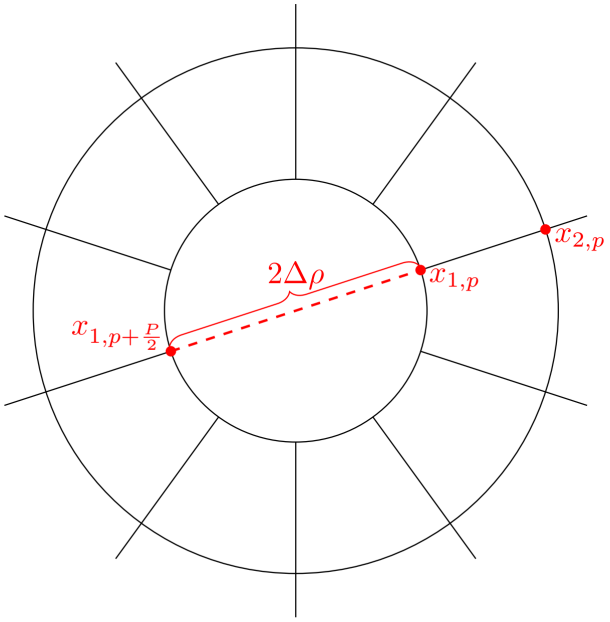

Figure 3.5: Grid points for approximation of $\frac{\partial^2 w}{\partial \mu^2}$ at $p = 1$

Comparing coefficients leads to

$$\begin{aligned}A + B + C &= 0, \\ \Delta\rho A - 2\Delta\rho C &= 0, \\ A\frac{(\Delta\rho)^2}{2} + 2C(\Delta\rho)^2 &= 1.\end{aligned}$$

This results in the solution $(A, B, C) = \frac{1}{(\Delta\rho)^2}(\frac{2}{3}, -1, \frac{1}{3})$. Thus,

$$\frac{\partial^2 w}{\partial \rho^2}(x_{1,p}, \xi_q) \approx \frac{2w_{2,p,q} - 3w_{1,p,q} + w_{1,p+\frac{P}{2},q}}{3(\Delta\rho)^2}.$$

Note that there is no derivative concerning ξ here, as it is constant. This means that the system of equations with $(R-1)PQ$ variables can be reduced to Q many

systems of equations with $(R-1)P$ many variables. These can therefore be calculated independently and thus in parallel. For fixed q and $r > 1$, (3.4) can be written as

$$\begin{aligned}
0 = {} & w_{r,p,q}\left(\frac{\varepsilon}{\rho_r\Delta\rho} + \frac{2\varepsilon}{(\Delta\rho)^2} + \frac{2\varepsilon}{\rho_r^2(\Delta\mu)^2} + \frac{\cos(\varphi-\mu)}{\Delta\rho} + \alpha\right) \\
& + w_{r+1,p,q}\left(-\frac{\varepsilon}{\rho_r\Delta\rho} - \frac{\varepsilon}{(\Delta\rho)^2} - \frac{\cos(\varphi-\mu)}{\Delta\rho}\right) \\
& + w_{r-1,p,q}\left(-\frac{\varepsilon}{(\Delta\rho)^2}\right) \\
& + w_{r,p+1,q}\left(-\frac{\varepsilon}{\rho_r^2(\Delta\mu)^2} - \frac{\sin(\varphi-\mu)}{2\rho_r\Delta\mu}\right) \\
& + w_{r,p-1,q}\left(-\frac{\varepsilon}{\rho_r^2(\Delta\mu)^2} + \frac{\sin(\varphi-\mu)}{2\rho_r\Delta\mu}\right)
\end{aligned}$$

and for $r = 1$ as

$$\begin{aligned}
0 = {} & w_{1,p,q}\left(\frac{\varepsilon}{\rho_1\Delta\rho} + \frac{\varepsilon}{(\Delta\rho)^2} + \frac{2\varepsilon}{\rho_1^2(\Delta\mu)^2} + \frac{\cos(\varphi-\mu)}{\Delta\rho} + \alpha\right) \\
& + w_{2,p,q}\left(-\frac{\varepsilon}{\rho_1\Delta\rho} - \frac{2\varepsilon}{3(\Delta\rho)^2} - \frac{\cos(\varphi-\mu)}{\Delta\rho}\right) \\
& + w_{1,p+\frac{P}{2},q}\left(-\frac{\varepsilon}{3(\Delta\rho)^2}\right) \\
& + w_{1,p+1,q}\left(-\frac{\varepsilon}{\rho_r^2(\Delta\mu)^2} - \frac{\sin(\varphi-\mu)}{2\rho_r\Delta\mu}\right) \\
& + w_{1,p-1,q}\left(-\frac{\varepsilon}{\rho_r^2(\Delta\mu)^2} + \frac{\sin(\varphi-\mu)}{2\rho_1\Delta\mu}\right).
\end{aligned}$$

The question remains on the accuracy of the reconstruction if $\mathcal{S}_\alpha^*$ is used instead of $\mathcal{I}_\alpha^*$. Unfortunately, no pattern for the optimal choice of the grid could be found here. Generally, the method only seems effective for certain grid parameters. For many combinations of radii and angles, the solution of the adjoint problem is so unstable that no iteration takes place at all. For all grids, the matrix that arises in each iteration of the finite differences appears to be nearly singular. To avoid this, the viscosity solutions were calculated. But this has not led to any improvement. Therefore, we calculate the minimum norm solution instead. To evaluate the quality of the adjoint operator via the transport or viscosity solutions, we first consider examples of vector fields f for which both $\mathcal{I}_0 f$ and $\mathcal{I}_0^*\mathcal{I}_0 f$ can be calculated analytically. In (A.3.1) these two operators were calculated for $f(x) = (a,b)^\top$, $a, b \in \mathbb{R}$ and it is verified that

$$\langle \mathcal{I}_0 f, \mathcal{I}_0 f\rangle_{L^2(\partial_+\Omega M)} = \langle f, \mathcal{I}_0^*\mathcal{I}_0 f\rangle_{L^2(S^1\tau'_M)} = 2\pi(a^2+b^2). \tag{3.5}$$

On the one hand, this confirms that the corresponding scalar products have been correctly derived and implemented. On the other hand, (3.5) offers the possibility

to test the adjoint operators $\mathcal{I}_0^*$ or $(\mathcal{S}_0^\varepsilon)^*$ for exactness due to the very precise computability of $\mathcal{I}_0 f$ and therefore, $\langle \mathcal{I}_0 f, \mathcal{I}_0 f \rangle_{L^2(\partial_+ \Omega M)}$. That is the reason for measuring the quality of the performance of the adjoint operators by introducing the relative errors

$$\operatorname{err}(\mathcal{I}_\alpha^*) := \frac{|\langle \mathcal{I}_\alpha f, \mathcal{I}_\alpha f \rangle - \langle f, \mathcal{I}_\alpha^* \mathcal{I}_\alpha f \rangle|}{\langle \mathcal{I}_\alpha f, \mathcal{I}_\alpha f \rangle} \tag{3.6}$$

and, respectively,

$$\operatorname{err}((\mathcal{S}_\alpha^\varepsilon)^*) := \frac{|\langle \mathcal{I}_\alpha f, \mathcal{I}_\alpha f \rangle - \langle f, (\mathcal{S}_\alpha^\varepsilon)^* \mathcal{I}_\alpha f \rangle|}{\langle \mathcal{I}_\alpha f, \mathcal{I}_\alpha f \rangle}. \tag{3.7}$$

For three distinct vector fields and various selections of ε, the errors are calculated, see Figures 3.6 - 3.8. A consistent trend is noted across all three cases, wherein the error exhibits similar behavior. As ε increases significantly, the error increases, while as ε tends toward zero, it appears to approach the error associated with the unperturbed transport equation. However, it is noteworthy that the observed errors are larger than those acquired through $\mathcal{I}_0^*$. This discrepancy arises due to the necessity of computing the minimum norm solution of the linear system when addressing the original and perturbated transport equation.

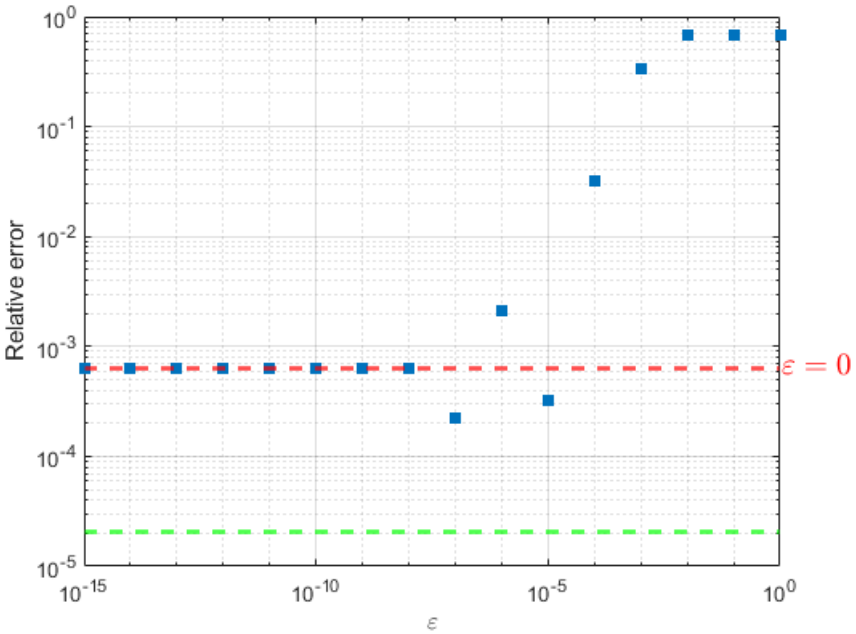

Figure 3.6: Relative errors $\operatorname{err}((\mathcal{S}_0^\varepsilon)^*)$ for $\varepsilon > 0$ (blue), $\operatorname{err}((\mathcal{S}_0^0)^*)$ (red) and $\operatorname{err}(\mathcal{I}_0^*)$ (green) for $f^{(1)}(x) = (x_1 + x_2, x_1 - x_2)^\top$

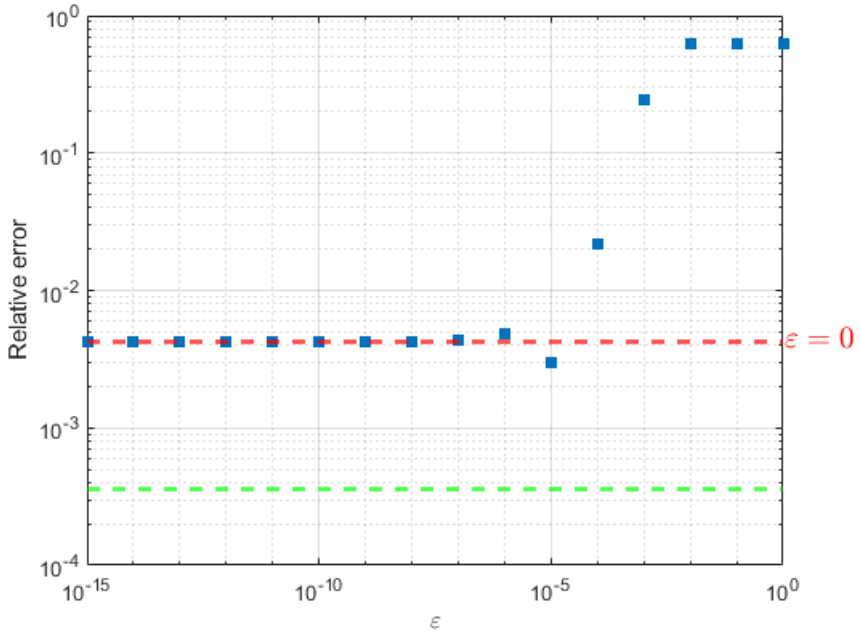

Figure 3.7: Relative errors $\mathrm{err}((\mathcal{S}_0^\varepsilon)^*)$ for $\varepsilon > 0$ (blue), $\mathrm{err}((\mathcal{S}_0^0)^*)$ (red) and $\mathrm{err}(\mathcal{I}_0^*)$ (green) for $f^{(2)}(x) = (x_1^2 - 2x_2^2, -2x_1x_2)^\top$

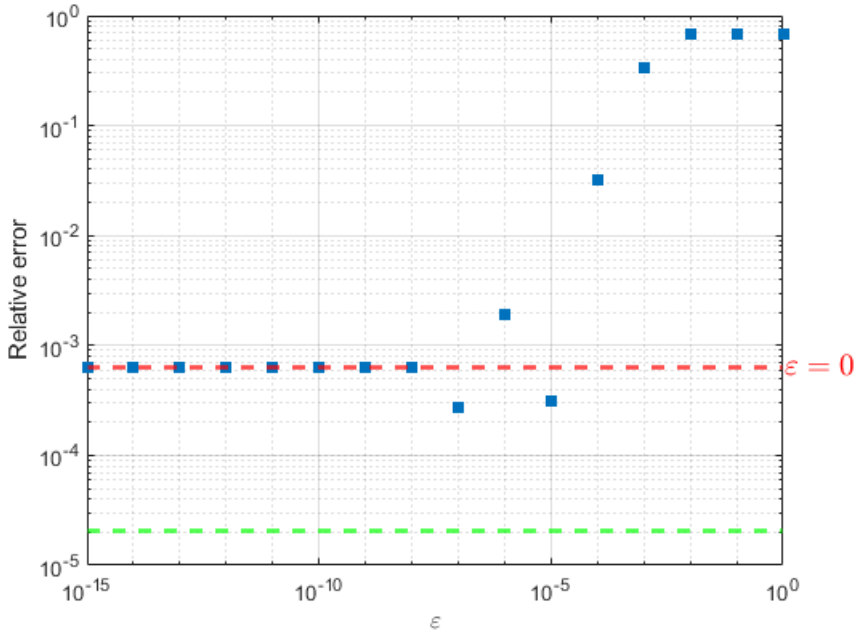

Figure 3.8: Relative errors $\mathrm{err}((\mathcal{S}_0^\varepsilon)^*)$ for $\varepsilon > 0$ (blue), $\mathrm{err}((\mathcal{S}_0^0)^*)$ (red) and $\mathrm{err}(\mathcal{I}_0^*)$ (green) for $f^{(3)}(x) = (x_1, -x_2)^\top$

The next investigation is solely confined to the case of $\alpha = 0$. The rationale behind this choice lies in the fact that the performance of $(\mathcal{S}_\alpha^\varepsilon)^*$ for $\varepsilon \geq 0$ significantly deteriorates with damping.

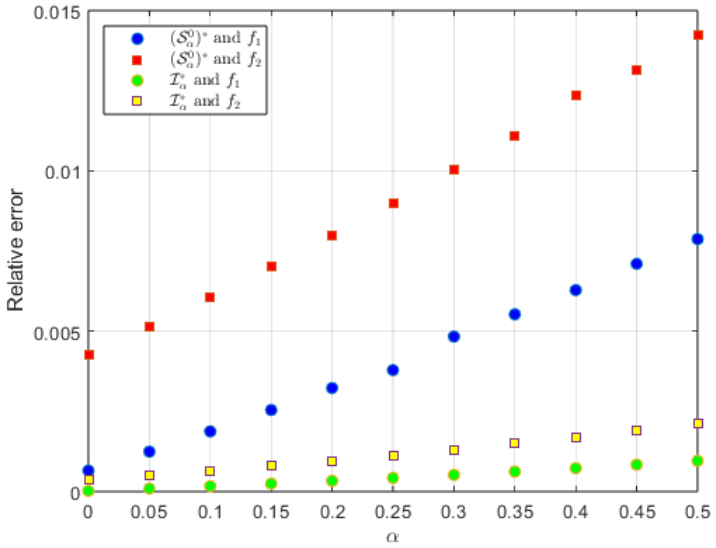

Figure 3.9: Validation of (3.6) and (3.7) for $\mathcal{I}_\alpha^*$ and $(\mathcal{S}_\alpha^0)^*$

Several observations can be made from Figure 3.9: Firstly, it appears that the relative error is linearly dependent on the choice of α for both types of adjoint operators and across both vector fields. Secondly, the error associated with $(\mathcal{S}_\alpha^0)^*$ is significantly larger than that of $(\mathcal{I}_\alpha)^*$. Only for f_1 and $\alpha = 0$ do both operators yield results within the same order of magnitude. This example emphazises that even $(\mathcal{S}_0^0)^*$ can lead to significant errors in certain fields.

Another drawback becomes evident when comparing the run time between the two approaches. When utilizing noise levels of 3% and 10% for the same grid and f_2, we measure the time required for the reconstruction, see Table 3.5.

Choice of adjoint	Noise level	Relative error	Run time
$\mathcal{I}_0^*$	3%	1.30%	5 min 5 s
	10%	3.39%	3 min 32 s
$\mathcal{S}_0^*$	3%	1.27%	178 min 53 s
	10%	3.34%	124 min 25 s

Table 3.5: Run time for reconstructing f_2 and relative L^2-error of Landweber iteration without Nesterov acceleration for both representations of adjoint operators

It is remarkable that the error in the reconstruction remains almost unchanged, while the run time for iterations using the PDE approach is significantly longer compared to the alternative method. Hence, there is little merit in extending the slower method to non-Euclidean metrics.

3.2 Numerical results for the non-Euclidean case

In the following, we allow the refractive index and the absorption coefficent to be variable. We will consider the following examples:

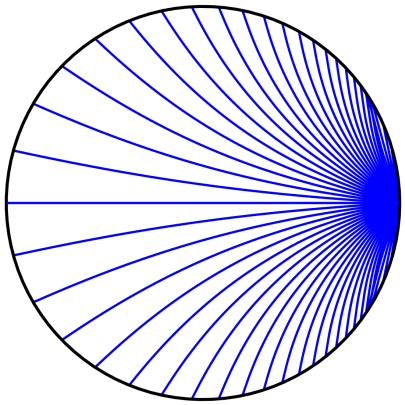

(a) $n_\lambda^{(1)}(x) = \frac{4}{3} + \lambda(x_1^2 + x_2^2)$, $\lambda = \frac{1}{2}$

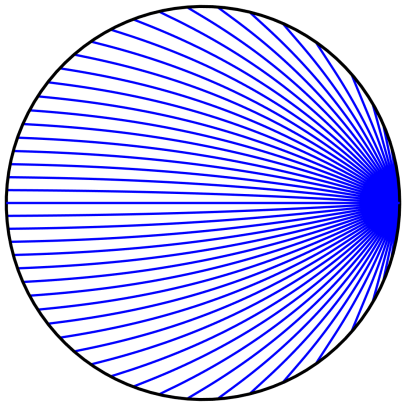

(b) $n^{(2)}(x) = 1 + \frac{1}{2}\exp(-x_1^2 - x_2^2)$

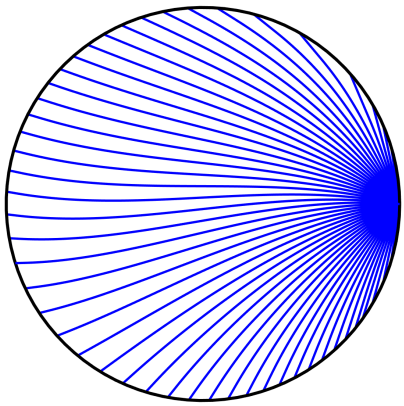

(c) $n^{(3)}(x) = 2 - x_1 x_2$

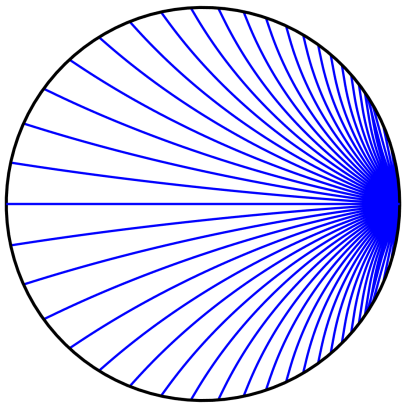

(d) $n^{(4)}(x) = 1 + \exp(x_1^2 + x_2^2 - 1)$

Figure 3.10: Sketch of geodesics starting in $x = (1, 0)^\top$ for several $n^{(i)}$

For $i = 1, \ldots, 4$ it can be verified that

$$\sup_{x \in M} \frac{\|\nabla n_{\frac{1}{2}}^{(1)}(x)\|}{n_{\frac{1}{2}}^{(1)}(x)} \geq 0.162 \qquad \sup_{x \in M} \frac{\|\nabla n^{(2)}(x)\|}{n^{(2)}(x)} \geq 0.109$$

$$\sup_{x \in M} \frac{\|\nabla n^{(3)}(x)\|}{n^{(3)}(x)} \geq 0.296 \qquad \sup_{x \in M} \frac{\|\nabla n^{(4)}(x)\|}{n^{(4)}(x)} \geq 0.091.$$

Hence, for small α_0 equation (2.60) is not necessarily satisfied. We will now determine to what extent the approximation of the forward and adjoint operators will change. Note that ξ depends on x if $n(x)$ does, i.e. we parameterize for $p = 1, \ldots, P$ and $q = 1, \ldots, Q$

$$x_p = \begin{pmatrix} \cos \mu_p \\ \sin \mu_p \end{pmatrix}, \qquad \mu_p = \frac{2\pi p}{P},$$

and

$$\xi_{p,q} = n^{-1}(x_p) \begin{pmatrix} \cos \varphi_q \\ \sin \varphi_q \end{pmatrix}, \qquad \varphi_q = \frac{2\pi q}{Q}.$$

The variable attenuation leads to the fact that the forward operator now consists of two nested integrations. To be able to approximate this using quadrature formulas, first the integration path $\gamma = \gamma_{x_p,\xi_{p,q}}$ must be calculated. Since a value $\neq 0$ can only be expected for $(x_p, \xi_{p,q})$ from $\partial_+ \Omega M$, we calculate the solution of the geodesic equation (2.25) backwards from $\tau = 0$ to $\tau = \tau_-(x_p, \xi_{p,q})$. This means that we have to multiply by -1 later in the quadrature. For each pair $(x_p, \xi_{p,q})$ we denote the grid points by τ_s, $s = 0, \ldots, S = S_{p,q}$, where $\tau_0 = \tau_+(x_p, \xi_{p,q})$ and $\tau_S = \tau_-(x_p, \xi_{p,q})$. The system of ordinary differential equations (2.26) is solved here using the Runge-Kutta method of order 4 (see (A.4)) and a constant step size $\Delta\tau$. We calculate further points $\gamma(\tau_s)$ of the geodesic until we obtain a point $\gamma(\tau_S)$ outside M. We now assume that $n(x)$ at ∂M deviates only slightly from 1. This is physically realistic. After all, we have required in our model that the analyzed object is surrounded by air. For correspondingly small $\Delta\tau$, we can therefore assume that $\gamma(\tau_S)$ does not deviate significantly from the actual trajectory. Therefore, we determine the true entry point $\gamma(\tau_S^*)$ as the intersection of the Euclidean line segment of $\gamma(\tau_{S-1})$ to $\tilde{\gamma}(\tau_S)$ and the boundary ∂M. The spacing of the sampling points for the evaluation of the integrals is therefore no longer constant. We approximate the increment $\Delta\tau^*$ between the last two points by scaling

$$\Delta\tau^* = \frac{\|\gamma(\tau_S) - \gamma(\tau_{S-1})\|_{euclid}}{\|\gamma(\tau_S^*) - \gamma(\tau_{S-1})\|_{euclid}} \cdot \Delta\tau.$$

Using the trapezoidal sum, the approximation $A_{p,q,s}$ of the inner integral in the exponential is given for $0 < s < S = S_{p,q}$ by

$$-\int_{\tau_s}^{0} \alpha(\gamma_{x_p,\xi_{p,q}}(\sigma))\mathrm{d}\sigma \approx A_{p,q,s} \coloneqq \frac{1}{2}\Delta\tau \left(\sum_{\tilde{s}=1}^{s-1} \alpha(\gamma_{x_p,\xi_{p,q}}(\tau_{\tilde{s}})) + \sum_{\tilde{s}=2}^{s} \alpha(\gamma_{x_p,\xi_{p,q}}(\tau_{\tilde{s}})) \right).$$

For $s = 0$ we obviously get $A_{p,q,0} = 0$. Only for $s = S$ do we specifically define

$$A_{p,q,S} = A_{p,q,S-1} + \frac{1}{2}\Delta\tau^* \left(\alpha(\gamma_{x_p,\xi_{p,q}}(\tau_{S-1})) + \alpha(\gamma_{x_p,\xi_{p,q}}(\tau_S))\right).$$

This yields

$$\begin{aligned}
\mathcal{I}_\alpha f(x_p, \xi_{p,q}) \approx & -\frac{\Delta\tau}{2} \sum_{s=0}^{S-2} \langle f(\gamma_{x_p,\xi_{p,q}}(\tau_s)), \dot{\gamma}_{x_p,\xi_{p,q}}(\tau_s)\rangle \exp(A_{p,q,s}) \\
& - \frac{\Delta\tau}{2} \sum_{s=1}^{S-1} \langle f(\gamma_{x_p,\xi_{p,q}}(\tau_s)), \dot{\gamma}_{x_p,\xi_{p,q}}(\tau_s)\rangle \exp(A_{p,q,s}) \\
& - \frac{\Delta\tau^*}{2} \langle f(\gamma_{x_p,\xi_{p,q}}(\tau_{S-1})), \dot{\gamma}_{x_p,\xi_{p,q}}(\tau_{S-1})\rangle \exp(A_{p,q,S-1}) \\
& - \frac{\Delta\tau^*}{2} \langle f(\gamma_{x_p,\xi_{p,q}}(\tau_S)), \dot{\gamma}_{x_p,\xi_{p,q}}(\tau_S)\rangle \exp(A_{p,q,S}).
\end{aligned}$$

Note that the above scalar products must all be considered in the corresponding metric. The treatment of the adjoint operator must also be slightly modified. Since now $x \in M$, we parameterize for $r = 1, \ldots, R$, $p = 1, \ldots, P$ and $q = 1, \ldots, Q$

$$x_{r,p} = \rho_r \begin{pmatrix} \cos\mu_p \\ \sin\mu_p \end{pmatrix}, \qquad \rho_r = \frac{r}{R}, \qquad \mu_p = \frac{2\pi p}{P},$$

and

$$\xi_{r,p,q} = n^{-1}(x_{r,p}) \begin{pmatrix} \cos\varphi_q \\ \sin\varphi_q \end{pmatrix}, \qquad \varphi_q = \frac{2\pi q}{Q}.$$

First, an integral must be approximated due to the variable assumed attenuation $\alpha(x)$. To this end, the integration line must also be calculated first, but in contrast to the forward operator, the geodesic equation is solved forward in time. Similarly, we therefore calculate further points of the geodesics with a step size $\Delta\tau$ starting from $\tau = 0$ until we leave the area M at τ_S. We determine the true exit point $\gamma(\tau_S^*)$ as the intersection of the Euclidean line segment of $\gamma(\tau_{S-1})$ to $\tilde{\gamma}(\tau_S)$ and the boundary ∂M. Hence, the last step size $\Delta\tau^*$ is defined as

$$\Delta\tau^* = \frac{\|\gamma(\tau_S) - \gamma(\tau_{S-1})\|_{euclid}}{\|\gamma(\tau_S^*) - \gamma(\tau_{S-1})\|_{eucid}} \cdot \Delta\tau.$$

For $N = 2$, Ξ_n is defined as

$$\Xi_n(x,\xi) = \frac{1}{2} n^{-1}(x) \langle \nabla n(x), \xi \rangle = \frac{1}{2} n^{-1}(x) \left(\partial_1 n(x) \xi_1 + \partial_2 n(x) \xi_2 \right).$$

That is why the approximation of the exponent in the exponential for $\gamma_{x_{r,p},\xi_{r,p,q}}$ is

$$\begin{aligned}
&- \int_0^{\tau_S} (\alpha + \Xi_n)(\gamma_{x_{r,p},\xi_{r,p,q}}(\sigma), \dot{\gamma}_{x_{r,p},\xi_{r,p,q}}(\sigma)) \mathrm{d}\sigma \\
&\approx -\frac{1}{2} \Delta\tau \left(\sum_{\tilde{s}=1}^{S-2} (\alpha + \Xi_n)(\gamma_{x_p,\xi_{p,q}}(\tau_s), \dot{\gamma}_{x_p,\xi_{p,q}}(\tau_s)) + \sum_{\tilde{s}=2}^{S-1} (\alpha + \Xi_n)(\gamma_{x_p,\xi_{p,q}}(\tau_s), \dot{\gamma}_{x_p,\xi_{p,q}}(\tau_s)) \right) \\
&\quad - \frac{1}{2} \Delta\tau^* \left((\alpha + \Xi_n)(\gamma_{x_p,\xi_{p,q}}(\tau_{S-1}), \dot{\gamma}_{x_p,\xi_{p,q}}(\tau_{S-1})) + (\alpha + \Xi_n)(\gamma_{x_p,\xi_{p,q}}(\tau_S), \dot{\gamma}_{x_p,\xi_{p,q}}(\tau_S)) \right).
\end{aligned}$$

We calculate the denominator of (2.95) by default as a scalar product over the metric g, i.e.,

$$\langle \nu_{\gamma_{x_{r,p},\xi_{r,p,q}}(\tau_S)}, \dot{\gamma}_{x_{r,p},\xi_{r,p,q}}(\tau_S) \rangle = n^{-2}(x_{r,p}) \langle \gamma_{x_{r,p},\xi_{r,p,q}}(\tau_S), \dot{\gamma}_{x_{r,p},\xi_{r,p,q}}(\tau_S) \rangle_{euclid}.$$

The last step is to evaluate the function h at $(\tilde{x}_{r,p}, \tilde{\xi}_{r,p,q}) \in \partial_+ \Omega M$. In contrast to the Euclidean case, $\tilde{x}_{r,p}$ and $\tilde{\xi}_{r,p,q}$ are not necessarily located on a grid. Therefore, a two-dimensional interpolation in the variables μ and φ is required. As in (3.2), $\tilde{\mu}$ and $\tilde{\varphi}$ exist such that

$$\tilde{x}_{r,p,q} = \begin{pmatrix} \cos\tilde{\mu} \\ \sin\tilde{\mu} \end{pmatrix}, \qquad \tilde{\xi}_{r,p,q} = \begin{pmatrix} \cos\tilde{\varphi} \\ \sin\tilde{\varphi} \end{pmatrix}.$$

The point $(\tilde{x}_{r,p,q}, \tilde{\xi}_{r,p,q})$ has the four adjacent points

$$\begin{aligned}
&\left(\left\lfloor \frac{\mu P}{2\pi} \right\rfloor, \left\lfloor \frac{\varphi Q}{2\pi} \right\rfloor \right), \ \left(\left\lfloor \frac{\mu P}{2\pi} \right\rfloor, \left\lfloor \frac{\varphi Q}{2\pi} \right\rfloor + 1 \right), \\
&\left(\left\lfloor \frac{\mu P}{2\pi} \right\rfloor + 1, \left\lfloor \frac{\varphi Q}{2\pi} \right\rfloor \right), \ \left(\left\lfloor \frac{\mu P}{2\pi} \right\rfloor + 1, \left\lfloor \frac{\varphi Q}{2\pi} \right\rfloor + 1 \right)
\end{aligned}$$

where again the indices are taken modulo P and Q, respectively. This results in

$$\begin{aligned}
h(\tilde{x}_{r,p,q}, \tilde{\xi}_{r,p,q}) \approx{}& \left(1 - \left(\frac{\mu P}{2\pi} - \left\lfloor \frac{\mu P}{2\pi} \right\rfloor \right) \right) \left(1 - \left(\frac{\varphi Q}{2\pi} - \left\lfloor \frac{\varphi Q}{2\pi} \right\rfloor \right) \right) H_{\lfloor \frac{\mu P}{2\pi} \rfloor, \lfloor \frac{\varphi Q}{2\pi} \rfloor} \\
&+ \left(\frac{\mu P}{2\pi} - \left\lfloor \frac{\mu P}{2\pi} \right\rfloor \right) \left(1 - \left(\frac{\varphi Q}{2\pi} - \left\lfloor \frac{\varphi Q}{2\pi} \right\rfloor \right) \right) H_{\lfloor \frac{\mu P}{2\pi} \rfloor + 1, \lfloor \frac{\varphi Q}{2\pi} \rfloor} \\
&+ \left(1 - \left(\frac{\mu P}{2\pi} - \left\lfloor \frac{\mu P}{2\pi} \right\rfloor \right) \right) \left(\frac{\varphi Q}{2\pi} - \left\lfloor \frac{\varphi Q}{2\pi} \right\rfloor \right) H_{\lfloor \frac{\mu P}{2\pi} \rfloor, \lfloor \frac{\varphi Q}{2\pi} \rfloor + 1} \\
&+ \left(\frac{\mu P}{2\pi} - \left\lfloor \frac{\mu P}{2\pi} \right\rfloor \right) \left(\frac{\varphi Q}{2\pi} - \left\lfloor \frac{\varphi Q}{2\pi} \right\rfloor \right) H_{\lfloor \frac{\mu P}{2\pi} \rfloor + 1, \lfloor \frac{\varphi Q}{2\pi} \rfloor + 1}.
\end{aligned}$$

Therefore, the approximation of the adjoint operator is given by

$$\begin{aligned}[\mathcal{I}_\alpha^* h](x_{r,p}) &= \int_{\Omega_{x_{r,p}}M} w(x_{r,p},\xi)\xi \mathrm{d}\omega_x(\xi) \\ &= \int_{\Omega_{x_{r,p}}M} w(x_{r,p},\xi(\varphi))\xi(\varphi)\mathrm{d}\varphi \\ &\approx \frac{2\pi}{Q}\sum_{q=1}^{Q} w(x_{r,p},\xi_{r,p,q})\xi_{r,p,q}.\end{aligned}$$

We want to apply this approximation to some examples. First, we consider $f^{(3)}(x) = (x_1, -x_2)^\top$ but with $\alpha = 0$ and very slowly varying refractive index

$$n^{(1)}_{0.002}(x) = 0.002|x|^2 + \frac{4}{3}.$$

This refractive index could be found in a domain filled with water that has not the same temperature everywhere. For a variety of noise levels, we get the following absolute errors in the reconstruction:

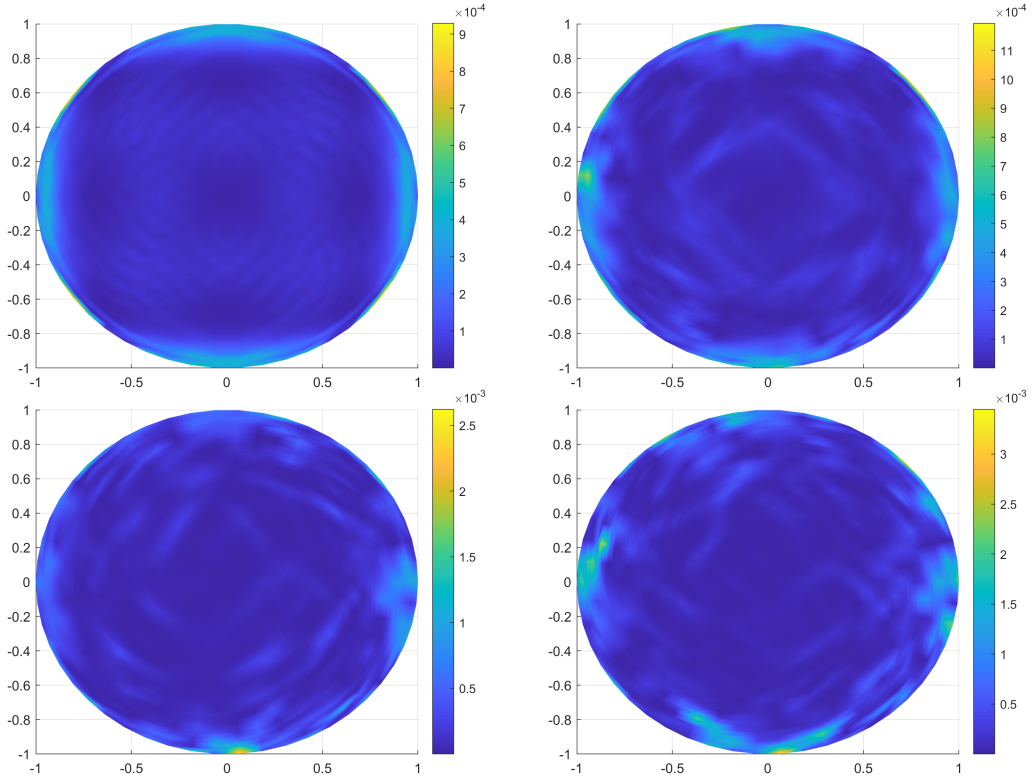

Figure 3.11: Absolute error for $(R, P, Q) = (34, 106, 106)$ and $\delta \in \{0, 0.01, 0.02, 0.03\}$ from the left top to the bottom

Next, we examine the extent to which the model with the inclusion of refraction effects also leads to an improvement in the reconstruction, when there is only a slight deviation from straight lines. At the same time, we want to compare the run times. For this purpose, we apply $\mathcal{I}_\alpha$ to a vector field, add noise to the result, and

then calculate the reconstruction once in the Euclidean ($n = 1$) and once within non-Euclidean setting ($n^{(1)}_{0.002}(x) = 1 + 0.002(x_1^2 + x_2^2)$). We use Landweber's method with a relaxation parameter of $\omega = 0.01$ and accelerate this with Nesterov's method ($k = 3$). With different choices of noise level and damping, we obtain the following data:

Noise level	Attenuation	Refraction (y/n)	Relative L^2-error	Run time
0	0.01	n	0.0555	1281 s
0	0.01	y	0.0132	3122 s
0.01	0.01	n	0.0559	655 s
0.01	0.01	y	0.0144	4149 s
0	0.02	n	0.0556	1579 s
0	0.02	y	0.0134	8734 s
0.01	0.02	n	0.0557	880 s
0.01	0.02	y	0.0145	6421 s

Table 3.6: Comparison of relative error after reconstructing with Euclidean and non-Euclidean model for $(R, P, Q) = (34, 106, 106)$

Table 3.6 clearly shows that, regardless of the choice of noise level or absorption coefficient, the method with refraction taken into account reduces the relative error by about 75%. On the other hand, we must accept a significantly higher run time for this purpose.

Allowing for greater fluctuations in $n(x)$ necessitates the use of the generalized model. Otherwise, the solutions would deviate even more significantly. Hereafter, we employ the refractive indices $n^{(2)}$, $n^{(3)}$, and $n^{(4)}$, combine them with various noise levels and attenuations, and apply them to $f^{(2)}$.

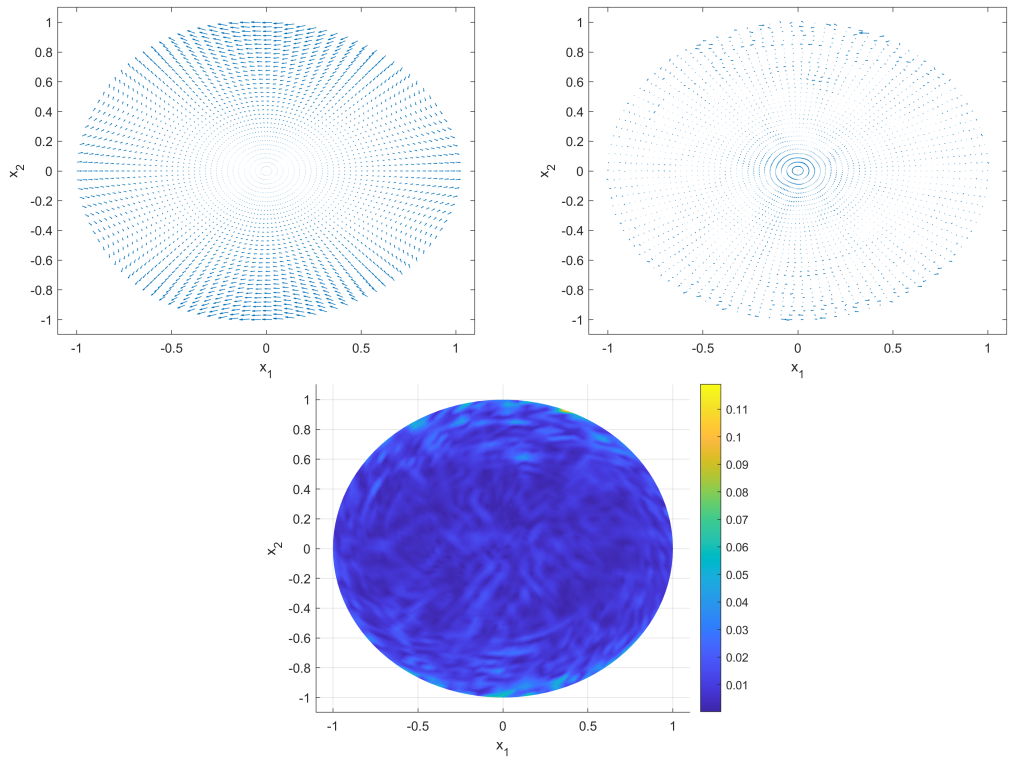

Figure 3.12: Quiver plot of reconstruction and difference to solution, and absolute error in each pixel of $f^{(2)}$ for $n^{(2)}$, $\delta = 4\%$, $\alpha = 0.1$; relative error is 3.26%

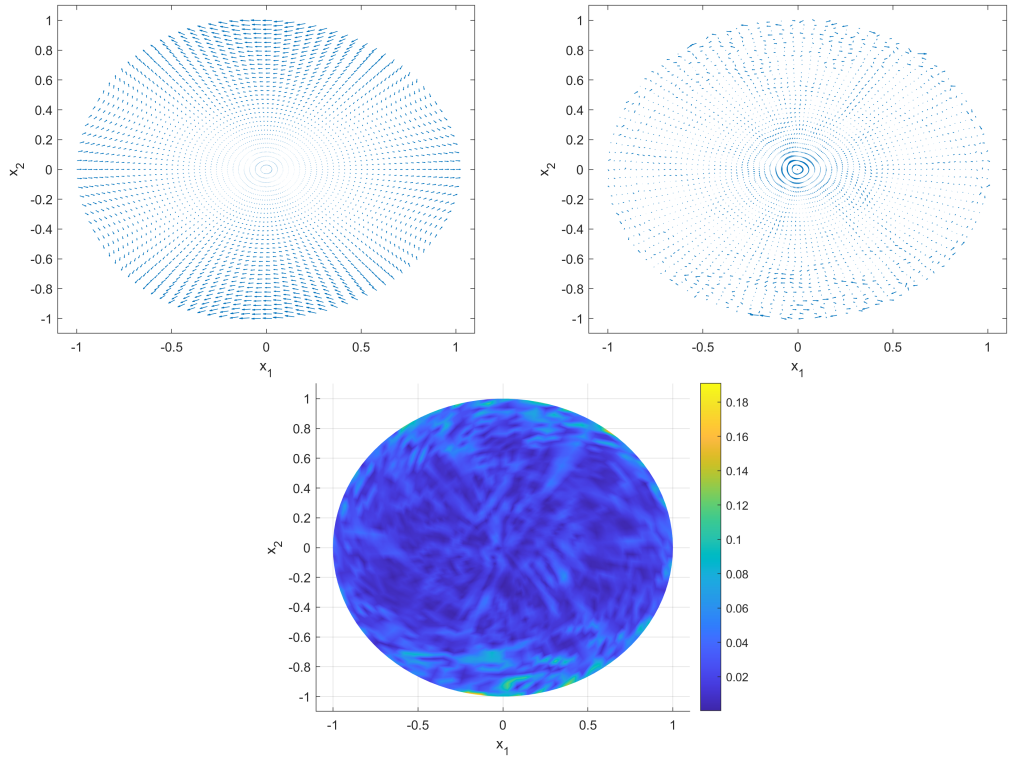

Figure 3.13: Quiver plot of reconstruction, difference to solution, and absolute error in each pixel of $f^{(2)}$ for $n^{(3)}$, $\delta = 12\%$, $\alpha = 0$; relative error is 5.03%

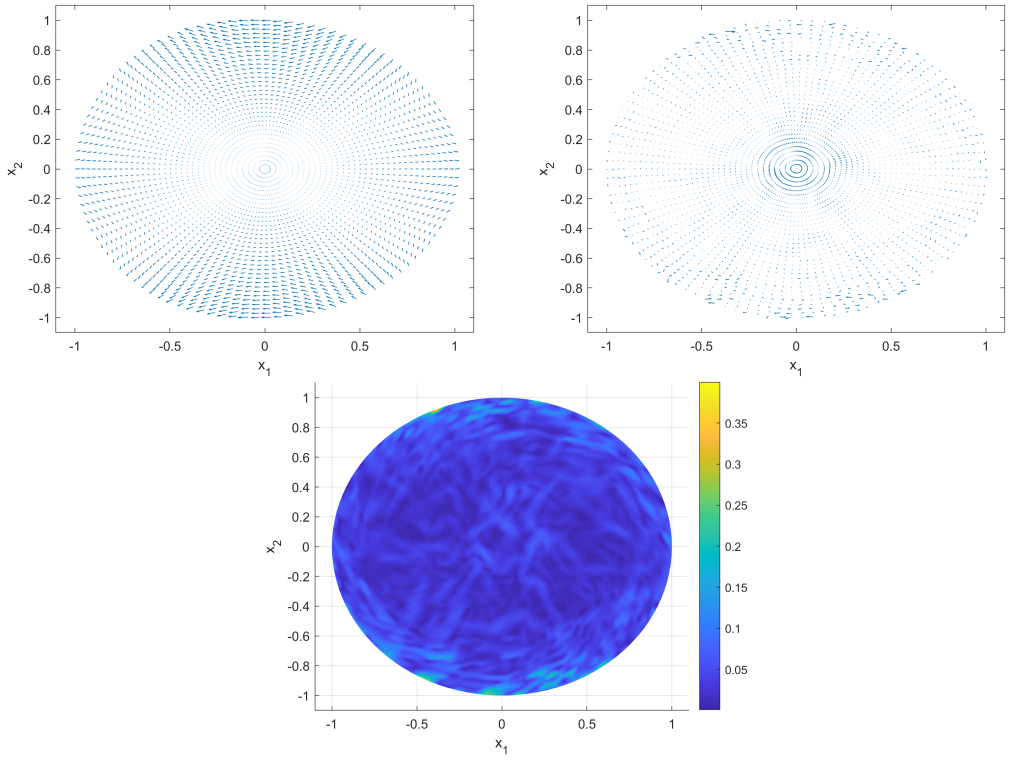

Figure 3.14: Quiver plot of reconstruction, difference to solution, and absolute error in each pixel of $f^{(2)}$ for $n^{(4)}$, $\delta = 20\%$, $\alpha = 0.1$; relative error is 8.75%

In the Euclidean part, we have seen how time-consuming the execution of $(\mathcal{S}_\alpha^\varepsilon)^*$ is and that this does not improve the reconstructions. With a variable refractive index, we would have to solve a much larger system of equations as described above, which will therefore increase the calculation time considerably. Therefore, no examples are given here for this case. We only show a numerical example of the solution of the boundary value problem that is solved by $\mathcal{S}_\alpha^\varepsilon$. Let

$$f^{(4)}(x) = \left(\frac{1}{x_1^2 + x_2^2 + 1}, x_1 + x_2 \right)^\top.$$

We choose $n^{(1)}(x)$ and $\alpha = 1$ such that (2.60) is satisfied:

$$\sup_{x \in M} \frac{\|\nabla n_1^{(1)}(x)\|}{n_1^{(1)}(x)} = \sup_{x \in M} \frac{2|x|}{(|x|^2 + \frac{4}{3})^3} \leq \frac{2}{\left(\frac{4}{3}\right)^3} \approx 0.844.$$

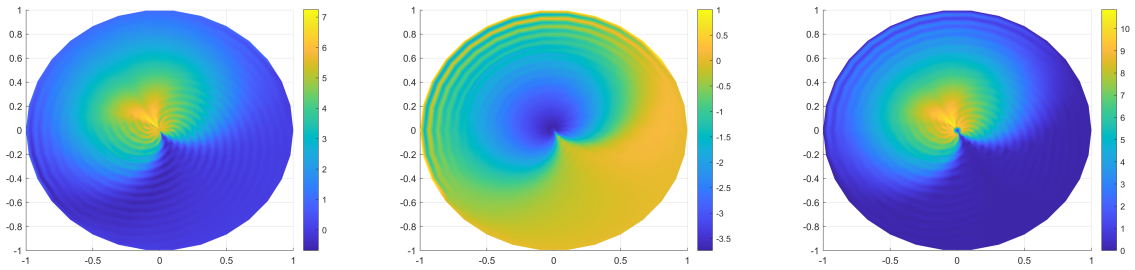

Figure 3.15: Solution of the transport equation, viscosity equation and the relative error for $(R, P, Q) = (30, 30, 10)$ and $\varepsilon = 10^{-3}$

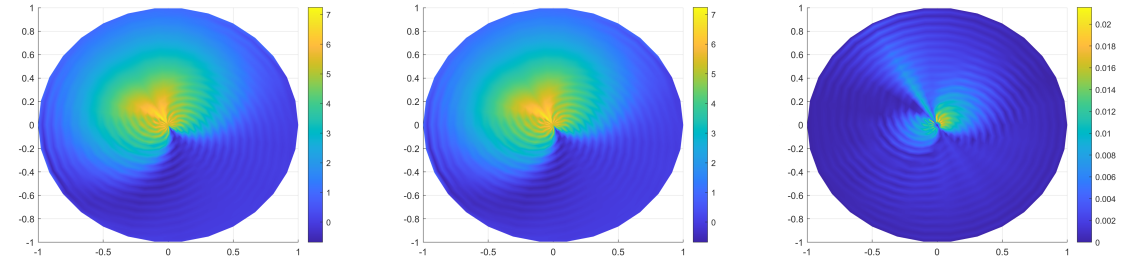

Figure 3.16: Solution of the transport equation, viscosity equation, and the relative error for $(R, P, Q) = (30, 30, 10)$ and $\varepsilon = 10^{-6}$

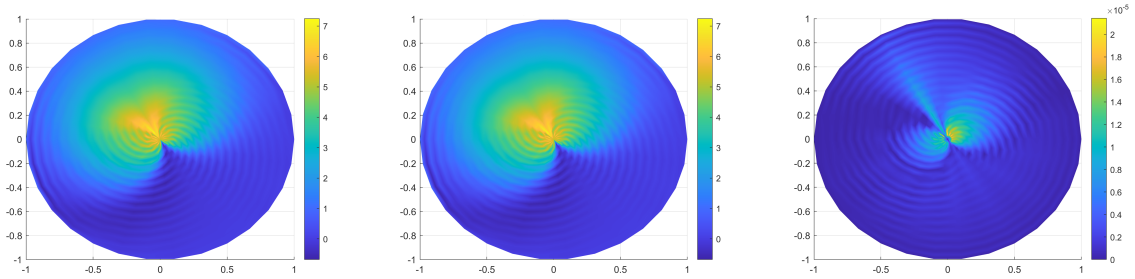

Figure 3.17: Solution of the transport equation, viscosity equation and the relative error for $(R, P, Q) = (30, 30, 10)$ and $\varepsilon = 10^{-9}$

The figures (3.15) - (3.17) are computed as described above. We see that the smaller ε gets the smaller the relative error in each grid point. We assume that the viscosity solution converges numerically to the transport solution as $\varepsilon \to 0$ for other choices of f, n, and α.

4 Conclusion and outlook

In the first part of this thesis, we derived a generalized model for tensor tomography that integrates both, absorption and refraction, and is also applicable to tensors that change over time. Having proven the continuity of the integral transformation, we have shown that it can also be interpreted as the boundary value of a transport equation. It was possible to derive the conditions under which unique weak viscosity solutions exist for the absorption coefficients and the refractive index. Based on this, the adjoint operator could also be specified in the form of a transport equation, with the difference that the solution of the actual PDE now takes place with full information about the boundary conditions. Here, too, the unambiguous solvability could be shown in the same sense as in the forward problem. An analytical solution could be found for the unperturbed transport equation so that there are now two possible representations of the adjoint problem.
We utilized this model to perform numerical experiments. Since the boundary values must be fully known for the solvability of a PDE, the integral representation is the suitable choice for the forward operator. Both variants can be implemented for the adjoint operator. Using these operators, we implemented the damped Landweber method. In the pursuit of optimal parameters for a polar grid, we identified a pattern when applying the integral operators and consistently utilized the optimal values. Beginning with a constant refractive index, excellent reconstructions of synthetic data were achieved, even at high noise levels. When solving the adjoint problem via the transport equation, very good results could be obtained for certain grids and in the absence of absorption. Unlike the integral operator, no pattern could be identified here. Furthermore, the computation time is significantly higher. However, it was confirmed through several examples that the viscosity solutions w_ε of the perturbed equation numerically converge towards the solution w of the transport equation. To circumvent uncertainty with arbitrary grids and long computation times, preference should be given to using the integral operator. This is why only this operator was further investigated for the non-Euclidean case. Here, we initially allowed only small fluctuations around the refractive index and observed a significant improvement compared to the Euclidean model. However, the computational effort increased up to 10 times. Finally, we also examined significant deviations in the signal and obtained very precise reconstructions for various absorption coefficients and high noise levels in the data. We were able to reduce the computational effort with the help of Nesterov acceleration. However, the method terminates when encountering large reconstruction errors. It is practical to utilize this method to save iteration steps and subsequently perform additional ordinary Landweber iterations with the solution that is still unsatisfactory. This approach has allowed for a reduction of approximately 25% in the number of iterations while maintaining a consistent residue level in our examples. The Landweber method demonstrated superior performance compared to

Tikhonov regularization in our experiments. Consequently, we focused on presenting the numerical results of the Landweber method, highlighting its effectiveness.

All necessary source code that is used for the numerical results is shared via GitHub under `https://github.com/tschus71/RDTT.git`.

Future research

Although the theory of the model has been provided in this thesis, there is no numerical example for tensor fields of rank greater than 1 and tensor fields that change over time. For example, one could assume that the analyzed object performs a rigid body motion, i.e., there is a time-dependent pair of a rotation matrix $A(t)$ and a transformation vector $b(t)$ so that we obtain for a reference field $f^{\text{ref}} \in C(S^m\tau'_M)$

$$f(t,x) = f^{\text{ref}}(A(t)x + b(t)).$$

Furthermore, it can be investigated how the reconstruction works for fields on a 3-dimensional domain. All three aspects mentioned above increase the dimension of the problem and thus the computational effort considerably.

Although all the generalizations mentioned so far are already very far-reaching, there is another possibility of generalization about one phenomenon: In this work, it has always been assumed that the studied material is isotropic. For isotropic materials, the refraction does not depend on the direction, but for anisotropic ones, this is the case. This means that for isotropic media the travel time from A to B is the same as from B to A, but for anisotropic this is generally not the case. This property is reflected in the metric tensor. For example, in [104] it is assumed that the metric tensor is given by

$$g_{ij} = \left[Q^T \begin{pmatrix} n_1^2 & 0 \\ 0 & n_2^2 \end{pmatrix} Q \right]_{ij}$$

where Q denotes a rotation matrix. The question arises as to how this affects the Γ_{ij}^k and, consequently, the solutions of the geodesic equation. Furthermore, it remains unclear whether a similar uniqueness condition for weak viscosity solutions of the transport equation exists in this case and what numerical results can be expected.

Finally, it remains an open question whether the solutions u_ε of the perturbed transport equation (2.56) converge with respect to a specific topology. And if so, it is also not clear whether the limit

$$\lim_{\varepsilon \to 0} u_\varepsilon$$

solves the original transport equation. Under certain assumptions for the tensor field f and the metric g one can show that

$$u_{\varepsilon_j} \to u \quad \text{as } j \to +\infty \quad \text{locally uniformly on } [0,T] \times \Omega M$$

for a subsequence $\{\varepsilon_j\}_{j\in\mathbb{N}}$ and a viscosity solution u (c.f. [100]). Alternatively, one can interpret $\mathcal{S}_\alpha^\varepsilon$, $\mathcal{S}_\alpha^{\varepsilon,d}$ as inexact operators, i.e. there is a number $\eta(\varepsilon)$ such that

$$\|\mathcal{S}_\alpha^{\varepsilon(,d)} - \mathcal{S}_\alpha^{0(,d)}\| \leq \eta(\varepsilon)$$

measuring the model uncertainty due to the degree of perturbation ε. This interpretation has for example been studied in [13],[14] and [100]. We define a family of Tikhonov functionals $\{\mathcal{J}_\varepsilon\}_{\varepsilon>0}$ by

$$\mathcal{J}_\varepsilon(f) \coloneqq \frac{1}{2}\|\mathcal{S}_\alpha^{\varepsilon(,d)} f - \phi^\delta\|^2 + \frac{\beta}{2}\|f\|^2.$$

The idea is to prove that

$$\mathcal{J}_\varepsilon \xrightarrow{\Gamma} \mathcal{J}_0$$

in the sense of Γ-convergence which is a special type of convergence of functionals. Given a Banach space X, a sequence $S_n \colon X \to [0,\infty]$ is said to Γ-converge to a limit $F \colon X \to [0,\infty]$ if the following to conditions hold:

- For any converging sequence (f_n) in X with $\lim_{n\to\infty} f_n = f \in X$ it holds that

$$S(f) \leq \liminf_{n\to\infty} S_n(f_n).$$

- For any $f \in X$ there is a sequence (f_n) in X converging to f such that

$$S(f) \geq \limsup_{n\to\infty} S_n(f_n).$$

Consequently, instead of proving the convergence of the forward operators directly, one shows the convergence of the respecting Tikhonov functionals. This is a milder condition because a converging sequence of forward operators leads to Γ-converging Tikhonov functionals. The following result from [14] is implied:

If the family of functionals $\{\mathcal{J}_\varepsilon\}_{\varepsilon>0}$ is uniformly mildly coercive and

$$\mathcal{J}_\varepsilon \xrightarrow{\Gamma} \mathcal{J}_0,$$

then any accumulation point of a minimizing sequence $\{f_\varepsilon\}$ of $\mathcal{J}_\varepsilon$ is a minimizer of $\mathcal{J}_0$.

As a consequence, this theorem guarantees that minimizers of $\mathcal{J}_\varepsilon$ are 'close' to those of $\mathcal{J}_0$. Therefore, the convergence of

$$u_\varepsilon \to u$$

is not necessarily demanded. Alternatively, one can use the criteria presented in [12] guaranteeing Γ-convergence as well as the convergence of minimizing sequences.

A Appendix

A.1 Proof of Theorem 2.8

First, we consider the case $N = 2$. Writing ξ in polar coordinates, we get

$$\xi = \begin{pmatrix} \xi^1 \\ \xi^2 \end{pmatrix} = n^{-1}(x) \begin{pmatrix} \cos\varphi \\ \sin\varphi \end{pmatrix}.$$

Next, we need the derivatives $\frac{\partial u}{\partial \xi^1}$ and $\frac{\partial u}{\partial \xi^2}$. We compute

$$\begin{aligned} \frac{\partial u}{\partial \xi^1} &= \frac{\partial u}{\partial \varphi}\frac{\partial \varphi}{\partial \xi^1} && \text{(A.1)} \\ &= \frac{\partial u}{\partial \varphi} \cdot \frac{\partial}{\partial \xi^1} \arctan\left(\frac{\xi^2}{\xi^1}\right) \\ &= \frac{\partial u}{\partial \varphi} \cdot \frac{-\frac{\xi^2}{(\xi^1)^2}}{1 + (\frac{\xi^2}{\xi^1})^2} \\ &= -\frac{\partial u}{\partial \varphi} \cdot \frac{n(x)\frac{\sin\varphi}{\cos^2\varphi}}{\frac{1}{\cos^2\varphi}} \\ &= -n(x)\sin\varphi \frac{\partial u}{\partial \varphi}. && \text{(A.2)} \end{aligned}$$

Similarly,

$$\begin{aligned} \frac{\partial u}{\partial \xi^2} &= \frac{\partial u}{\partial \varphi}\frac{\partial \varphi}{\partial \xi^2} && \text{(A.3)} \\ &= \frac{\partial u}{\partial \varphi} \cdot \frac{\partial}{\partial \xi^2} \arctan\left(\frac{\xi^2}{\xi^1}\right) \\ &= \frac{\partial u}{\partial \varphi} \cdot \frac{\frac{1}{\xi^1}}{1 + (\frac{\xi^2}{\xi^1})^2} \\ &= \frac{\partial u}{\partial \varphi} \cdot \frac{n(x)\frac{1}{\cos\varphi}}{\frac{1}{\cos^2\varphi}} \\ &= n(x)\cos\varphi \frac{\partial u}{\partial \varphi}. && \text{(A.4)} \end{aligned}$$

We use (2.27) and (2.28) and write the left-hand side of (2.51) as

$$
\begin{aligned}
&-\int_{\Omega_x M} \Gamma_{ij}^k \xi^i \xi^j \frac{\partial u}{\partial \xi^k} w \mathrm{d}\omega_x(\xi) \\
&= \int_0^{2\pi} n^{-1}(x) \left(n^{-2}(x) \frac{\partial n}{\partial x_k}(x) - 2\xi^k \langle \xi, \nabla n(x) \rangle \right) \frac{\partial u(x,\xi)}{\partial \xi^k} u(x,\xi) \mathrm{d}\varphi.
\end{aligned}
$$

Using (A.1) and (A.3), we obtain for $k = 1, 2$

$$
\begin{aligned}
&\left(n^{-2}(x) \frac{\partial n}{\partial x_1}(x) - 2\xi^1 \langle \xi, \nabla n(x) \rangle \right) \frac{\partial u(x,\xi)}{\partial \xi^1} \\
&= \left(n^{-2}(x) \frac{\partial n}{\partial x_1}(x) - 2n^{-1}(x) \cos\varphi \left(n^{-1}(x) \frac{\partial n}{\partial x_1}(x) \cos\varphi + n^{-1}(x) \frac{\partial n}{\partial x_2}(x) \sin\varphi \right) \right) \times \\
&\quad \times \left(-n(x) \sin\varphi \frac{\partial u}{\partial \varphi} \right) \\
&= \left(-n^{-1}(x) \frac{\partial n}{\partial x_1}(x) \sin\varphi + 2n^{-1}(x) \frac{\partial n}{\partial x_1}(x) \cos^2\varphi \sin\varphi + 2n^{-1}(x) \frac{\partial n}{\partial x_2}(x) \cos\varphi \sin^2\varphi \right) \frac{\partial u}{\partial \varphi} \\
&= \left(n^{-1}(x) \frac{\partial n}{\partial x_1}(x) (2\cos^2\varphi \sin\varphi - \sin\varphi) + 2n^{-1}(x) \frac{\partial n}{\partial x_2}(x) \cos\varphi \sin^2\varphi \right) \frac{\partial u}{\partial \varphi}
\end{aligned}
$$

and

$$
\begin{aligned}
&\left(n^{-2}(x) \frac{\partial n}{\partial x_2}(x) - 2\xi^2 \langle \xi, \nabla n(x) \rangle \right) \frac{\partial u(x,\xi)}{\partial \xi^2} \\
&= \left(n^{-2}(x) \frac{\partial n}{\partial x_2}(x) - 2n^{-1}(x) \sin\varphi \left(n^{-1}(x) \frac{\partial n}{\partial x_1}(x) \cos\varphi + n^{-1}(x) \frac{\partial n}{\partial x_2}(x) \sin\varphi \right) \right) \times \\
&\quad \times \left(n(x) \cos\varphi \frac{\partial u}{\partial \varphi} \right) \\
&= \left(n^{-1}(x) \frac{\partial n}{\partial x_2}(x) \cos\varphi - 2n^{-1}(x) \frac{\partial n}{\partial x_1}(x) \cos^2\varphi \sin\varphi - 2n^{-1}(x) \frac{\partial n}{\partial x_2}(x) \cos\varphi \sin^2\varphi \right) \frac{\partial u}{\partial \varphi} \\
&= \left(n^{-1}(x) \frac{\partial n}{\partial x_1}(x) (-2\cos^2\varphi \sin\varphi) + n^{-1}(x) \frac{\partial n}{\partial x_2}(x) (\cos\varphi - 2\cos\varphi \sin^2\varphi) \right) \frac{\partial u}{\partial \varphi}.
\end{aligned}
$$

Cancellation of terms yields

$$
-\int_{\Omega_x M} \Gamma_{ij}^k \xi^i \xi^j \frac{\partial u}{\partial \xi^k} w \mathrm{d}\omega_x(\xi) = \int_0^{2\pi} n^{-2}(x) \left(-\frac{\partial n}{\partial x_1}(x) \sin\varphi + \frac{\partial n}{\partial x_2}(x) \cos\varphi \right) \frac{\partial u}{\partial \varphi} w \mathrm{d}\varphi.
$$

Integration by parts leads to

$$\begin{aligned}
&\int_0^{2\pi} n^{-2}(x)\left(-\frac{\partial n}{\partial x_1}(x)\sin\varphi+\frac{\partial n}{\partial x_2}(x)\cos\varphi\right)\frac{\partial u}{\partial\varphi}w\mathrm{d}\varphi\\
&=-\int_0^{2\pi} n^{-2}(x)\left(-\frac{\partial n(x)}{\partial x_1}\sin\varphi+\frac{\partial n(x)}{\partial x_2}\cos\varphi\right)\frac{\partial w}{\partial\varphi}u\\
&\quad+n^{-2}(x)\left(\frac{\partial n(x)}{\partial x_1}\cos\varphi+\frac{\partial n(x)}{\partial x_2}\sin\varphi\right)uw\mathrm{d}\varphi\\
&=\int_{\Omega_x M}\Gamma_{ij}^k\xi^i\xi^j\frac{\partial w}{\partial\xi^k}u\mathrm{d}\omega_x(\xi)+\int_{\Omega_x M} n^{-1}(x)\langle\nabla n,\xi\rangle\ uw\omega_x(\xi).
\end{aligned}$$

The analog can be done for $N=3$. Writing ξ in spherical coordinates as

$$\xi=\begin{pmatrix}\xi^1\\ \xi^2\\ \xi^3\end{pmatrix}=n^{-1}(x)\begin{pmatrix}\cos\varphi\sin\theta\\ \sin\varphi\sin\theta\\ \cos\theta\end{pmatrix}.$$

To obtain the derivatives $\frac{\partial u}{\partial\xi^1}$, $\frac{\partial u}{\partial\xi^2}$ and $\frac{\partial u}{\partial\xi^3}$ we compute:

$$\begin{aligned}
\frac{\partial u}{\partial\varphi}\frac{\partial\varphi}{\partial\xi^1}&=\frac{\partial u}{\partial\varphi}\cdot\frac{\partial}{\partial\xi^1}\arctan\left(\frac{\xi^2}{\xi^1}\right)\\
&=\frac{\partial u}{\partial\varphi}\cdot\frac{-\frac{\xi^2}{(\xi^1)^2}}{1+(\frac{\xi^2}{\xi^1})^2}\\
&=-\frac{\partial u}{\partial\varphi}\cdot\frac{n(x)\frac{\sin\varphi}{\cos^2\varphi\sin\theta}}{\frac{1}{\cos^2\varphi}}\\
&=-n(x)\frac{\sin\varphi}{\sin\theta}\frac{\partial u}{\partial\varphi},
\end{aligned}$$

$$\begin{aligned}
\frac{\partial u}{\partial\theta}\frac{\partial\theta}{\partial\xi^1}&=\frac{\partial u}{\partial\theta}\frac{\partial}{\partial\xi^1}\arctan\left(\frac{\sqrt{(\xi^1)^2+(\xi^2)^2}}{\xi^3}\right)\\
&=\frac{\partial u}{\partial\theta}\frac{\frac{\xi^1}{\xi^3\sqrt{(\xi^1)^2+(\xi^2)^2}}}{1+\frac{(\xi^1)^2+(\xi^2)^2}{(\xi^3)^2}}\\
&=n(x)\cos\varphi\cos\theta\frac{\partial u}{\partial\theta}.
\end{aligned}$$

Hence,

$$\frac{\partial u}{\partial\xi^1}=\frac{\partial u}{\partial\varphi}\frac{\partial\varphi}{\partial\xi^1}+\frac{\partial u}{\partial\theta}\frac{\partial\theta}{\partial\xi^1}=-n(x)\frac{\sin\varphi}{\sin\theta}\frac{\partial u}{\partial\varphi}+n(x)\cos\varphi\cos\theta\frac{\partial u}{\partial\theta}. \tag{A.5}$$

In the same way we get

$$\begin{aligned}\frac{\partial u}{\partial \varphi}\frac{\partial \varphi}{\partial \xi^2} &= \frac{\partial u}{\partial \varphi}\cdot\frac{\partial}{\partial \xi^2}\arctan\left(\frac{\xi^2}{\xi^1}\right)\\ &= \frac{\partial u}{\partial \varphi}\cdot\frac{\frac{1}{\xi^1}}{1+(\frac{\xi^2}{\xi^1})^2}\\ &= \frac{\partial u}{\partial \varphi}\cdot\frac{n(x)\frac{1}{\cos\varphi\sin\theta}}{\frac{1}{\cos^2\varphi}}\\ &= n(x)\frac{\cos\varphi}{\sin\theta}\frac{\partial u}{\partial \varphi},\end{aligned}$$

$$\begin{aligned}\frac{\partial u}{\partial \theta}\frac{\partial \theta}{\partial \xi^2} &= \frac{\partial u}{\partial \theta}\frac{\partial}{\partial \xi^2}\arctan\left(\frac{\sqrt{(\xi^1)^2+(\xi^2)^2}}{\xi^3}\right)\\ &= \frac{\partial u}{\partial \theta}\frac{\frac{\xi^2}{\xi^3\sqrt{(\xi^1)^2+(\xi^2)^2}}}{1+\frac{(\xi^1)^2+(\xi^2)^2}{(\xi^3)^2}}\\ &= n(x)\sin\varphi\cos\theta\frac{\partial u}{\partial \theta},\end{aligned}$$

and thus,

$$\frac{\partial u}{\partial \xi^2} = \frac{\partial u}{\partial \varphi}\frac{\partial \varphi}{\partial \xi^2} + \frac{\partial u}{\partial \theta}\frac{\partial \theta}{\partial \xi^2} = n(x)\frac{\cos\varphi}{\sin\theta}\frac{\partial u}{\partial \varphi} + n(x)\sin\varphi\cos\theta\frac{\partial u}{\partial \theta}, \tag{A.6}$$

as well as

$$\begin{aligned}\frac{\partial u}{\partial \xi^3} = \frac{\partial u}{\partial \theta}\frac{\partial \theta}{\partial \xi^3} &= \frac{\partial u}{\partial \theta}\cdot\frac{\partial}{\partial \xi^3}\arctan\left(\frac{\xi^2}{\xi^1}\right)\\ &= \frac{\partial u}{\partial \theta}\cdot\frac{-\sqrt{(\xi^1)^2+(\xi^2)^2}/(\xi^3)^2}{\frac{1}{\cos^2\theta}}\\ &= -n(x)\sin\theta\frac{\partial u}{\partial \theta}.\end{aligned} \tag{A.7}$$

Using (2.29) and (2.27) we write the left-hand side of (2.53) as

$$\begin{aligned}&-\int_{\Omega_x M}\Gamma^k_{ij}\xi^i\xi^j\frac{\partial u}{\partial \xi^k}u\mathrm{d}\omega_x(\xi)\\ &=\int_0^{2\pi}\int_0^{\pi} n^{-1}(x)\left(n^{-2}(x)\frac{\partial n(x)}{\partial x_k} - 2\xi^k\langle\xi,\nabla n(x)\rangle\right)\frac{\partial u(x,\xi)}{\partial x_k}w(x,\xi)\sin\theta\mathrm{d}\theta\mathrm{d}\varphi.\end{aligned}$$

Next, we use (A.5), (A.6) and (A.7) to obtain separately for $k = 1$

$$\begin{aligned}
&\left(n^{-2}(x)\frac{\partial n(x)}{\partial x_1} - 2\xi^1\langle\xi, \nabla n\rangle\right)\frac{\partial u}{\partial \xi^1}\sin\theta \\
&= \left(n^{-1}(x)\frac{\partial u}{\partial \theta}\right)\Big(\partial_1 n\cos\varphi\cos\theta\sin\theta - 2\partial_1 n\cos^3\varphi\cos\theta\sin^3\theta \\
&\quad -2\partial_2 n\cos^2\varphi\sin\varphi\cos\theta\sin^3\theta - 2\partial_3 n\cos^2\varphi\cos^2\theta\sin^2\theta\Big) \\
&\quad + \left(n^{-1}(x)\frac{\partial u}{\partial \varphi}\right)\Big(-\partial_1 n\sin\varphi + 2\partial_1 n\cos^2\varphi\sin\varphi\sin^2\theta \\
&\quad +2\partial_2 n\cos\varphi\sin^2\varphi\sin^2\theta + 2\partial_3 n\cos\varphi\sin\varphi\cos\theta\sin\theta\Big), \qquad \text{(A.8)}
\end{aligned}$$

for $k = 2$

$$\begin{aligned}
&\left(n^{-2}(x)\frac{\partial n(x)}{\partial x_2} - 2\xi^2\langle\xi, \nabla n\rangle\right)\frac{\partial u}{\partial \xi^2}\sin\theta \\
&= \left(n^{-1}(x)\frac{\partial u}{\partial \theta}\right)\Big(\partial_2 n\sin\varphi\cos\theta\sin\theta - 2\partial_1 n\cos\varphi\sin^2\varphi\cos\theta\sin^3\theta \\
&\quad -2\partial_2 n\sin^3\varphi\cos\theta\sin^3\theta - 2\partial_3 n\sin^2\varphi\cos^2\theta\sin^2\theta\Big) \\
&\quad + \left(n^{-1}(x)\frac{\partial u}{\partial \varphi}\right)\Big(\partial_2 n\cos\varphi - 2\partial_1 n\cos^2\varphi\sin\varphi\sin^2\theta \\
&\quad -2\partial_2 n\cos\varphi\sin^2\varphi\sin^2\theta - 2\partial_3 n\cos\varphi\sin\varphi\cos\theta\sin\theta\Big), \qquad \text{(A.9)}
\end{aligned}$$

and for $k = 3$

$$\begin{aligned}
&\left(n^{-2}(x)\frac{\partial n(x)}{\partial x_3} - 2\xi^3\langle\xi, \nabla n\rangle\right)\frac{\partial u}{\partial \xi^3}\sin\theta \\
&= \left(n^{-1}(x)\frac{\partial u}{\partial \theta}\right)\times \\
&\times\Big(-\partial_3 n\sin^2\theta + 2\partial_1 n\cos\varphi\cos\theta\sin^3\theta + 2\partial_2 n\sin\varphi\cos\theta\sin^3\theta + 2\partial_3 n\cos^2\theta\sin^2\theta\Big). \qquad \text{(A.10)}
\end{aligned}$$

After some simplifications we get

$$\begin{aligned}
&\left(n^{-2}(x)\frac{\partial n}{\partial x_k}(x) - 2\xi^k\langle\xi, \nabla n(x)\rangle\right)\frac{\partial u}{\partial \xi^k}\sin\theta \\
&= n^{-1}(x)(\partial_1 n\sin\theta\cos\theta\cos\varphi + \partial_2 n\sin\theta\cos\theta\sin\varphi - \partial_3 n\sin^2\theta)\frac{\partial u}{\partial \theta} \\
&\quad + n^{-1}(x)(\partial_2 n\cos\varphi - \partial_1 n\sin\varphi)\frac{\partial u}{\partial \varphi}
\end{aligned}$$

and thus,

$$\begin{aligned}
&\int_0^{2\pi}\int_0^{\pi} n^{-1}(x)\left(n^{-2}(x)\frac{\partial n}{\partial x^i}(x) - 2\xi^k\langle\xi,\nabla n(x)\rangle\right)\frac{\partial u(x,\xi)}{\partial \xi^k}w(x,\xi)\sin\theta \mathrm{d}\theta\mathrm{d}\varphi\\
&= \int_0^{2\pi}\int_0^{\pi} n^{-2}(x)(\partial_1 n\sin\theta\cos\theta\cos\varphi + \partial_2 n\sin\theta\cos\theta\sin\varphi - \partial_3 n\sin^2\theta)\frac{\partial u}{\partial\theta}w\mathrm{d}\theta\mathrm{d}\varphi\\
&+ \int_0^{2\pi}\int_0^{\pi} n^{-2}(x)(\partial_2 n\cos\varphi - \partial_1 n\sin\varphi)\frac{\partial u}{\partial\varphi}w\mathrm{d}\theta\mathrm{d}\varphi.
\end{aligned}$$

An integration by parts with respect to θ in the first integral leads to

$$\begin{aligned}
&\int_0^{2\pi}\int_0^{\pi} n^{-2}(x)(\partial_1 n\sin\theta\cos\theta\cos\varphi + \partial_2 n\sin\theta\cos\theta\sin\varphi - \partial_3 n\sin^2\theta)\frac{\partial u}{\partial\theta}w\mathrm{d}\theta\mathrm{d}\varphi\\
&= \int_0^{2\pi}\left[n^{-2}(x)(\partial_1 n\sin\theta\cos\theta\cos\varphi + \partial_2 n\sin\theta\cos\theta\sin\varphi - \partial_3 n\sin^2\theta)u^2\right]_0^{\pi}\mathrm{d}\varphi\\
&\quad - \int_0^{\pi}\int_0^{2\pi} n^{-2}(x)(\partial_1 n\sin\theta\cos\theta\cos\varphi + \partial_2 n\sin\theta\cos\theta\sin\varphi - \partial_3 n\sin^2\theta)\frac{\partial w}{\partial\theta}u\mathrm{d}\varphi\mathrm{d}\theta\\
&\quad - \int_0^{\pi}\int_0^{2\pi} n^{-2}(x)\partial_1 n\cos\varphi(\cos^2\theta - \sin^2\theta)uw\mathrm{d}\varphi\mathrm{d}\theta\\
&\quad - \int_0^{\pi}\int_0^{2\pi} n^{-2}(x)(\partial_2 n\sin\varphi(\cos^2\theta - \sin^2\theta) - 2\partial_3 n\sin\theta\cos\theta)uw\mathrm{d}\varphi\mathrm{d}\theta.
\end{aligned}$$

An according integration by parts with respect to φ yields

$$\begin{aligned}
&\int_0^{2\pi}\int_0^{\pi} n^{-2}(x)(\partial_2 n\cos\varphi - \partial_1 n\sin\varphi)\frac{\partial u}{\partial\varphi}w\mathrm{d}\theta\mathrm{d}\varphi\\
&= \int_0^{\pi}\left[n^{-2}(x)\left(\partial_2 n(x)\cos\varphi - \partial_1 n(x)\sin\varphi\right)uw\right]_0^{2\pi}\mathrm{d}\theta\\
&\quad - \int_0^{\pi}\int_0^{2\pi} u\frac{\partial w}{\partial\varphi}n^{-2}(x)\left(\partial_2 n(x)\cos\varphi - \partial_1 n(x)\sin\varphi\right)\mathrm{d}\varphi\mathrm{d}\theta\\
&\quad - \int_0^{\pi}\int_0^{2\pi} uwn^{-2}(x)\left(-\partial_2 n(x)\sin\varphi - \partial_1 n(x)\cos\varphi\right)\mathrm{d}\varphi\mathrm{d}\theta.
\end{aligned}$$

Because of the periodicity of the trigonometric functions, the first integral vanishes in each case and we arrive at

$$
\begin{aligned}
&\int_{\Omega_x M} n^{-1}(x)\left(n^{-2}(x)\frac{\partial n}{\partial x_k}(x)-2\xi^k\langle\xi,\nabla n(x)\rangle\right)\frac{\partial u}{\partial \xi^k}u\mathrm{d}\omega_x(\xi)\\
=&-\int_0^{\pi}\int_0^{2\pi} n^{-2}(x)(\partial_1 n\sin\theta\cos\theta\cos\varphi+\partial_2 n\sin\theta\cos\theta\sin\varphi-\partial_3 n\sin^2\theta)\frac{\partial w}{\partial\theta}u\mathrm{d}\varphi\mathrm{d}\theta\\
&-\int_0^{\pi}\int_0^{2\pi} u\frac{\partial w}{\partial\varphi}n^{-2}(x)\left(\partial_2 n(x)\cos\varphi-\partial_1 n(x)\sin\varphi\right)\mathrm{d}\varphi\mathrm{d}\theta\\
&-\int_0^{\pi}\int_0^{2\pi} n^{-2}(x)\partial_1 n\cos\varphi(\cos^2\theta-\sin^2\theta)uw\mathrm{d}\varphi\mathrm{d}\theta\\
&-\int_0^{\pi}\int_0^{2\pi} n^{-2}(x)(\partial_2 n\sin\varphi(\cos^2\theta-\sin^2\theta)-2\partial_3 n\sin\theta\cos\theta)uw\mathrm{d}\varphi\mathrm{d}\theta\\
&-\int_0^{\pi}\int_0^{2\pi} n^{-2}(x)\left(-\partial_2 n(x)\sin\varphi-\partial_1 n(x)\cos\varphi\right)uw\mathrm{d}\varphi\mathrm{d}\theta\\
=&\int_{\Omega_x M}\Gamma_{ij}^k\xi^i\xi^j\frac{\partial w}{\partial\xi^k}u\mathrm{d}\omega_x(\xi)+2\int_{\Omega_x M} n^{-1}\langle\nabla n,\xi\rangle uw\mathrm{d}\omega_x(\xi).
\end{aligned}
$$

A.2 Gradient and Laplacian in spherical coordinates

In the Euclidean case, the Laplacian in spherical coordinates (c.f. [10]), applied to a scalar function Φ, is given by

$$\Delta\Phi = \frac{1}{r^2}\frac{\partial}{\partial r}\left(r^2\frac{\partial\Phi}{\partial r}\right) + \frac{1}{r^2\sin\theta}\frac{\partial}{\partial\theta}\left(\sin\theta\frac{\partial\Phi}{\partial\theta}\right) + \frac{1}{r^2\sin\theta^2}\frac{\partial^2\Phi}{\partial\varphi^2}.$$

For $N = 2$ the angle θ can be set as a constant $\frac{\pi}{2}$ and therefore,

$$\Delta\Phi = \frac{1}{r}\frac{\partial}{\partial r}\left(r\frac{\partial\Phi}{\partial r}\right) + \frac{1}{r^2}\frac{\partial^2\Phi}{\partial\varphi^2}.$$

On the Riemannian manifold (M, g) the Laplacian becomes the Laplace-Beltrami operator Δu of a scalar function $u \in C^2(\Omega M)$. In cartesian coordinates we use (1.26) to compute

$$\begin{aligned}\Delta u &= \frac{1}{\sqrt{\det g}}\sum_{i,j=1}^{N}\left(\frac{\partial}{\partial x_i}\left(\sqrt{\det g}g^{ij}\frac{\partial u}{\partial x_j}\right) + \frac{\partial}{\partial\xi^i}\left(\sqrt{\det g}g^{ij}\frac{\partial u}{\partial\xi^j}\right)\right)\\ &= n^{-N}(x)\sum_{i,j=1}^{N}\left(\frac{\partial}{\partial x_i}\left(n^{N-2}(x)\frac{\partial u}{\partial x_i}\right) + n^{N-2}(x)\frac{\partial^2 u}{\partial(\xi^i)^2}\right)\\ &= n^{-2}(x)\sum_{i=1}^{N}\left(\frac{\partial^2 u}{\partial x_i^2} + \frac{\partial^2 u}{\partial(\xi^i)^2}\right) + (N-2)n^{-3}(x)\sum_{i=1}^{N}\frac{\partial n}{\partial x_i}\frac{\partial u}{\partial x_i}. \qquad \text{(A.11)}\end{aligned}$$

In polar coordinates, we parameterize similarly to the proof of 2.8. For $N = 2$ we get

$$\xi = \begin{pmatrix}\xi^1\\ \xi^2\end{pmatrix} = n^{-1}(x)\begin{pmatrix}\cos\varphi\\ \sin\varphi.\end{pmatrix}, \qquad x = \begin{pmatrix}x_1\\ x_2\end{pmatrix} = r\begin{pmatrix}\cos\mu\\ \sin\mu.\end{pmatrix}$$

Hence, (A.11) becomes

$$\Delta u = n^{-2}(x)\left(\frac{1}{r^2}\frac{\partial}{\partial r}\left(r^2\frac{\partial u}{\partial r}\right) + \frac{1}{r^2}\frac{\partial^2 u}{\partial\mu^2} + \frac{\partial^2 u}{\partial\varphi^2}\right).$$

Accordingly for $N = 3$, we parametrize

$$x = \begin{pmatrix}x_1\\ x_2\\ x_3\end{pmatrix} = r\begin{pmatrix}\cos\mu\sin\eta\\ \sin\mu\sin\eta\\ \cos\eta\end{pmatrix}, \qquad \xi = \begin{pmatrix}\xi^1\\ \xi^2\\ \xi^3\end{pmatrix} = n^{-1}(x)\begin{pmatrix}\cos\varphi\sin\theta\\ \sin\varphi\sin\theta\\ \cos\theta\end{pmatrix}.$$

Observing that

$$\begin{aligned}\sum_{i=1}^{N}\frac{\partial n}{\partial x_i}\frac{\partial u}{\partial x_i} &= \langle\nabla_{\text{euclid}}n,\nabla_{\text{euclid}}u\rangle_{\text{euclid}}\\ &= \frac{\partial n}{\partial r}\frac{\partial u}{\partial r}+\frac{1}{r^2\sin^2\eta}\frac{\partial n}{\partial\mu}\frac{\partial u}{\partial\mu}+\frac{1}{r^2}\frac{\partial n}{\partial\eta}\frac{\partial\mu}{\partial\eta}.\end{aligned}$$

we obtain

$$\begin{aligned}\Delta u = n^{-2}(x)&\left(\frac{1}{r^2}\frac{\partial}{\partial r}\left(r^2\frac{\partial\Phi}{\partial r}\right)+\frac{1}{r^2\sin\theta}\frac{\partial}{\partial\theta}\left(\sin\theta\frac{\partial\Phi}{\partial\theta}\right)+\frac{1}{r^2\sin\theta^2}\frac{\partial^2\Phi}{\partial\varphi^2}\right)+\frac{1}{\sin^2\theta}\frac{\partial^2u}{\partial\varphi^2}\\ &+n^{-3}(x)\left(\frac{\partial n}{\partial r}\frac{\partial u}{\partial r}+\frac{1}{r^2\sin^2\eta}\frac{\partial n}{\partial\mu}\frac{\partial u}{\partial\mu}+\frac{1}{r^2}\frac{\partial n}{\partial\eta}\frac{\partial u}{\partial\eta}\right).\end{aligned}$$

A.3 Computation of integral transforms for some examples

Chapter 2 introduced $\mathcal{I}_\alpha^{(d)}$ for tensor fields. For the numerical application and analysis of the solution methods from Chapter 3, the transformations are calculated for some examples where the integration is also possible analytically. For all examples, we consider $N = 2$ and g as the Euclidean metric. We parametrize x by

$$x = \begin{pmatrix} x_1 \\ x_2 \end{pmatrix} = \begin{pmatrix} r\cos\mu \\ r\sin\mu \end{pmatrix}, \quad r \in [0,1], \mu \in [0, 2\pi]$$

$$\xi = \begin{pmatrix} \xi^1 \\ \xi^2 \end{pmatrix} = \begin{pmatrix} \cos\varphi \\ \sin\varphi \end{pmatrix}, \qquad \varphi \in [0, 2\pi].$$

A.3.1 Constant vector field

For constants A and B let

$$f^{(0)}(x_1, x_2) = \begin{pmatrix} A \\ B \end{pmatrix}.$$

Then,

$$\begin{aligned}
[\mathcal{I}_{\alpha_0} f^{(0)}](x,\xi) &= \int_{\tau_-(x,\xi)}^{0} \langle f(x+\tau\xi), \xi\rangle e^{\alpha_0\tau} \mathrm{d}\tau \\
&= \int_{\tau_-(x,\xi)}^{0} (A\xi^1 + B\xi^2) e^{\alpha_0\tau} \mathrm{d}\tau \\
&= \frac{A\xi^1 + B\xi^2}{\alpha_0} \left(1 - e^{\alpha_0 \tau_-(x,\xi)}\right)
\end{aligned}$$

and

$$[\mathcal{I}_0 f^{(0)}](x,\xi) = -(A\xi^1 + B\xi^2)\tau_-(x,\xi).$$

We want to compute $||\mathcal{I}_0 f^{(0)}||_{L^2(\partial_+\Omega M)}$ for $f(x) = (A,B)^\top$.

$$\mathcal{I}_0 f^{(0)}(x,\xi) = -(A\xi^1 + B\xi^2)\tau_-(x,\xi) = (A\xi^1 + B\xi^2)\left(\langle x,\xi\rangle + \sqrt{\langle x,\xi\rangle^2 + 1 - \langle x, x\rangle}\right).$$

$$\begin{aligned}
\langle \mathcal{I}_0 f^{(0)}, \mathcal{I}_0 f^{(0)} \rangle_{L^2(\partial_+\Omega M)} &= \int_{\partial_+\Omega M} |\mathcal{I}_0 f^{(0)}(x,\xi)|^2 \mathrm{d}\sigma_+(\xi) \\
&= \int_{\partial_+\Omega M} (A\xi^1 + B\xi^2)^2 \left(\langle x,\xi\rangle + |\langle x,\xi\rangle|\right)^2 \mathrm{d}\sigma_+(\xi)
\end{aligned}$$

Parametrizing $x = (\cos\mu, \sin\mu)^\top$, $\xi = (\cos\varphi, \sin\varphi)^\top$,

$$\langle \mathcal{I}_0 f^{(0)}, \mathcal{I}_0 f^{(0)} \rangle_{L^2(\partial_+\Omega M)} = \int_0^{2\pi} (A\cos\varphi + B\sin\varphi)^2 \int_0^{2\pi} \left(\cos(\mu-\varphi) + |\cos(\mu-\varphi)|\right)^2 \mathrm{d}\mu \mathrm{d}\varphi.$$

Since the integrand of the inner integral is 2π-periodic, we have

$$\begin{aligned}
&\int_0^{2\pi} \left(\cos(\mu-\varphi) + |\cos(\mu-\varphi)|\right)^2 \mathrm{d}\mu \\
&= \int_0^{\frac{\pi}{2}} \left(\cos(\mu) + |\cos(\mu)|\right)^2 \mathrm{d}\mu + \int_{\frac{\pi}{2}}^{\frac{3\pi}{2}} \left(\cos(\mu) + |\cos(\mu)|\right)^2 \mathrm{d}\mu \\
&+ \int_{\frac{3\pi}{2}}^{2\pi} \left(\cos(\mu) + |\cos(\mu)|\right)^2 \mathrm{d}\mu \\
&= \int_0^{\frac{\pi}{2}} 4\cos^2(\mu)\mathrm{d}\mu + \int_{\frac{3\pi}{2}}^{2\pi} 4\cos^2(\mu)\mathrm{d}\mu \\
&= [\sin(2\mu) + 2\mu]_0^{\frac{\pi}{2}} + [\sin(2\mu) + 2\mu]_{\frac{3\pi}{2}}^{2\pi} \\
&= 2\pi
\end{aligned}$$

and therefore,

$$\begin{aligned}
\langle \mathcal{I}_0 f^{(0)}, \mathcal{I}_0 f^{(0)} \rangle_{L^2(\partial_+\Omega M)} &= 2\pi \int_0^{2\pi} (A\cos\varphi + B\sin\varphi)^2 \mathrm{d}\varphi \\
&= 2\pi^2 (A^2 + B^2).
\end{aligned}$$

Hence,

$$\|\mathcal{I}_0 f^{(0)}\|_{L^2(\partial_+\Omega M)} = \sqrt{2(A^2+B^2)}\pi.$$

For $A, B \in \mathbb{R}$ we want to verify that

$$\langle \mathcal{I}_0 f^{(0)}, \mathcal{I}_0 f^{(0)} \rangle_{L^2(\partial_+\Omega M)} = \langle f^{(0)}, \mathcal{I}_0^* \mathcal{I}_0 f^{(0)} \rangle_{L^2(S^1\tau'_M)}.$$

We have

$$\begin{aligned}
\mathcal{I}_0 f^{(0)}(x,\xi) &= -(A\xi^1 + B\xi^2)\tau_-(x,\xi) \\
&= (A\xi^1 + B\xi^2)\left(\langle x,\xi\rangle + \sqrt{\langle x,\xi\rangle^2 + 1 - \langle x,x\rangle}\right) \\
&=: h(x,\xi).
\end{aligned}$$

Thus, for $(\tilde{x},\tilde{\xi}) \in \Omega M$,

$$
\begin{aligned}
&h(\tilde{x}+\tau_+(\tilde{x},\tilde{\xi})\tilde{\xi},\tilde{\xi})\\
&=(A\tilde{\xi}_1+B\tilde{\xi}_2)\left(\langle\tilde{x}+\tau_+(\tilde{x},\tilde{\xi})\tilde{\xi},\tilde{\xi}\rangle+\sqrt{\langle\tilde{x}+\tau_+(\tilde{x},\tilde{\xi})\tilde{\xi},\tilde{\xi}\rangle^2+1-\underbrace{|\tilde{x}+\tau_+(\tilde{x},\tilde{\xi})\tilde{\xi}|^2}_{=1}}\right)\\
&=(A\tilde{\xi}_1+B\tilde{\xi}_2)\left(\langle\tilde{x},\tilde{\xi}\rangle+\tau_+(\tilde{x},\tilde{\xi})+\sqrt{(\langle\tilde{x},\tilde{\xi}\rangle+\tau_+(\tilde{x},\tilde{\xi}))^2}\right)\\
&=2(A\tilde{\xi}_1+B\tilde{\xi}_2)\sqrt{\langle\tilde{x},\tilde{\xi}\rangle^2+1-|\tilde{x}|^2}.
\end{aligned}
$$

Consequently, we have

$$
w(\tilde{x},\tilde{\xi})=\frac{h(\tilde{x}+\tau_+(\tilde{x},\tilde{\xi})\tilde{\xi},\tilde{\xi})}{\langle\tilde{x},\tilde{\xi}\rangle+\tau_+(\tilde{x},\tilde{\xi})}=2(A\tilde{\xi}_1+B\tilde{\xi}_2)
$$

and therefore,

$$
\mathcal{I}_0^*\mathcal{I}_0 f^{(0)}=\int_0^{2\pi}2(A\cos\varphi+B\sin\varphi)\begin{pmatrix}\cos\varphi\\ \sin\varphi\end{pmatrix}\mathrm{d}\varphi=2\pi\begin{pmatrix}A\\ B\end{pmatrix}.
$$

Hence, we obtain as expected

$$
\begin{aligned}
\langle f^{(0)},\mathcal{I}_0^*\mathcal{I}_0 f^{(0)}\rangle_{L^2(S^1\tau'_M)}&=\int_M 2\pi(A^2+B^2)\mathrm{d}V\\
&=2\pi(A^2+B^2)\int_0^1\int_0^{2\pi}r\mathrm{d}\mu\mathrm{d}r\\
&=2\pi^2(A^2+B^2).
\end{aligned}
$$

This example will be used to prove the accuracy of the implemented adjoint operator.

A.3.2 Variable vector field

Let $c>0$ be constant. We define

$$
f(x_1,x_2)=\begin{pmatrix}x_1\\ cx_2\end{pmatrix}.
$$

Then,

$$
\begin{aligned}
[\mathcal{I}_{\alpha_0} f](x,\xi) &= \int_{\tau_-(x,\xi)}^{0} \left[(x_1+\tau\xi^1)\xi^1 + c(x_2+\tau\xi^2)\xi^2\right] e^{\alpha_0\tau}\mathrm{d}\tau \\
&= \int_{\tau_-(x,\xi)}^{0} \left[(x_1\xi^1 + cx_2\xi^2) + \tau((\xi^1)^2 + c(\xi^2)^2)\right] e^{\alpha_0\tau}\mathrm{d}\tau \\
&= \left[e^{\alpha_0\tau}\left(\frac{(\xi^1)^2+c(\xi^2)^2}{\alpha}\tau + \frac{x_1\xi^1+cx_2\xi^2}{\alpha_0} - \frac{(\xi^1)^2+c(\xi^2)^2}{\alpha_0^2}\right)\right]_{\tau_-(x,\xi)}^{0} \\
&= \frac{x_1\xi^1+cx_2\xi^2}{\alpha_0} - \frac{(\xi^1)^2+c(\xi^2)^2}{\alpha_0^2} \\
&- e^{\alpha_0\tau_-(x,\xi)}\left(\frac{(\xi^1)^2+c(\xi^2)^2}{\alpha}\tau_-(x,\xi) + \frac{x_1\xi^1+cx_2\xi^2}{\alpha_0} - \frac{(\xi^1)^2+c(\xi^2)^2}{\alpha_0^2}\right)
\end{aligned}
$$

and

$$
\begin{aligned}
[\mathcal{I}_0 f](x,\xi) &= \int_{\tau_-(x,\xi)}^{0} \left[(x_1+\tau\xi^1)\xi^1 + c(x_2+\tau\xi^2)\xi^2\right] \mathrm{d}\tau \\
&= \int_{\tau_-(x,\xi)}^{0} \left[(x_1\xi^1 + cx_2\xi^2) + \tau((\xi^1)^2 + c(\xi^2)^2)\right] \mathrm{d}\tau \\
&= -(x_1\xi^1 + cx_2\xi^2)\tau_-(x,\xi) - \frac{1}{2}((\xi^1)^2 + c(\xi^2)^2)\tau_-^2(x,\xi).
\end{aligned}
$$

A.4 Runge-Kutta method

We consider the following first-order differential equation:

$$y'(t) = f(y(t)), \qquad y(t_0) = y_0.$$

The fourth-order Runge-Kutta method is given by

$$\begin{aligned} k_1 &= f(y(t_0)) = f(y_0) \\ k_2 &= f\left(y_0 + k_1 \frac{\Delta t}{2}\right) \\ k_3 &= f\left(y_0 + k_2 \frac{\Delta t}{2}\right) \\ k_4 &= f(y_0 + k_3 \Delta t). \end{aligned}$$

and

$$\begin{aligned} y(t_0 + \Delta t) &\approx y(t_0) + \frac{k_1 + 2k_2 + 2k_3 + k_4}{6} \Delta t \\ &= \left(\frac{1}{6}k_1 + \frac{1}{3}k_2 + \frac{1}{3}k_3 + \frac{1}{6}k_4\right) \Delta t. \end{aligned}$$

Bibliography

[1] H.K. Aben. Magnetophotoelasticity—photoelasticity in a magnetic field. *Experimental Mechanics*, 10(3):97–105, 1970.

[2] H.K. Aben and A.É. Puro. Photoelastic tomography for three-dimensional flow birefringence studies. *Inverse Problems*, 13(2):215, 1997.

[3] G. Ainsworth and Y.M. Assylbekov. On the range of the attenuated magnetic ray transform for connections and Higgs fields. *arXiv preprint arXiv:1311.4582*, 2013.

[4] Amal Alphonse, Charles Elliott, and Björn Stinner. An abstract framework for parabolic PDEs on evolving spaces. *Portugaliae Mathematica*, pages 1–46, 2015.

[5] D.L. Anderson and A.M. Dziewonski. Seismic tomography. *Scientific American*, 251(4):60–71, 1984.

[6] Y.E. Anikonov and L. N. Pestov. Integral geometry and the structure of Riemannian spaces. *J. Inv. Ill-Posed Prob.*, 1(3):177–191, 1993.

[7] Y.E. Anikonov, S.B. Gorshkalev, S.V. Maltseva, Y.S. Volkov, and E.Y. Derevtsov. A criterion for the horizontal homogeneity of a medium in the inverse kinematic problem of seismics. *Journal of Mathematical Sciences*, 195 (6):741–753, 2013.

[8] Y.M. Assylbekov and P. Stefanov. Sharp stability estimate for the geodesic ray transform. *Inverse problems*, 36(2):025013, 2020.

[9] H. Attouch and J. Peypouquet. The rate of convergence of Nesterov's accelerated forward-backward method is actually faster than 1/k^2. *SIAM Journal on Optimization*, 26(3):1824–1834, 2016.

[10] M. Bartelmann, B. Feuerbacher, T. Krüger, D. Lüst, A. Rebhan, and A. Wipf. *Theoretische Physik*. Springer, 2015.

[11] A. Beck and M. Teboulle. A fast iterative shrinkage-thresholding algorithm for linear inverse problems. *SIAM journal on imaging sciences*, 2(1):183–202, 2009.

[12] A. Belenkin, M. Hartz, and T. Schuster. A note on Γ-convergence of Tikhonov functionals for nonlinear inverse problems. *arXiv preprint arXiv:2208.05780*, 2022.

[13] S.E. Blanke, B.N. Hahn, and A. Wald. Inverse problems with inexact forward operator: iterative regularization and application in dynamic imaging. *Inverse Problems*, 36(12):124001, 2020.

[14] A. Braides. *Gamma-convergence for Beginners*, volume 22. Clarendon Press, 2002.

[15] H. Braun and A. Hauck. Tomographic reconstruction of vector fields. *IEEE Transactions on signal processing*, 39(2):464–471, 1991.

[16] A.V. Bronnikov. Numerical solution of the identification problem for the attenuated radon transform. *Inverse Problems*, 15(5):1315, 1999.

[17] A.A. Bukgheim. *Mathematical Methods and Modelling in Hydrocarbon Exploration and Production. Mathematics in Industry*, volume 7, chapter Modern Techniques in Seismic Tomography. Springer, Berlin, Heidelberg, 2005. A. Iske, T. Randen (Eds.).

[18] National Research Council et al. Mathematics and physics of emerging biomedical imaging. 1996.

[19] M.G. Crandall, H. Ishii, and P.-L. Lions. User's guide to viscosity solutions of second order partial differential equations. *Bulletin of the American mathematical society*, 27(1):1–67, 1992.

[20] N.S. Dairbekov, G.P. Paternain, P. Stefanov, and G. Uhlmann. The boundary rigidity problem in the presence of a magnetic field. *Advances in mathematics*, 216(2):535–609, 2007.

[21] M. Defrise and G.T. Gullberg. 3D reconstruction of tensors and vectors. 2005.

[22] W. Demtröder. *Experimentalphysik 2–Elektrizität und Optik*, volume 3. Springer Berlin, Heidelberg, 2004.

[23] W. Demtröder. *Experimentalphysik 1: Mechanik und Wärme*, volume 1. Springer Berlin Heidelberg, 2008.

[24] E.Y. Derevtsov and I.E. Svetov. Tomography of tensor fields in the plane. *Eurasian J. Math. Comp. Appl.*, 3(2):24–68, 2015.

[25] E.Y. Derevtsov, Y.S. Volkov, and Schuster T. *Differential Equations and Uniqueness Theorems for the Generalized Attenuated Ray Transforms of Tensor Fields.*

[26] E.Y. Derevtsov, R. Dietz, A.K. Louis, and T. Schuster. Influence of refraction to the accuracy of a solution for the 2D-emission tomography problem. *Journal of Inverse and Ill-Posed Problems*, 8(2):161–191, 2000.

[27] E.Y. Derevtsov, A.K. Louis, and T. Schuster. Two approaches to the problem of defect correction in vector field tomography solving boundary value problems. *J. Inv. Ill-Posed Prob.*, 12:597–626, 2004.

[28] E.Y. Derevtsov, V.V. Pikalov, and T. Schuster. Application of local operators for numerical reconstruction of the singular support of a vector field by its known ray transforms. *Journal of Physics: Conference Series*, 135, 2008. Article ID 012035.

[29] E.Y. Derevtsov, I.E. Svetov, Y.S. Volkov, and T. Schuster. Numerical B-spline solution of emission and vector 2D tomography problems for media with absorbtion and refraction. In *Proceedings 2008 IEEE Region 8 International Conference on Computational Technologies in Electrical and Electronics Engineering SIBIRCON-08*, pages 212–217, Novosibirsk Scientific Center, Novosibirsk, Russia, 2008.

[30] E.Y. Derevtsov, A.K. Louis, S.V. Maltseva, A.P. Polyakova, and I.E. Svetov. Numerical solvers based on the method of approximate inverse for 2D vector and 2-tensor tomography problems. *Inverse Problems*, 33:17pp., 2017.

[31] E.Y. Derevtsov, Y.S. Volkov, and T. Schuster. Generalized attenuated ray transforms and their integral angular moments. *Applied Mathematics and Computation*, page 409, 2021.

[32] L. Desbat, S. Roux, and P. Grangeat. Compensation of some time dependent deformations in tomography. *IEEE Transact. Med. Imag.*, 26(2):261–269, 2007.

[33] Marco Donatelli. On nondecreasing sequences of regularization parameters for nonstationary iterated tikhonov. *Numerical Algorithms*, 60:651–668, 2012.

[34] H.W. Engl, M. Hanke, and A. Neubauer. *Regularization of inverse problems*, volume 375. Springer Science & Business Media, 1996.

[35] D.V. Finch. Uniqueness for the attenuated x-ray transform in the physical range. *Inverse problems*, 2(2):197, 1986.

[36] O. Forster. *Analysis 3*. Springer Spektrum, 2009.

[37] D. Gourion and D. Noll. The inverse problem of emission tomography. *Inverse Problems*, 18(5):1435, 2002.

[38] J.S. Hadamard. *Lectures on Cauchy's problem in linear partial differential equations*, volume 18. Yale university press, 1923.

[39] B. Hahn. Efficient algorithms for linear dynamic inverse problems with known motion. *Inverse Problems*, 30, 2014. Article ID 035008.

[40] B. Hahn. Motion estimation and compensation strategies in dynamic computerized tomography. *Sensing and Imaging*, 18:1–20, 2017.

[41] B. Hahn. A motion artefact study and locally deforming objects in computerized tomography. *Inverse Problems*, 33, 2017. 114001.

[42] P.C. Hansen. *Discrete inverse problems: insight and algorithms*. SIAM, 2010.

[43] A. Hertle. On the injectivity of the attenuated radon transform. *Proceedings of the American Mathematical Society*, 92(2):201–205, 1984.

[44] Q. Huang. Attenuated vector tomography–an approach to image flow vector fields with doppler. 2008.

[45] S. Hubmer and R. Ramlau. Convergence analysis of a two-point gradient method for nonlinear ill-posed problems. *Inverse Problems*, 33(9):095004, 2017.

[46] K. Jänich. *Vektoranalysis*, volume 5. Springer Berlin, Heidelberg, 2005.

[47] J. Jost. *Riemannian geometry and geometric analysis*, volume 42005. Springer, 2008.

[48] P. Juhlin. Principles of Doppler tomography. Technical report, Center for Mathematical Sciences, Lund Institute of Technology, SE-221 00 Lund, Schweden, 1992.

[49] V.P. Karassiov and A.V. Masalov. The method of polarization tomography of radiation in quantum optics. *Journal of Experimental and Theoretical Physics*, 99(1):51–60, 2004.

[50] A. Katsevich. An approach to motion compensation in tomography. In Y. Censor, M. Jiang, and G. Wang, editors, *Biomedical Mathematics: Promising Directions in Imaging, Therapy Planning and Inverse Problems*, pages 221–242, Madison, Wisconsin, 2010. Medical Physics Publishing.

[51] A. Katsevich. An accurate approximate algorithm for motion compensation in two-dimensional tomography. *Inverse Problems*, 26, 2010. article ID 065007 (16 pp).

[52] S.G. Kazantsev and A.A. Bukhgeim. Inversion of the scalar and vector attenuated X-ray transforms in a unit disc. *J. Ill-Posed Inv. Probl.*, 15(7):735–765, 2007.

[53] H. Kielhöfer. *Variationsrechnung*, volume 1. Vieweg+Teubner Verlag Wiesbaden, 2010.

[54] A. Kirsch et al. *An introduction to the mathematical theory of inverse problems*, volume 120. Springer, 2011.

[55] R.V. Kuranov, V.V. Sapozhnikova, I.V. Turchin, E.V. Zagainova, V.M. Gelikonov, V.A. Kamensky, L.B. Snopova, and N.N. Prodanetz. Complementary use of cross-polarization and standard OCT for differential diagnosis of pathological tissues. *Optics Express*, 10(15):707–713, 2002.

[56] W.R.B. Lionheart and P.J. Withers. Diffraction tomography of strain. *Inverse Problems*, 31:17pp, 2015. Article ID 045005.

[57] J.L. Lions. *Optimal Control of Systems Governed by Partial Differential Equations*. Springer, Berlin, Heidelberg, 1971.

[58] A.K. Louis. *Inverse und schlecht gestellte Probleme*. Springer-Verlag, 2013.

[59] S. Minakshisundaram and Å. Pleijel. Some properties of the eigenfunctions of the Laplace-operator on riemannian manifolds. *Canadian Journal of Mathematics*, 1(3):242–256, 1949.

[60] G.J. Minity. On a "monotonicity" method for the solution of nonlinear equations in banach spaces. *University of Michigan*, 1963.

[61] F. Monard. Numerical implementation of geodesic X-ray transforms and their inversion. *SIAM J. Imag. Sci.*, 7(2), 2014.

[62] Z. Nashed. The theory of Tikhonov regularization for Fredholm equations of the first kind. *Siam Review*, 28(1):116–118, 1986.

[63] F. Natterer. Inverting the attenuated vectorial Radon transform. *J. Inverse and Ill-Posed Probl.*, 13(1):93–101, 2005. doi: doi:10.1515/1569394053583720. URL `https://doi.org/10.1515/1569394053583720`.

[64] F. Natterer and K.P. Hadeler. Efficient implementation of 'optimal' algorithms in computerized tomography. *Mathematical Methods in the Applied Sciences*, 2 (4):545–555, 1980.

[65] Y.E. Nesterov. A method of solving a convex programming problem with convergence rate $\mathcal{O}(k^2)$. In *Doklady Akademii Nauk*, volume 269, pages 543–547. Russian Academy of Sciences, 1983.

[66] S.J. Norton. Tomographic reconstruction of 2-D vector fields: Application to flow imaging. *Geophysics Journal*, 97:161–168, 1988.

[67] R. Novikov and V.A. Sharafutdinov. On the problem of polarization tomography: I. *Inverse problems*, 23(3):1229, 2007.

[68] R.G. Novikov. An inversion formula for the attenuated X-ray transformation. *Arkiv för matematik*, 40(1):145–167, 2002.

[69] R.G. Novikov. On the range characterization for the two-dimensional attenuated X-ray transformation. *Inverse problems*, 18(3):677, 2002.

[70] N.F. Osman and J.L. Prince. 3D vector tomography on bounded domains. *Inverse problems*, 14(1):185–196, 1998.

[71] V.Y. Panin, G.L. Zeng, M. Defrise, and G.T. Gullberg. Diffusion tensor MR imaging of principal directions: a tensor tomography approach. *Phys. Med. Biol.*, 47:2737–2757, 2002.

[72] G.P. Paternain, M. Salo, and G. Uhlmann. Tensor tomography on surfaces. *Inventiones mathematicae*, 193(1):229–247, 2013.

[73] L. Pestov and G. Uhlmann. On the characterization of the range and inversion formulas for the geodesic X-ray transform. *Internat. Math. Res. Notices*, 80: 4331–4347, 2004.

[74] P. Petersen. *Riemannian Geometry*. Springer Science and Business Media, 2006.

[75] T. Pfitzenreiter and T. Schuster. Tomographic reconstruction of the curl and divergence of 2D vector fields taking refractions into account. *SIAM J. on Imaging Sci.*, 4:40–56, 2011.

[76] A.É. Puro and D.D. Karov. Tensor field tomography of residual stresses. *Optics and Spectroscopy*, 103(4):678–682, 2007.

[77] A.É. Puro and D.D. Karov. Inverse problem of thermoelasticity of fiber gratings. *Journal of Thermal Stresses*, 39(5):500–512, 2016.

[78] R. Ramlau, R. Clackdoyle, F. Noo, and G. Bal. Accurate attenuation correction in spect imaging using optimization of bilinear functions and assuming an unknown spatially-varying attenuation distribution. *ZAMM-Journal of Applied Mathematics and Mechanics/Zeitschrift für Angewandte Mathematik und Mechanik: Applied Mathematics and Mechanics*, 80(9):613–621, 2000.

[79] A. Rieder. *Keine Probleme mit inversen Problemen: eine Einführung in ihre stabile Lösung*. Springer-Verlag, 2013.

[80] Tomas Roubicek. *Nonlinear Partial Differential Equations with Applications*. Birkhäuser, 2010.

[81] D. Rouseff, K.B. Winters, and T.E. Ewart. Reconstruction of oceanic microstructure by tomography: a numerical feasibility study. *Journal of Geophysical Research: Oceans*, 96(C5):8823–8833, 1991.

[82] K. Sadiq and A. Tamasan. On the range characterization of the two-dimensional attenuated Doppler transform. *SIAM Journal on Mathematical Analysis*, 47 (3):2001–2021, 2015.

[83] U. Schmitt and A.K. Louis. Efficient algorithms for the regularization of dynamic inverse problems: I. Theory. *Inverse Problems*, 18:645–658, 2002.

[84] U. Schmitt, A.K. Louis, C. Wolters, and M. Vauhkonen. Efficient algorithms for the regularization of dynamic inverse problems: II. Applications. *Inverse Problems*, 18:659–676, 2002.

[85] F. Schmitz, P. Nägele, and J. Daube. Bochner-Räume. *Universität Freiburg*, 2016.

[86] U. Schröder and T. Schuster. An iterative method to reconstruct the refractive index of a medium from time-of-flight measurements. *Inverse Problems*, 32(8): 085009, 2016.

[87] V.A. Sharafutdinov. *Integral geometry of tensor fields*. De Gruyter, 1994.

[88] V.A. Sharafutdinov. Finiteness theorem for the ray transform on a Riemannian manifold. *Inverse Problems*, 11(5):1039, 1995.

[89] V.A. Sharafutdinov. Ray transform on Riemannian manifolds. eight lectures on integral geometry. *preprint*, 1999.

[90] V.A. Sharafutdinov. Slice-by-slice reconstruction algorithm for vector tomography with incomplete data. *Inverse Problems*, 23:2603–2627, 2007.

[91] V.A. Sharafutdinov. The problem of polarization tomography: II. *Inverse Problems*, 24(3):035010, 2008.

[92] R.E. Showalter. *Monotone Operators in Banach Space and Nonlinear Partial Differential Equations*. American Mathematical Society, 1997.

[93] H. Sielschott and W. Derichs. Use of collocation methods under inclusion of a priori information in acoustic pyrometry. In *Proc. European Concerted Action on Process Tomography, Bergen, Norway*, pages 110–117, 1995.

[94] B. Spain. *Tensor Calculus: a concise course*. Courier Corporation, 2003.

[95] G. Sparr and K. Strahlen. Vector field tomography: an overview. *IMA Volumes in Mathematics and its Applications; Computational Radiology and Imaging: Therapy and Diagnostic*, 110, 1998.

[96] P. Stefanov. Support theorems for the light ray transform on analytic Lorentzian manifolds. *Proceedings of the American Mathematical Society*, 145(3):1259–1274, 2017.

[97] P. Stefanov and G. Uhlmann. Stability estimates for the X-ray transform of tensor fields and boundary rigidity. *Duke Math. J.*, 123(3):445–467, 2004.

[98] P. Stefanov, G. Uhlmann, and A. Vasy. Inverting the local geodesic X-ray transform on tensors. *Journal d'Analyse Mathematique*, 136(1):151–208, 2018.

[99] A. Tamasan. Tomographic reconstruction of vector fields in variable background media. *Inverse Problems*, 23(5):2197, 2007.

[100] H.V. Tran. *Hamilton–Jacobi equations: theory and applications*, volume 213. American Mathematical Soc., 2021.

[101] L. Vierus and T. Schuster. Well-defined forward operators in dynamic diffractive tensor tomography using viscosity solutions of transport equations. 2021.

[102] J. Wagner. *Erste Schritte in die Theoretische Physik*, volume 1. Springer Spektrum Berlin, Heidelberg, 2019.

[103] W. Walt. *Ordinary differential equations*, volume 182. Springer Science & Business Media, 1998.

[104] X. Yin and H. Xie. New metric tensors for anisotropic mesh generation. *arXiv preprint arXiv:1105.3254*, 2011.

[105] E. Zeidler. *Nonlinear Functional Analysis and Its Applications: II/B: Nonlinear Monotone Operators*. Springer Science and Business Media, 2013.